

Homotopy solutions for flows in a rotating frame



By

Tariq Javed

DEPARTMENT OF MATHEMATICS
QUAID-I-AZAM UNIVERSITY
ISLAMABAD, PAKISTAN
2008

Homotopy solutions for flows in a rotating frame



By
Tariq Javed

Supervised by
Dr. Tasawar Hayat

DEPARTMENT OF MATHEMATICS
QUAID-I-AZAM UNIVERSITY
ISLAMABAD, PAKISTAN
2008

Homotopy solutions for flows in a rotating frame

By

Tariq Javed

A Thesis

Submitted in the Partial Fulfillment of the

Requirements for the Degree of

DOCTOR OF PHILOSOPHY

IN

MATHEMATICS

Supervised By

Dr. Tasawar Hayat

DEPARTMENT OF MATHEMATICS
QUAID-I-AZAM UNIVERSITY
ISLAMABAD, PAKISTAN
2008

CERTIFICATE

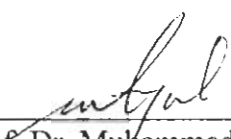
Homotopy solutions for flows in a rotating frame

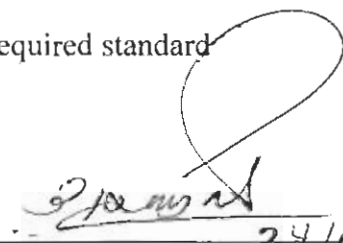
By

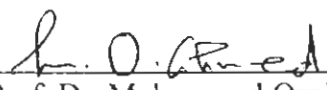
Tariq Javed

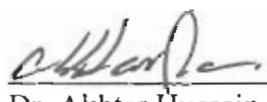
A THESIS SUBMITTED IN THE PARTIAL FULFILMENT OF THE REQUIREMENTS
FOR THE DEGREE OF THE DOCTOR OF PHILOSOPHY

We accept this dissertation as conforming to the required standard

1. 
Prof. Dr. Muhammad Ayub
(Chairman)

2. 
Dr. Tasawar Hayat
(Supervisor) 24/6/08

3. 
Prof. Dr. Muhammad Ozair Ahmad
(External Examiner)

4. 
Dr. Akhtar Hussain
(External Examiner)

DEPARTMENT OF MATHEMATICS
QUAID-I-AZAM UNIVERSITY
ISLAMABAD, PAKISTAN
2008

Dedicated to

The most dedicated one

Dr. Tasawar Hayat

And
To the memory of

Muhammad Amjad
(I miss you)

Acknowledgements

My last remaining task is to acknowledge all those that have contribute to the work described in this thesis. This is an impossible task, given many people that have helped me to design, implement, criticize, sponsor and evangelize the work. I am going to try anyway, and if your name is not listed, rest assured that my gratitude is not less than for those listed below.

This thesis would not have been possible without the kind support, the trenchant critiques, the probing questions and the creative abilities of my supervisor Dr. Tasawar Hayat. With his too much busy schedule, he always uses to take his precious time for his students regularly. His capacity to combine critique with an immediate empathy and commitment towards workers and others engaged in struggle always inspire me. While his friendship always refreshing, enhanced my PhD Experience. Honestly I have no words to pay my deepest gratitude, I cannot thank him enough.

I am grateful to Dr. Muhammad Yaqoob Nasir (Ex-chairman) and Prof. Dr. Muhammad Ayub, Chairman Department of Mathematics for providing friendly environment for the research work at the department.

Institutionally, I am very grateful for my years at the Quaid-I Azam University, made possible by the Higher Education Commission of Pakistan for financial support.

I took many courses during my PhD program from which I learn a great deal. I would like to thank all my teachers for their dedication and time. I remain indebted to them for providing me the means to learn and understand.

Where would I be without my friends? I am extraordinary fortunate in having Dr. Sajid, Dr. Iftikhar, Nasir and Zaheer as my closest friend with whom I spent a lot of time here. I could never have embarked and started and finished up all of this so easily without their prior support in research. We share really beautiful hues of life together.

I also gratefully acknowledge my friends Dr. Mazhar and Sher Baz Khan, we spend wonderful moments together. Thank you for all the moments we've shared, moments filled with shared dreams and wishes, secrets, laughers. Each precious second will be treasured in my heart forever.

I feel responsible to acknowledge the role of Fluid mechanics Group in the development of research activity up to the highest possible level. Dr. Sajid is always playing a vital role in this crucial activity "Group Meeting" of FMG. Dr. Masood Khan is also thanked for their efforts in the meetings. In absence of Dr. Tasawar Hayat, it looks very difficult to lead it in a right direction. I feel honor to thank Dr. Masood Khan and Dr. Sohail Nadeem, they always treated me as their friend.

Many thanks go in particular senior colleagues "Sir"Amjad & Ramzan, Amer Mann, Haidar Zamam, Mazhar tiwana and Ahmer. I always feel happy and comfort to be with them in their research room. All of my rest of friends at QAU Hostel especially Amanullah Dar, Tariq, Hannan, Sajid,...who have shared so many special moments, contributing a common story whose colourful pages now lead me towards a new chapter of life. I wish I could mention each individually.

I am deeply grateful to my friends of Murtaza, Sajeel, Faisal, Saqib, Yasir, Ashfaq, Kamran, Tariq, Azhar, Qadeer and especially Shafiq, I really learn a lot from him.

There are a number of people in my everyday circle of colleagues who have enriched me academic and non-academic life in various ways. I would like to thanks Mr. Niaz, Nayyar, Qumar, Umar, Usman and Majid. Thank you all. Maratib and his company is especially thankful, who have helped in shaping my thoughts and being source to understand different tedious aspects.

My parents deserve special attention for their inseparable support and prayers. My father in the first place is the person who put fundament my learning character, showing me the joy of intellectual pursuit ever since I was a child. My mother is the one who sincerely raised me with her caring and gentle love. Words fail me to express appreciation to my younger brother Tahir and Rizwan. It was theirs vision, care and persistent confidence in me, they have taken the load of my shoulder for so long time. It was almost four years ago that set this journey in motion and due to their handwork and sacrifice that enabled me to be the one to take it this far. It is largely due to their efforts that I am as I am today. I would like to express my sincere thanks to my sisters and brothers in-law especially Bhai Khalil who constantly provide emotional support and took care of me in many aspects. Many many thanks to my cousin Bhai Afzal, Rafi, Kamran and Uncles, who is always been a moral support for me in my life.

I am highly thankful to my childhood friends Abdulkhaliq and his family, Noor Ahmed and Ashfaq and his brothers.

Many thanks to the Staff members Saeed sb, Hameed sb, Sheraz sb, Bilal, Sajid, Miskeen and Noman whose friendship and support have made the department more than a temporary place of study for students and alumni from around the country.

Last but be no means least, my thanks although, I cannot pay, to all those who always pray for me and most importantly, I would like to thank almighty Allah, for it is under his grace that we live, learn and flourish.

22-06-2008

TARIQ JAVED

Contents

1	Introduction	6
1.1	Literature survey and basic equations	6
1.2	Magnetohydrodynamic (MHD) rotating flows	6
1.3	Flows over a stretching/shrinking surface	8
1.4	Basic equations	9
1.5	Constitutive equations	10
1.6	Boundary layer equations	12
1.7	Homotopy analysis method	13
1.8	Homotopy-Padé approximation	15
2	Hydromagnetic rotating flow of a viscous fluid over a shrinking surface	17
2.1	Mathematical formulation	17
2.2	Analytic solution	19
2.3	Convergence of the analytic solution	28
2.4	Results and discussion	28
3	Three-dimensional rotating flow induced by a shrinking sheet for suction	33
3.1	Description of the problem	33
3.2	Analytic solution	35
3.3	Convergence of the HAM solution	39
3.4	Results and discussion	40

4	Homotopy analysis for the rotating flow over a non-linear stretching surface	49
4.1	Problem formulation	49
4.2	HAM solution of the problem	52
4.3	Convergence of the analytic solution	56
4.4	Results and discussion	59
5	MHD rotating flow of a second grade fluid over a shrinking surface	66
5.1	Mathematical formulation	66
5.2	Solution by homotopy analysis method	68
5.3	Convergence of the analytic solution	73
5.4	Results and discussion	75
6	The influence of Hall current on rotating flow of a third grade fluid in a porous medium	81
6.1	Mathematical formulation	81
6.2	Analytic solution	85
6.3	Convergence of the analytic solution	88
6.4	Results and discussion	89
7	Heat transfer analysis on the rotating flow of a third grade fluid	97
7.1	Formulation of the problem	97
7.2	HAM solution for $F(z)$	99
7.3	HAM solution for $\theta(z)$	100
7.4	Convergence of the solution	101
7.5	Results and discussion	103
8	Conclusions	109

Preface

The study of fluid flow has a variety of applications in medicine, science and technology. The formulation of the Cauchy stress for various fluids is a difficult problem. Due to the great diversity in the physical structure of fluids, it is impossible to establish a single constitutive equation. Therefore several constitutive equations describing the fluid behavior for instance stress differences, shear thinning or shear thickening, stress relaxation and elastic effects etc. are proposed. It is known that Newtonian fluids can be described by the Navier-Stokes equations. Non-Newtonian fluids are mainly classified under three categories namely the differential type, rate type and integral type. One of the simplest subclass of differential type fluids is second grade. Although second grade model is able to predict the normal stress differences but third grade model is required in examining shear thinning or thickening when the shear viscosity is constant. Many flow problems of classical hydrodynamics have received new attentions recently in the general context of magnetohydrodynamics (MHD). In the past few years magnetohydrodynamics (MHD) has gained considerable importance because of its diverse applications in physics and engineering. In astrophysical and geophysical applications it is useful to study the stellar and solar structures, solar storms and flares, radio propagation through the ionosphere etc. In engineering its applications are in MHD generators, MHD pumps and MHD bearings. The concept of magnetohydrodynamics has been also utilized in the development of boundary layer flows over a stretching surface. Such flows have important engineering applications. Examples of such processes include the hot rolling, wire drawing, glass-fiber and paper production. Sheet stretching is also commonly used in polymer industry. Production of plastic sheets and foils, for example, involves extrusion of molten polymers through a slit die with the extrudates being collected by a wind-up roll upon solidification. There are abundant number of existing articles through various aspects that deal with the stretching flow problems. However the investigations on the flows due to a shrinking sheet are scarcely available in the literature. These are even not available for the hydrodynamic situation. With all the facts highlighted above this thesis runs as follows.

In chapter one, we include the review relevant to the MHD rotating flows, stretching and shrinking flows for viscous and non-Newtonian fluids. The basic flow equations, constitutive equations, homotopy analysis method and homotopy Padé approximation are also presented

in this chapter.

Chapter two discusses the two-dimensional boundary layer flow of a viscous fluid over a porous shrinking sheet. The equations are modeled when the MHD fluid and the shrinking surface are in a state of solid body rotation. It is concluded that suction solution in shrinking flow is only possible for the MHD fluid. The results of this chapter have been published in **Nonlinear Dynamics** 51 (2008) 259.

Chapter three extends the flow analysis of chapter two in three dimensions when the fluid is bounded between the two plates. Emphasis is given to the results of wall shear stress. It is found that influences of Hartman number and rotation parameter on the wall shear stress are different. However the role of suction parameter on the shear stress is similar to that of the rotation parameter. These observations are in press in **Chaos, Solitons and Fractals** (2007).

Porous materials have critical role in many scientific and engineering applications. Typical examples include catalysis, hydrology, tissue engineering, powder technology, wetting and drying processes. The fluid flow through porous media occurs in the fields of agriculture engineering to study the underground water resources, seepage of water in the river beds, in petroleum technology and transpiration cooling. In view of such applications, the MHD rotating flow of a viscous fluid over a non-linear stretching surface is studied in chapter four. The flow analysis is based in the absence of electric and induced magnetic fields. An incompressible viscous fluid occupies the porous half space. The influence of porosity parameter on the flow is found similar to that of the Hartman number. The contents of this chapter have been submitted for publication in **Phys. Lett. A**.

Chapter five is prepared to analyze the MHD rotating flow of a second grade fluid bounded by a shrinking sheet. Flow modeling is done and influence of second grade parameter is seen. It is revealed that the role of second grade parameter on horizontal and vertical velocity components is opposite. Here the magnitude of horizontal velocity component decreases by increasing the second grade parameter. These observations are in press for publication in **Phys. Lett. A** 372 (2008) 3264.

Much attention has been given to the flows in porous media which involve the classical Darcy's law valid for a viscous fluid. The investigations dealing with the flows of non-Newtonian

fluids through modified Darcy's law are less. In view of this reason chapter six investigates the Hall effect on hydromagnetic Poiseuille flow of a third grade fluid in a rotating frame. The modified Darcy's law for a third grade fluid is first developed and then used in the problem formulation. Such flow occurs for high magnetic field or low collision frequency. The presented analysis depict that the influence of Hall parameter and third grade parameter are similar on the velocity components. The main points of this chapter are published in **J. Porous Media 10 (2007) 807**.

Chapter seven illustrates the flow and heat transfer characteristics of a third grade fluid between two porous plates. Both plates and fluid exhibit rigid body rotation. It is found that third grade material parameter causes a reduction in the temperature profile. The behavior of rotation parameter and third grade parameter on the temperature profile is same. These conclusions have been published in **Acta Mechanica 191 (2007) 219**.

Chapter 1

Introduction

1.1 Literature survey and basic equations

This chapter includes the review of the previous investigations relevant to MHD rotating flows and flows over stretching and shrinking surfaces. The basic and constitutive equations governing the flow are given. Moreover the basic ideas of homotopy analysis method and Padé approximant are explained.

1.2 Magnetohydrodynamic (MHD) rotating flows

Due to theoretical and practical interest, the flow with magnetic field has attracted the attention of the investigators during the last few decades. In the presence of magnetic field the fluid particles experience a force induced by the electric current which results in the modification of the flow. In fact the Lorentz force is the interaction between the transverse magnetic field and the electrically conducting fluid. Interest in MHD flow began in 1918, when Hartman [1] invented the electromagnetic pump. Historically, Rossow [2] initiated the MHD boundary layer flow on a semi-infinite flat plate. Since then a large amount of literature is developed on this subject. The recent attempts in this direction are made by Hayat et al. [3–5], Misra et al. [6], Amkadni et al. [7], Sadeghy et al. [8], Khan et al. [9, 10], Abbas et al. [11], Sekhar et al. [12], Ibrahim et al. [13], Cortell [14], Pantokratoras [15], Pattison et al. [16], Liu et al. [17], Aliakbar et al. [18], Hakan et al. [19], Ni et al. [20, 21], Osalusi et al. [22], Pahlavan

et al. [23]. Samulyak et al. [24], EL-Kabeir et al. [25], Salem et al. [26], Eklabe et al. [27] and Abel et al. [28]. Further the scientific research of the fluid systems in rotating environments has considerable bearing on the problems of geophysical and astrophysical interest and fluid engineering applications. Chandrasekhar [29–31] discussed the influence of Coriolis force on problems of thermal instability and on stability of a viscous MHD flow. Lehnert [32,33] pointed out the Coriolis force effects on the MHD waves in the sun. Vidyanidhi [34] and Nanda and Mohanty [35] developed the steady rotating flow in a channel when pressure gradient is constant. Gupta [36] obtained an exact solution of the steady rotating flow past a porous plate. He showed that steady asymptotic solution for suction and injection cases are possible in a rotating frame. Soundalgekar and Pop [37] extended the Gupta's analysis [36] to the MHD fluid case. Loper [38] demonstrated the steady hydromagnetic boundary layer flow analysis near a rotating electrically conducting plate. In another paper, Loper [39] constructed the general solution for the linearized Ekman-Hartman layer on a spherical boundary. Hsueh [40] considered the problem of viscous fluid flow over a corrugated bottom in a rotating system. Potter and Chawla [41] and Gilman [42] investigated the stability of Ekman and Ekman-Hartman layers respectively. Vajravelu and Debnath [43] discussed the convective rotating flow in a wavy channel. Furthermore, some works have been done to investigate the time-dependent hydromagnetic flows as the boundary and initial value problems. Thornley [44] has studied the rotating flow of hydrodynamic viscous fluid bounded by an oscillating plate. The fluid occupies the semi-infinite space. The case of fluid between two plates the lower of which is oscillating and upper at rest is also discussed. Debnath [45] examined the rotating flow of a viscous MHD fluid over an oscillating rigid plate. In a series of papers, Debnath and his coworkers [46–48] analyzed the rotating flows of a viscous fluid for magnetohydrodynamic rigid and porous boundaries and Hall effect cases. The unsteady flow of a rotating MHD fluid induced by periodic pressure gradient in a channel is studied by Seth and Jana [49]. The influence of heat transfer and Hall current on the hydromagnetic flow has been seen by Mazumder et al. [50]. In another paper, Mazumder [51] found an exact solution for an oscillatory Couette flow in a rotating frame. Ganapathy [52] proposed an alternate solution for the problem considered in ref. [51]. Singh [53] extended the analysis of ref. [51] to MHD effects. More recently the hydromagnetic rotating flows of non-Newtonian fluids which take into account various physical features are investigated by Hayat et al. [54–58] and Siddiqui et al. [59,60].

1.3 Flows over a stretching/shrinking surface

The flows in which the sheet is stretched in its own plane with the velocity proportional to the distance from a fixed point is known as the stretching flows. These flows have relevance in several industrial applications. Investigations of boundary layer flows of an incompressible fluid over a stretched surface particularly include aerodynamic extrusion of plastic sheets, liquid film in condensation processes, cooling of a metallic plate, the glass fibre production and so on. The solution of stretching flow problem is substantially different from that of boundary layer flow bounded by a stationary surface (Blasius flow). Howarth [61] discussed the flat-plate flow by Runge-Kutta numerical scheme. Abussita [62] analyzed the Blasius flow and discussed the existence of the solution. Wang [63] demonstrated the approximate solution for Blasius flow using Adomian decomposition method. Interest in the boundary layer flows over a stretching surface is initiated by Sakiadis [64] and then followed by many other researchers. He examined the analysis over a stretched surface with a constant velocity for two-dimensional and axisymmetric flows. Tsou et al. [65] experimentally confirmed the numerical results of Sakiadis [66] for heat transfer in the boundary layer flow induced by a stretching surface with a constant velocity. Erickson [67] extended the Sakiadis' work to mass transfer situation.

There are very few cases in which the closed form solution of the Navier-Stokes equations is possible. Fortunately an analytic closed form solution is possible for the steady two-dimensional flow of a stretching surface. Crane [68] gave solution for the two-dimensional flow. The worth-mentioning fact of Cranes' problem is that it is still possible to obtain a closed form solution even when numerous other features for example suction, magnetic field, viscoelasticity of the fluid etc. are considered (see Andersson [69], Troy et al. [70], Ariel [71]). Moreover heat transfer and non-Newtonian effects on the stretching flow have been also analyzed (see Dandapat and Gupta [72], Cheng and Huang [73], Gupta and Gupta [74], Chen and Char [75], Dutta [76], Vajravelu [77], Hayat et al. [78,79] and Sajid et al. [80–82]). It should be pointed out that the flow and heat transfer over a stretching surface have key importance in engineering applications. Such applications may include heat treatment of materials manufactured in an extrusion process and a casting process of materials. Since the material quality depends upon the cooling of stretching sheets therefore control of the temperature is important. Hence knowledge of flow and heat transfer in such systems plays a critical role.

In the existing studies on stretching flows little attention has been given to non-linear velocity of a stretching surface and slip condition. Some works which take into account such physical features are developed by Vajravelu [83] and Hayat et al. [84]. Magyari and Keller [85] and Sajid and Hayat [86] also considered the exponentially stretching surface. Vajravelu and Kumar [87] also obtained the analytical and numerical solutions for non-linear system arising in three-dimensional rotating flow. Literature survey indicates that most of the researchers in the field investigated the flow due to a stretching surface through various aspects. Little is known up to yet about the flow caused by a shrinking surface. To the best of our information only two such studies [88, 89] exist. In [88] Wang presented unsteady shrinking film solution and in [89], Miklavcic and Wang proved the existence and uniqueness of steady hydrodynamic flow due to a shrinking sheet for a specific value of the suction parameter. Cortell [90] generalized the flow analysis of ref. [87] in the regime of MHD fluids.

1.4 Basic equations

The equations of magnetohydrodynamics which can describe the flow and heat transfer characteristics are

(a) Maxwell's equations

$$\begin{aligned} \operatorname{div} \mathbf{E} &= 0, \quad \operatorname{div} \mathbf{B} = 0, \\ \operatorname{curl} \mathbf{E} &= -\frac{\partial \mathbf{B}}{\partial t}, \quad \operatorname{curl} \mathbf{B} = \mu_m \mathbf{J}. \end{aligned} \quad (1.1)$$

These Maxwell's equations holds only when the displacement current is negligible.

(b) Ohms' law

$$\mathbf{J} = \sigma (\mathbf{E} + \mathbf{V} \times \mathbf{B}). \quad (1.2)$$

(c) The incompressibility condition

$$\operatorname{div} \mathbf{V} = 0. \quad (1.3)$$

(d) The momentum equation in porous media [91]

$$\rho \frac{d\mathbf{V}}{dt} = \text{div } \boldsymbol{\tau} + \rho \mathbf{b} + \mathbf{R}. \quad (1.4)$$

(e) The energy equation

$$\rho c_p \frac{dT}{dt} = \boldsymbol{\tau} \cdot \mathbf{L} - \text{div } \mathbf{q}. \quad (1.5)$$

Here \mathbf{E} and \mathbf{B} are the total electric and magnetic fields, μ_m is the magnetic permeability, t is the time, \mathbf{J} is the current density, \mathbf{V} is the velocity, σ is the electrical conductivity, ρ is the fluid density, \mathbf{b} the body force, \mathbf{R} is the Darcy's resistance, c_p is the specific heat, T is the temperature, \mathbf{q} is the heat flux, d/dt is the material derivative, \mathbf{L} is the velocity gradient and the Cauchy stress tensor $\boldsymbol{\tau}$ is given by

$$\boldsymbol{\tau} = \begin{pmatrix} \tau_{xx} & \tau_{xy} & \tau_{xz} \\ \tau_{yx} & \tau_{yy} & \tau_{yz} \\ \tau_{zx} & \tau_{zy} & \tau_{zz} \end{pmatrix}. \quad (1.6)$$

Note that in above equations displacement currents, free charges and radiation effects are absent; τ_{xx} , τ_{yy} and τ_{zz} are the normal stresses and τ_{xy} , τ_{xz} , τ_{yx} , τ_{yz} , τ_{zx} and τ_{zy} are the shear stresses.

In rotating frame Eq. (1.4) takes the form

$$\rho \left(\frac{d\mathbf{V}}{dt} + 2\boldsymbol{\Omega} \times \mathbf{V} + \boldsymbol{\Omega} \times (\boldsymbol{\Omega} \times \mathbf{r}) \right) = \text{div } \boldsymbol{\tau} + \rho \mathbf{b} + \mathbf{R}, \quad (1.7)$$

in which $\boldsymbol{\Omega}$ is the angular velocity, the second and third terms on the left hand side of above equation are the Coriolis and centrifugal forces respectively.

1.5 Constitutive equations

It is an established fact that many models have been suggested to analyze the response of various fluids. The fluids obeying Newton's law of viscosity can be characterized by the Navier-Stokes equation. However there are fluids of high molecular weight for which Navier-Stokes theory is inadequate. These fluids are termed as the non-Newtonian fluids. Unlike the Newtonian fluids

the flow of non-Newtonian fluids cannot be described by a single relationship between stress and deformation rate. Amongst the several models of fluids, the Navier-Stokes, second and third grade fluids which are the subclasses of differential type fluids are considered here.

The Cauchy stress tensor τ in an incompressible homogeneous fluid of grade three is [92]:

$$\tau = -p\mathbf{I} + \mu\mathbf{A}_1 + \alpha_1\mathbf{A}_2 + \alpha_2\mathbf{A}_1^2 + \beta_1\mathbf{A}_3 + \beta_2(\mathbf{A}_2\mathbf{A}_1 + \mathbf{A}_1\mathbf{A}_2) + \beta_3(\text{tr}\mathbf{A}_1^2)\mathbf{A}_1, \quad (1.8)$$

in which μ is the dynamic viscosity, p is the pressure, \mathbf{I} is the identity tensor, α_n ($n = 1, 2$) and β_n ($n = 1 - 3$) are the material moduli. The first three Rivlin-Ericksen tensors \mathbf{A}_n ($n = 1 - 3$) are defined as follows:

$$\begin{aligned} \mathbf{A}_1 &= \mathbf{L} + \mathbf{L}^T, \\ \mathbf{A}_n &= \frac{d\mathbf{A}_n}{dt} + \mathbf{A}_{n-1}\mathbf{L} + \mathbf{L}^T\mathbf{A}_{n-1} \quad n = 2, 3. \end{aligned} \quad (1.9)$$

It should be pointed out that Eq. (1.8) is considered as a third order approximation to an incompressible simple fluid in the sense of retardation. However, the model is properly frame invariant and can be used as an exact model in its own right. Fosdick and Rajagopal [93] examined the thermodynamics and stability of model (1.8). They conclude that if the fluid is thermodynamically compatible in the sense that all flows of the fluid meet the Clausius-Duhem inequality and the assumption that the specific Helmholtz free energy of the fluid is minimum when the fluid is locally at rest, then

$$\mu \geq 0, \quad \alpha_1 \geq 0, \quad |\alpha_1 + \alpha_2| \leq \sqrt{24\mu\beta_3}, \quad \beta_1 = \beta_2 = 0, \quad \beta_3 \geq 0. \quad (1.10)$$

Therefore the model (1.8) now is

$$\tau = -p\mathbf{I} + \mu\mathbf{A}_1 + \alpha_1\mathbf{A}_2 + \alpha_2\mathbf{A}_1^2 + \beta_3(\text{tr}\mathbf{A}_1^2)\mathbf{A}_1. \quad (1.11)$$

For second grade fluid $\beta_1 = \beta_2 = \beta_3 = 0$ and thus

$$\tau = -p\mathbf{I} + \mu\mathbf{A}_1 + \alpha_1\mathbf{A}_2 + \alpha_2\mathbf{A}_1^2, \quad (1.12)$$

whence [94]

$$\mu \geq 0, \alpha_1 \geq 0, \alpha_1 + \alpha_2 = 0. \quad (1.13)$$

Equation (1.12) for Navier-Stokes fluid can be reduced by choosing $\alpha_1 = \alpha_2 = 0$ and hence

$$\boldsymbol{\tau} = -p\mathbf{I} + \mu\mathbf{A}_1. \quad (1.14)$$

1.6 Boundary layer equations

Here we consider the following scalar equations for a rotating viscous flow

$$u \frac{\partial u}{\partial x} + w \frac{\partial u}{\partial z} - 2\Omega v - \Omega^2 x = -\frac{1}{\rho} \frac{\partial p}{\partial x} + \nu \left(\frac{\partial^2 u}{\partial x^2} + \frac{\partial^2 u}{\partial z^2} \right), \quad (1.15)$$

$$u \frac{\partial v}{\partial x} + w \frac{\partial v}{\partial z} + 2\Omega u = \nu \left(\frac{\partial^2 v}{\partial x^2} + \frac{\partial^2 v}{\partial z^2} \right), \quad (1.16)$$

$$u \frac{\partial w}{\partial x} + w \frac{\partial w}{\partial z} = -\frac{1}{\rho} \frac{\partial p}{\partial z} + \nu \left(\frac{\partial^2 w}{\partial x^2} + \frac{\partial^2 w}{\partial z^2} \right) \quad (1.17)$$

and an incompressibility condition

$$\frac{\partial u}{\partial x} + \frac{\partial w}{\partial z} = 0. \quad (1.18)$$

Here ν indicates the kinematic viscosity, $\mathbf{V} = (u, v, w)$, $\boldsymbol{\Omega}$ is the constant angular velocity with which the system is rotating about the z -axis. Defining

$$\begin{aligned} x^* &= \frac{x}{L}, \quad z^* = \frac{z}{\delta}, \quad \Omega^* = \frac{\Omega L}{U}, \\ u^* &= \frac{u}{U}, \quad w^* = \frac{wL}{U\delta}, \quad p^* = \frac{p}{\rho U^2} \end{aligned} \quad (1.19)$$

where L is the horizontal length scale, δ is the boundary layer thickness at $x = L$ and U is the fluid velocity in the x -direction parallel to the solid boundary. Now we obtain

$$u^* \frac{\partial u^*}{\partial x^*} + w^* \frac{\partial u^*}{\partial z^*} - 2\Omega^* v^* - \Omega^{*2} x^* = -\frac{\partial p^*}{\partial x^*} + \frac{\nu}{UL} \left(\frac{\partial^2 u^*}{\partial x^{*2}} + \left(\frac{L}{\delta} \right)^2 \frac{\partial^2 u^*}{\partial z^{*2}} \right), \quad (1.20)$$

$$u^* \frac{\partial v^*}{\partial x^*} + w^* \frac{\partial v^*}{\partial z^*} + 2\Omega^* u^* = \frac{\nu}{UL} \left(\frac{\partial^2 v^*}{\partial x^{*2}} + \left(\frac{L}{\delta} \right)^2 \frac{\partial^2 v^*}{\partial z^{*2}} \right), \quad (1.21)$$

$$u^* \frac{\partial w^*}{\partial x^*} + w^* \frac{\partial u^*}{\partial z^*} = - \left(\frac{L}{\delta} \right)^2 \frac{\partial p^*}{\partial z^*} + \frac{v}{UL} \left(\frac{\partial^2 u^*}{\partial x^{*2}} + \left(\frac{L}{\delta} \right)^2 \frac{\partial^2 w^*}{\partial z^{*2}} \right), \quad (1.22)$$

$$\frac{\partial u^*}{\partial x^*} + \frac{\partial w^*}{\partial z^*} = 0. \quad (1.23)$$

Selecting

$$\frac{v}{UL} \left(\frac{L}{\delta} \right)^2 = O(1) \quad (1.24)$$

and omitting asterisks one has

$$u \frac{\partial u}{\partial x} + w \frac{\partial u}{\partial z} - 2\Omega v - \Omega^2 x = - \frac{\partial p}{\partial x} + \frac{1}{R} \frac{\partial^2 u}{\partial x^2} + \frac{\partial^2 u}{\partial z^2}. \quad (1.25)$$

$$u \frac{\partial v}{\partial x} + w \frac{\partial v}{\partial z} + 2\Omega u = \frac{1}{R} \frac{\partial^2 v}{\partial x^2} + \frac{\partial^2 v}{\partial z^2}, \quad (1.26)$$

$$\frac{1}{R} \left(u \frac{\partial w}{\partial x} + w \frac{\partial w}{\partial z} \right) = - \frac{\partial p}{\partial z} + \frac{1}{R^2} \left(\frac{\partial^2 u}{\partial x^2} + R \frac{\partial^2 w}{\partial z^2} \right), \quad (1.27)$$

$$\frac{\partial u}{\partial x} + \frac{\partial w}{\partial z} = 0 \quad (1.28)$$

in which $\text{Re}(= UL/v)$ is the Reynold number. When $R \rightarrow \infty$ then above equations reduce to

$$u \frac{\partial u}{\partial x} + w \frac{\partial u}{\partial z} - 2\Omega v = - \frac{\partial \bar{p}}{\partial x} + \frac{\partial^2 u}{\partial z^2}, \quad (1.29)$$

$$u \frac{\partial v}{\partial x} + w \frac{\partial v}{\partial z} + 2\Omega u = \frac{\partial^2 v}{\partial z^2}, \quad (1.30)$$

$$\frac{\partial p}{\partial z} = 0, \quad (1.31)$$

$$\frac{\partial u}{\partial x} + \frac{\partial w}{\partial z} = 0, \quad (1.32)$$

where the modified pressure is

$$\bar{p} = p - \frac{1}{2} \Omega^2 (x^2 + y^2). \quad (1.33)$$

1.7 Homotopy analysis method

Perturbation methods have been widely used by the engineers in obtaining results especially for non-linear problems. Such methods require small parameters so that approximate solution can

be expressed in term of series. It is not necessary that all problems involve such small parameter. Therefore it seems important to have another analytic method which does not require small parameters at all. Keeping this fact in view Liao [95] has developed homotopy analysis method (HAM) which is independent upon small parameter assumption. Some recent investigations in the literature that contain HAM solutions may be mentioned in the refs. [?, 96-124]. The basic idea of HAM is described as follows.

Consider a nonlinear equation governed by

$$A(u) + f(r) = 0, \tag{1.34}$$

where A is a nonlinear operator, $f(r)$ is a known function and u is an unknown function. By means of homotopy analysis method, one first constructs a family of equations

$$(1 - q)\mathcal{L}[\widehat{v}(r, p) - u_0(r)] = q\hbar \{A[\widehat{v}(r, p) - f(r)]\}. \tag{1.35}$$

where $u_0(r)$ is an initial guess chosen by using the ‘‘Rule of solution expression’’ such that it satisfies the boundary conditions, \mathcal{L} is an auxiliary linear operator is to be chosen in such a way that it must generate the set of base functions that are used to define the initial guess, \hbar is an auxiliary parameter, $q \in [0, 1]$ is an embedding parameter, $\widehat{v}(r, q)$ is an unknown function of r and q . Liao [125] expanded $\widehat{v}(r, q)$ in Taylor series about the embedding parameter

$$\widehat{v}(r, p) = u_0(r) + \sum_{m=1}^{\infty} u_m(r) q^m, \tag{1.36}$$

where

$$u_m(r) = \frac{1}{m!} \left. \frac{\partial^m \widehat{v}(r, q)}{\partial q^m} \right|_{q=0}. \tag{1.37}$$

The convergence of the series (1.36) depends upon the auxiliary parameter \hbar . If it is convergent at $q = 1$, one has

$$u(r) = u_0(r) + \sum_{m=1}^{\infty} u_m(r). \tag{1.38}$$

Differentiating the zeroth order deformation equation (1.35) n -times with respect to p and then dividing them by $n!$ and finally setting $q = 0$ we obtain the following n th-order deformation

equation

$$\mathcal{L}[u_m(r) - \chi_m u_{m-1}(r)] = \hbar \mathcal{R}_m(r), \quad (1.39)$$

in which

$$\chi_m = \begin{cases} 0, & m \leq 1, \\ 1, & m > 1, \end{cases} \quad (1.40)$$

$$\mathcal{R}_m(r) = \frac{1}{(m-1)!} \times \left\{ \frac{d^{k-1}}{dq^{k-1}} A \left[u_0(r) + \sum_{m=1}^{\infty} u_m(r) q^m \right] \right\} \Big|_{q=0}. \quad (1.41)$$

There are many different ways to get the higher order deformation equations. However, according to the fundamental theorem in calculus [126], the term $u_m(r)$ in the series (1.36) is unique. Note that the HAM contains an auxiliary parameters \hbar , which provides us with a simple way to control and adjust the convergence of the series solution (1.38).

1.8 Homotopy-Padé approximation

A Padé approximant of a given power series is a rational function of numerator degree m and the denominator degree n whose power series agrees with the given one upto degrees $m+n$ inclusively. The Padé approximant that can be thought of as a generalization of a Taylor Polynomial. A Padé approximant often yields better approximation of the function than truncating its Taylor series, and it may still work where the Taylor series does not converge. In many cases the traditional Padé technique can greatly increase the convergence region and rate of approximations. For a given series

$$\sum_{n=0}^{\infty} a_n r^n \quad (1.42)$$

the corresponding $[m, n]$ Padé approximant is

$$\frac{\sum_{k=0}^m b_{m,k} r^k}{\sum_{k=0}^n c_{n,k} r^k} \quad (1.43)$$

in which $b_{m,k}$ and $c_{m,k}$ are determined by the coefficients a_i ($i = 0, 1, 2, 3, \dots, m+n$). The so-called homotopy-Padé technique [127] was proposed by combining the traditional Padé technique and homotopy analysis method. For convergence of series (1.36) at $q = 1$, we first employ the traditional $[m, n]$ Padé technique about the embedding parameter q to obtain $[m, n]$ Padé approximant

$$\frac{\sum_{k=0}^m B_{m,k}(r)q^k}{\sum_{k=0}^n C_{m,k}(r)q^k}, \quad (1.44)$$

where the coefficients $B_{m,k}(r)$ and $C_{m,k}(r)$ are determined by the first several approximations $u_0(r), u_1(r), \dots, u_{m+n}(r)$. On setting $q = 1$ in Eq. (1.44) one can write

$$\frac{\sum_{k=0}^m B_{m,k}(r)}{\sum_{k=0}^n C_{m,k}(r)}. \quad (1.45)$$

In general, the $[m, m]$ homotopy-Padé approximation can be expressed as

$$\frac{\sum_{k=0}^{m^2+m+1} B_1^{m,k}(r)}{\sum_{k=0}^{m^2+m+1} C_1^{m,k}(r)}, \quad (1.46)$$

In above equation $B_1^{m,k}(r)$ and $C_1^{m,k}(r)$ are coefficients. It is very interesting that these coefficients are found to be independent of the auxiliary parameter \hbar . Comparing Eqs. (1.43) and (1.46) we find that in accuracy the $[m, m]$ homotopy-Padé approximation is equivalent to the traditional $[m^2 + m + 1, m^2 + m + 1]$ Padé approximant. Similarly, the so-called homotopy-Padé technique can be applied to accelerate the convergence of the related series.

Chapter 2

Hydromagnetic rotating flow of a viscous fluid over a shrinking surface

This chapter deals with the magnetohydrodynamic (MHD) rotating boundary layer flow of a viscous fluid induced by the porous shrinking surface. The similarity transformations are used to reduce the partial differential equations into a system of two coupled ordinary differential equations. Analytic solution of the governing non-linear problem is developed by employing homotopy analysis method (HAM). The solution is presented in the form of an infinite series and convergence of the obtained series is given explicitly. The influence of the emerging parameters on the velocity fields is presented graphically and discussed. It is worth mentioning to note that for the shrinking surface, the meaningful convergent solutions are possible only for the MHD flows. The electromagnetic force is responsible for such meaningful solutions.

2.1 Mathematical formulation

Consider the steady laminar MHD boundary layer flow of a viscous fluid caused by a two dimensional shrinking surface in a rotating frame of reference. In mathematical modelling, we use the Cartesian coordinate system (x, y, z) with Ω being the angular velocity of the rotating fluid in the z -direction. In addition a constant magnetic field \mathbf{B}_0 is applied in the z -direction. There is no applied and induced electric fields. Under the assumption of small magnetic Reynolds number, the induced magnetic field is neglected. Therefore, the Eqs. (1.3),

(1.7) and (1.14) under the boundary layer approximations and no pressure gradient are reduced in the following forms:

$$\frac{\partial u}{\partial x} + \frac{\partial w}{\partial z} = 0, \quad (2.1)$$

$$u \frac{\partial u}{\partial x} + w \frac{\partial u}{\partial z} - 2\Omega v = \nu \frac{\partial^2 u}{\partial z^2} - \frac{\sigma B_0^2}{\rho} u, \quad (2.2)$$

$$u \frac{\partial v}{\partial x} + w \frac{\partial v}{\partial z} + 2\Omega u = \nu \frac{\partial^2 v}{\partial z^2} - \frac{\sigma B_0^2}{\rho} v, \quad (2.3)$$

where $\nu = \mu/\rho$ is the kinematic viscosity, σ is the electrical conductivity and u, v and w are the velocity components in x, y and z -directions, respectively.

The boundary conditions are

$$\begin{aligned} u &= -ax, & v &= 0, & w &= -W & \text{at } z &= 0, \\ u &\rightarrow 0, & v &\rightarrow 0 & & & \text{as } z &\rightarrow \infty \end{aligned} \quad (2.4)$$

in which $a > 0$ is the shrinking constant and $W > 0$ is the suction velocity. Introducing the following similarity transformations

$$u = ax f'(\eta), \quad v = ax g(\eta), \quad w = -\sqrt{a\nu} f(\eta), \quad \eta = \sqrt{\frac{a}{\nu}} z \quad (2.5)$$

equation (2.1) is identically satisfied and Eqs. (2.2) and (2.3) become

$$f''' - f'^2 + f f'' + 2\lambda g - M^2 f' = 0, \quad (2.6)$$

$$g'' - f' g + f g' - 2\lambda f' - M^2 g = 0, \quad (2.7)$$

$$\begin{aligned} f &= s, & f' &= -1, & g &= 0 & \text{at } \eta &= 0, \\ f' &\rightarrow 0, & g &\rightarrow 0 & & & \text{as } \eta &\rightarrow \infty, \end{aligned} \quad (2.8)$$

where the Hartman number (M), suction (s) and rotation (λ) parameters are respectively given by $M = \sigma B_0^2 / \rho a$, $s = W / \sqrt{a\nu}$ and $\lambda = \Omega / a$ and prime indicates the differentiation with respect to η .

2.2 Analytic solution

For the HAM solution of Eqs. (2.6) and (2.7) subject to conditions (2.8), we choose the following initial guess approximations for the functions f and g

$$f_0(\eta) = s - 1 + e^{-\eta}, \quad g_0(\eta) = \eta e^{-\eta}. \quad (2.9)$$

Here

$$\mathcal{L}_1(f) = f''' - f', \quad \mathcal{L}_2(f) = f'' - f \quad (2.10)$$

are the auxiliary linear operators satisfying

$$\mathcal{L}_1 [C_1 + C_2 e^\eta + C_3 e^{-\eta}] = 0, \quad \mathcal{L}_2 [C_4 e^\eta + C_5 e^{-\eta}] = 0, \quad (2.11)$$

where $C_i : i = 1 - 5$ are arbitrary constants.

Zeroth order deformation problems

The problem at the zeroth order are given by

$$(1 - q) \mathcal{L}_1 [\hat{f}(\eta, q) - f_0(\eta)] = q \hbar \mathcal{N}_1 [\hat{f}(\eta, q), \hat{g}(\eta, q)], \quad (2.12)$$

$$(1 - q) \mathcal{L}_2 [\hat{g}(\eta, q) - g_0(\eta)] = q \hbar \mathcal{N}_2 [\hat{f}(\eta, q), \hat{g}(\eta, q)], \quad (2.13)$$

$$\begin{aligned} \hat{f}(0, q) &= s, & \hat{f}'(0, q) &= -1, & \hat{f}'(\infty, q) &= 0, \\ \hat{g}(0, q) &= 0, & \hat{g}(\infty, q) &= 0, \end{aligned} \quad (2.14)$$

$$\begin{aligned} \mathcal{N}_1 [\hat{f}(\eta, q), \hat{g}(\eta, q)] &= \frac{\partial^3 \hat{f}(\eta, q)}{\partial \eta^3} - M^2 \frac{\partial \hat{f}(\eta, q)}{\partial \eta} + 2\lambda \hat{g}(\eta, q) \\ &\quad - \left(\frac{\partial \hat{f}(\eta, q)}{\partial \eta} \right)^2 + \hat{f}(\eta, q) \frac{\partial^2 \hat{f}(\eta, q)}{\partial \eta^2}, \end{aligned} \quad (2.15)$$

$$\begin{aligned} \mathcal{N}_2 \left[\widehat{f}(\eta, q), \widehat{g}(\eta, q) \right] &= \frac{\partial^2 \widehat{g}(\eta, q)}{\partial \eta^2} - M^2 \widehat{g}(\eta, q) - 2\lambda \frac{\partial \widehat{f}(\eta, q)}{\partial \eta} \\ &\quad - \frac{\partial \widehat{f}(\eta, q)}{\partial \eta} \widehat{g}(\eta, q) + \widehat{f}(\eta, q) \frac{\partial \widehat{g}(\eta, q)}{\partial \eta} \end{aligned} \quad (2.16)$$

in which $q \in [0, 1]$ is the embedding parameter and \hbar is the auxiliary nonzero parameter. For $q = 0$ and $q = 1$, we respectively have

$$\begin{aligned} \widehat{f}(\eta, 0) &= f_0(\eta), & \widehat{f}(\eta, 1) &= f(\eta), \\ \widehat{g}(\eta, 0) &= g_0(\eta), & \widehat{g}(\eta, 1) &= g(\eta). \end{aligned} \quad (2.17)$$

As q increases from 0 to 1, $\widehat{f}(\eta, q)$, $\widehat{g}(\eta, q)$ varies from the initial guesses $f_0(\eta)$, $g_0(\eta)$ to the exact solutions $f(\eta)$, $g(\eta)$. By Taylor's theorem and Eq. (2.17), one can write

$$f(\eta, q) = f_0(\eta) + \sum_{m=1}^{\infty} f_m(\eta) q^m, \quad g(\eta, q) = g_0(\eta) + \sum_{m=1}^{\infty} g_m(\eta) q^m, \quad (2.18)$$

where

$$f_m(\eta) = \frac{1}{m!} \left. \frac{\partial^m \widehat{f}(\eta, q)}{\partial q^m} \right|_{q=0}, \quad g_m(\eta) = \frac{1}{m!} \left. \frac{\partial^m \widehat{g}(\eta, q)}{\partial q^m} \right|_{q=0}.$$

The convergence of the two series in Eq. (2.18) depends on the auxiliary parameter \hbar . Assume that \hbar is chosen in such a way that the two series in Eq. (2.18) are convergent at $q = 1$, then due to Eq. (2.17) we get

$$f(\eta) = f_0(\eta) + \sum_{m=1}^{\infty} f_m(\eta), \quad g(\eta) = g_0(\eta) + \sum_{m=1}^{\infty} g_m(\eta). \quad (2.19)$$

m -th-order deformation problems

Differentiating the zeroth order deformation Eqs. (2.12) and (2.13) with respect to the embedding parameter p , m -times and then dividing by $m!$ and finally setting $p = 0$, we get the m th order deformation problem as follows:

$$\mathcal{L}_1 [f_m(\eta) - \chi_m f_{m-1}(\eta)] = \hbar \mathcal{R}_m^f(\eta), \quad \mathcal{L}_2 [g_m(\eta) - \chi_m g_{m-1}(\eta)] = \hbar \mathcal{R}_m^g(\eta), \quad (2.20)$$

$$f_m(0) = f'_m(0) = f'_m(\infty) = g_m(0) = g_m(\infty) = 0. \quad (2.21)$$

$$\begin{aligned}\mathcal{R}_m^f(\eta) &= f_{m-1}'''(\eta) - M^2 f_{m-1}'(\eta) + 2\lambda g_{m-1}(\eta) \\ &\quad + \sum_{k=0}^{m-1} [f_{m-1-k}(\eta) f_k''(\eta) - f_{m-1-k}'(\eta) f_k'(\eta)],\end{aligned}\quad (2.22)$$

$$\begin{aligned}\mathcal{R}_m^g(\eta) &= g_{m-1}''(\eta) - M^2 g_{m-1}(\eta) - 2\lambda f_{m-1}'(\eta) \\ &\quad + \sum_{k=0}^{m-1} [f_{m-1-k}(\eta) g_k'(\eta) - f_{m-1-k}'(\eta) g_k(\eta)],\end{aligned}\quad (2.23)$$

where χ_m is defined in Eq. (1.40). We use the symbolic computation software MATHEMATICA now to solve the linear Eqs. (2.20) and (2.21) upto first few order of approximations. It is found that the solution of the problem can be expressed as an infinite series of the form

$$f_m(\eta) = \sum_{n=0}^{m+1} \sum_{q=0}^{m+1-n} a_{m,n}^q \eta^q e^{-n\eta}, \quad g_m(\eta) = \sum_{n=0}^{m+1} \sum_{q=0}^{m+1-n} A_{m,n}^q \eta^q e^{-n\eta}, \quad m > 0. \quad (2.24)$$

In order to find the recurrence formulas for the unknown coefficients in above equation, we proceed as follows. Now

$$\begin{aligned}f_m'(\eta) &= \sum_{n=0}^{m+1} \left[\sum_{q=1}^{m+1-n} k a_{m,n}^q \eta^{q-1} - n \sum_{q=0}^{m+1-n} a_{m,n}^q \eta^q \right] e^{-n\eta} \\ &= \sum_{n=0}^{m+1} \left[\sum_{q=0}^{m+1-n} (q+1) a_{m,n}^{q+1} \eta^q - n \sum_{q=0}^{m+1-n} a_{m,n}^q \eta^q \right] e^{-n\eta} \\ &= \sum_{n=0}^{m+1} \sum_{q=0}^{m+1-n} [(q+1) a_{m,n}^{q+1} - n a_{m,n}^q] \eta^q e^{-n\eta} \\ &= \sum_{n=0}^{m+1} \sum_{q=0}^{m+1-n} b_{m,n}^q \eta^q e^{-n\eta},\end{aligned}\quad (2.25)$$

where

$$b_{m,n}^q = (q+1) a_{m,n}^{q+1} - n a_{m,n}^q. \quad (2.26)$$

Employing a similar procedure, other derivatives involved in Eq. (2.24) are given by

$$f_m''(\eta) = \sum_{n=0}^{m+1} \sum_{q=0}^{m+1-n} c_{m,n}^q \eta^q e^{-n\eta}, \quad (2.27)$$

$$f_m'''(\eta) = \sum_{n=0}^{m+1} \sum_{q=0}^{m+1-n} d_{m,n}^q \eta^q e^{-n\eta}, \quad (2.28)$$

$$g_m'(\eta) = \sum_{n=0}^{m+1} \sum_{q=0}^{m+1-n} B_{m,n}^q \eta^q e^{-n\eta}, \quad (2.29)$$

$$g_m''(\eta) = \sum_{n=0}^{m+1} \sum_{q=0}^{m+1-n} C_{m,n}^q \eta^q e^{-n\eta}. \quad (2.30)$$

$$c_{m,n}^q = (q+1) b_{m,n}^{q+1} - n b_{m,n}^q, \quad (2.31)$$

$$d_{m,n}^q = (q+1) c_{m,n}^{q+1} - n c_{m,n}^q. \quad (2.32)$$

$$B_{m,n}^q = (q+1) A_{m,n}^{q+1} - n A_{m,n}^q, \quad (2.33)$$

$$C_{m,n}^q = (q+1) B_{m,n}^{q+1} - n B_{m,n}^q. \quad (2.34)$$

Now for the product term $f_{m-1-k}(\eta) f_k''(\eta)$, when $0 \leq k \leq m-1$, we get from Eqs. (2.24) and (2.27) as

$$\begin{aligned} f_{m-1-k}(\eta) f_k''(\eta) &= \left(\sum_{i=0}^{m-k} \sum_{j=0}^{m-k-i} \alpha_{m-1-k,i}^j \eta^j e^{-i\eta} \right) \left(\sum_{p=0}^{k+1} \sum_{r=0}^{k+1-p} c_{k,p}^r \eta^r e^{-p\eta} \right) \\ &= \sum_{p=0}^{k+1} \sum_{i=0}^{m-k} e^{-(i+p)\eta} \left(\sum_{r=0}^{k+1-p} \sum_{j=0}^{m-k-i} c_{k,p}^r \alpha_{m-1-k,i}^j \eta^{(j+r)} \right) \\ &= \sum_{n=0}^{k+1} e^{-n\eta} \sum_{p=\max\{0, n+k-m\}}^{\min\{n, k+1\}} \left(\sum_{r=0}^{k+1-p} \sum_{j=0}^{m-k-i} c_{k,p}^r \alpha_{m-1-k,i}^j \eta^{(j+r)} \right) \\ &= \sum_{n=0}^{k+1} e^{-n\eta} \sum_{p=\max\{0, n+k-m\}}^{\min\{n, k+1\}} \sum_{q=0}^{m+1-n} \sum_{r=\max\{0, q+n-p+k-m\}}^{\max\{q, k+1-p\}} c_{k,p}^r \alpha_{m-1-k, n-p}^{q-r} \eta^q \\ &= \sum_{n=0}^{k+1} \sum_{q=0}^{m+1-n} \times \left(\sum_{p=\max\{0, n+k-m\}}^{\min\{n, k+1\}} \sum_{r=\max\{0, q+n-p+k-m\}}^{\max\{q, k+1-p\}} c_{k,p}^r \alpha_{m-1-k, n-p}^{q-r} \right) \eta^q e^{-n\eta} \quad (2.35) \end{aligned}$$

which can be further simplified as

$$\begin{aligned}
\sum_{k=0}^{m-1} f_{m-1-k}(\eta) f_k''(\eta) &= \sum_{n=0}^{k+1} e^{-n\eta} \sum_{q=0}^{m+1-n} \eta^q \\
&\times \left(\sum_{k=0}^{m-1} \sum_{p=\max\{0, n+k-m\}}^{\min\{n, k+1\}} \sum_{r=\max\{0, q+n-p+k-m\}}^{\max\{q, k+1-p\}} C_{k,p}^r \alpha_{m-1-k, n-p}^{q-r} \right), \\
&= \sum_{n=0}^{k+1} \sum_{q=0}^{m+1-n} \delta_{m,n}^q \eta^q e^{-n\eta}.
\end{aligned} \tag{2.36}$$

where

$$\delta_{m,n}^q = \sum_{k=0}^{m-1} \sum_{p=\max\{0, n+k-m\}}^{\min\{n, k+1\}} \sum_{r=\max\{0, q+n-p+k-m\}}^{\max\{q, k+1-p\}} C_{k,p}^r \alpha_{m-1-k, n-p}^{q-r}. \tag{2.37}$$

Employing the same methodology, we get

$$\sum_{k=0}^{m-1} f'_{m-1-k}(\eta) f_k'(\eta) = \sum_{n=0}^{k+1} \sum_{q=0}^{m+1-n} \Delta_{m,n}^q \eta^q e^{-n\eta}, \tag{2.38}$$

$$\sum_{k=0}^{m-1} f_{m-1-k}(\eta) g_k'(\eta) = \sum_{n=0}^{k+1} \sum_{q=0}^{m+1-n} \Lambda_{m,n}^q \eta^q e^{-n\eta}, \tag{2.39}$$

$$\sum_{k=0}^{m-1} f'_{m-1-k}(\eta) g_k(\eta) = \sum_{n=0}^{k+1} \sum_{q=0}^{m+1-n} \Gamma_{m,n}^q \eta^q e^{-n\eta}, \tag{2.40}$$

where

$$\Delta_{m,n}^q = \sum_{k=0}^{m-1} \sum_{i=\max\{0, n-m+k\}}^{\min\{n, k+1\}} \sum_{j=\max\{0, q-m+k+n-i\}}^{\min\{q, k+1-i\}} b_{k,i}^j b_{m-1-k, n-i}^{q-j}, \tag{2.41}$$

$$\Lambda_{m,n}^q = \sum_{k=0}^{m-1} \sum_{i=\max\{0, n-m+k\}}^{\min\{n, k+1\}} \sum_{j=\max\{0, q-m+k+n-i\}}^{\min\{q, k+1-i\}} B_{k,i}^j \alpha_{m-1-k, n-i}^{q-j}, \tag{2.42}$$

$$\Gamma_{m,n}^q = \sum_{k=0}^{m-1} \sum_{i=\max\{0, n-m+k\}}^{\min\{n, k+1\}} \sum_{j=\max\{0, q-m+k+n-i\}}^{\min\{q, k+1-i\}} A_{k,i}^j b_{m-1-k, n-i}^{q-j}, \tag{2.43}$$

and hence Eqs. (2.22) and (2.23) can be written as

$$\Psi_{m,n}^q = \hbar \left[\chi_{m+2-n-q} \left(d_{m-1,n}^q - M^2 b_{m-1,n}^q + 2\lambda A_{m-1,n}^q \right) + \delta_{m,n}^q - \Delta_{m,n}^q \right], \quad (2.44)$$

$$\Theta_{m,n}^q = \hbar \left[\chi_{m+2-n-q} \left(C_{m-1,n}^q - M^2 A_{m-1,n}^q + 2\lambda b_{m-1,n}^q \right) + \Lambda_{m,n}^q - \Gamma_{m,n}^q \right]. \quad (2.45)$$

Substituting Eqs. (2.44) and (2.45) into Eq. (2.20) we have

$$\mathcal{L}_1 [f_m(\eta) - \chi_m f_{m-1}(\eta)] = \sum_{n=0}^{m+1} \sum_{q=0}^{m+1-n} \Psi_{m,n}^q \eta^q e^{-n\eta}, \quad (2.46)$$

$$\mathcal{L}_2 [g_m(\eta) - \chi_m g_{m-1}(\eta)] = \sum_{n=0}^{m+1} \sum_{q=0}^{m+1-n} \Theta_{m,n}^q \eta^q e^{-n\eta}. \quad (2.47)$$

In order to obtain the solution of Eq. (2.46), we have to solve the following equation

$$y'''(\eta) - y'(\eta) = \eta^q e^{-n\eta}. \quad (2.48)$$

Case (1): For $n = 1$, above equation gives

$$y(\eta) = \sum_{k=0}^{q+1} \sum_{p=0}^{q+1-k} \frac{q!}{k! 2^{q+2-k-p}} \eta^k e^{-\eta}. \quad (2.49)$$

Setting

$$\mu_{1,k}^q = \sum_{p=0}^{q+1-k} \frac{q!}{k! 2^{q+2-k-p}}, \quad q \geq 0, \quad 0 \leq k \leq q+1 \quad (2.50)$$

Eq. (2.49) takes the form

$$y(\eta) = \sum_{k=0}^{q+1} \mu_{1,k}^q \eta^k e^{-\eta}. \quad (2.51)$$

Case (2): When $n \geq 2$, Eq. (2.48) has a solution

$$y(\eta) = \sum_{k=0}^q \sum_{r=0}^{q-k} \sum_{p=0}^{q-k-r} \frac{-q!}{k! n^{r+1} (n-1)^{q+1-k-r-p} (n+1)^{p+1}} \eta^k e^{-n\eta} \quad (2.52)$$

or

$$y(\eta) = \sum_{k=0}^q \mu_{n,k}^q \eta^k e^{-n\eta} \quad (2.53)$$

where

$$\begin{aligned} \mu_{n,k}^q &= \sum_{r=0}^{q-k} \sum_{p=0}^{q-k-r} \frac{q!}{k!n^{r+1}(n-1)^{q+1-k-r-p}(n+1)^{p+1}}, \\ 0 &\leq k \leq q, \quad q \geq 0, \quad n \geq 2. \end{aligned} \quad (2.54)$$

Similarly for the solution of Eq. (2.47), our interest lies in finding the solution of the following differential equation

$$x''(\eta) - x(\eta) = \eta^q e^{-n\eta}. \quad (2.55)$$

Case (1): For $n = 1$, the above equation is satisfied by

$$x(\eta) = \sum_{k=1}^{q+1} \mu_{1,k}^q \eta^k e^{-\eta}, \quad (2.56)$$

where

$$\mu_{1,k}^q = \sum_{p=0}^{2q+2} \frac{(-1)^{2q+1-2k-p} q!}{k! 2^{q+2-k}}, \quad q \geq 0, \quad 1 \leq k \leq q+1. \quad (2.57)$$

Case (2): When $n \geq 2$, the Eq. (2.55) has a solution

$$x(\eta) = \sum_{k=0}^q \mu_{n,k}^q \eta^k e^{-n\eta}, \quad (2.58)$$

in which

$$\begin{aligned} \mu_{n,k}^q &= \sum_{p=0}^{q-k} \frac{q!}{k!(n-1)^{q+1-k-p}(n+1)^{p+1}}, \\ 0 &\leq k \leq q, \quad q \geq 0, \quad n \geq 2. \end{aligned} \quad (2.59)$$

Thus we deduce the following solution of the Eqs. (2.46) and (2.47) respectively as

$$\begin{aligned}
f_m(\eta) - \chi_m f_{m-1}(\eta) &= \sum_{q=0}^{m+1} \sum_{k=1}^{q+1} \Psi_{m,0}^q \mu_{0,k}^q \eta^k + \sum_{q=0}^m \sum_{k=0}^{q+1} \Psi_{m,1}^q \mu_{1,k}^q \eta^k e^{-\eta} \\
&+ \sum_{n=2}^{m+1} \sum_{q=0}^{m+1-n} \sum_{k=0}^q \Psi_{m,n}^q \mu_{n,k}^q \eta^k e^{-n\eta} \\
&+ C_1^m + C_2^m e^{-\eta} + C_3^m e^\eta, \tag{2.60}
\end{aligned}$$

$$\begin{aligned}
g_m(\eta) - \chi_m g_{m-1}(\eta) &= \sum_{q=0}^{m+1} \sum_{k=0}^q \Theta_{m,0}^q \mu_{0,k}^q \eta^k + \sum_{q=0}^m \sum_{k=1}^{q+1} \Theta_{m,1}^q \mu_{1,k}^q \eta^k e^{-\eta} \\
&+ \sum_{n=2}^{m+1} \sum_{q=0}^{m+1-n} \sum_{k=0}^q \Theta_{m,n}^q \mu_{n,k}^q \eta^k e^{-n\eta} \\
&+ C_4^m e^\eta + C_5^m e^{-\eta}, \tag{2.61}
\end{aligned}$$

where $C_1^m, C_2^m, C_3^m, C_4^m$ and C_5^m are integral constants. Using the boundary conditions (2.21), we have

$$C_1^m = - \sum_{q=0}^m \Psi_{m,1}^q \mu_{1,1}^q - \sum_{n=2}^{m+1} \sum_{q=0}^{m+1-n} \Psi_{m,n}^q \left(\mu_{n,1}^q - (n-1) \mu_{n,0}^q \right), \tag{2.62}$$

$$C_2^m = \sum_{q=0}^m \Psi_{m,1}^q \left(\mu_{1,1}^q - \mu_{1,0}^q \right) + \sum_{n=2}^{m+1} \sum_{q=0}^{m+1-n} \Psi_{m,n}^q \left(\mu_{n,1}^q - n \mu_{n,0}^q \right), \tag{2.63}$$

$$C_3^m = 0, \quad C_4^m = 0, \tag{2.64}$$

$$C_5^m = - \sum_{n=2}^{m+1} \sum_{q=0}^{m+1-n} \Theta_{m,n}^q \mu_{n,0}^q. \tag{2.65}$$

Now

$$f(\eta) = \sum_{m=0}^{\infty} f_m(\eta) = \lim_{M \rightarrow \infty} \left[\sum_{m=0}^M a_{m,0}^0 + \sum_{n=1}^{M+1} e^{-n\eta} \left(\sum_{m=n-1}^M \sum_{k=0}^{m+1-n} a_{m,n}^k \eta^k \right) \right], \tag{2.66}$$

$$g(\eta) = \sum_{m=0}^{\infty} g_m(\eta) = \lim_{M \rightarrow \infty} \left[\sum_{n=1}^{M+1} e^{-n\eta} \left(\sum_{m=n-1}^M \sum_{k=0}^{m+1-n} A_{m,n}^k \eta^k \right) \right], \tag{2.67}$$

where

$$a_{m,0}^0 = \chi_m \chi_{m+2} a_{m-1,0}^0 - \sum_{q=0}^m \Psi_{m,1}^q \mu_{1,1}^q - \sum_{n=2}^{m+1} \left[\begin{array}{c} (n-1) \Psi_{m,n}^0 \mu_{n,0}^0 \\ + \sum_{q=1}^{m+1-n} \Psi_{m,n}^q \left((n-1) \mu_{n,0}^q - \mu_{n,1}^q \right) \end{array} \right], \quad (2.68)$$

$$a_{m,0}^k = \chi_m \chi_{m+1-k} a_{m-1,0}^k, \quad 1 \leq k \leq m+1, \quad (2.69)$$

$$a_{m,1}^0 = \chi_m \chi_{m+1} a_{m-1,1}^0 + \sum_{q=0}^m \Psi_{m,1}^q \mu_{1,1}^q + \sum_{n=2}^{m+1} \left\{ n \Psi_{m,n}^0 \mu_{n,0}^0 + \sum_{q=1}^{m+1-n} \Psi_{m,n}^q \left(n \mu_{n,0}^q - \mu_{n,1}^q \right) \right\}, \quad (2.70)$$

$$a_{m,1}^k = \chi_m \chi_{m-k+1} a_{m-1,1}^k + \sum_{q=k-1}^m \Psi_{m,1}^q \mu_{1,k}^q, \quad 1 \leq k \leq m+1, \quad (2.71)$$

$$a_{m,n}^k = \chi_m \chi_{m+2-n-k} a_{m-1,n}^k + \sum_{q=k}^{m+1-n} \Psi_{m,n}^q \mu_{n,k}^q, \quad 2 \leq n \leq m+1, \quad 0 \leq k \leq m+1-n, \quad (2.72)$$

$$A_{m,1}^0 = \chi_m \chi_{m+1} A_{m-1,1}^0 - \sum_{n=2}^{m+1} \sum_{q=0}^{m+1-n} \Theta_{m,n}^q \nu_{n,0}^q, \quad (2.73)$$

$$A_{m,1}^k = \chi_m \chi_{m-k+1} A_{m-1,1}^k + \sum_{q=k-1}^m \Theta_{m,1}^q \nu_{1,k}^q, \quad 1 \leq k \leq m+1, \quad (2.74)$$

$$A_{m,n}^k = \chi_m \chi_{m+2-n-k} A_{m-1,n}^k + \sum_{q=k}^{m+1-n} \Theta_{m,n}^q \nu_{n,k}^q, \quad 2 \leq n \leq m+1, \quad 0 \leq k \leq m+1-n, \quad (2.75)$$

$$a_{0,0}^0 = s-1, \quad a_{0,1}^0 = 1, \quad a_{0,1}^1 = 1. \quad (2.76)$$

2.3 Convergence of the analytic solution

The explicit, analytic expressions given by Eqs. (2.66) and (2.67) contain the auxiliary parameter \hbar . As pointed out by Liao [95] this parameter plays a vital role in finding the convergence region and rate of approximation for the homotopy analysis method. For this purpose the \hbar -curves are plotted for the 25th order of approximations for both f and g in Fig. 2.1. Figure 2.1 clearly indicates that the admissible values of the parameter \hbar are $-0.45 \leq \hbar < -0.1$. Our calculations depict that the series given by Eqs. (2.66) and (2.67) converge in the whole region of η when $\hbar = -0.25$.

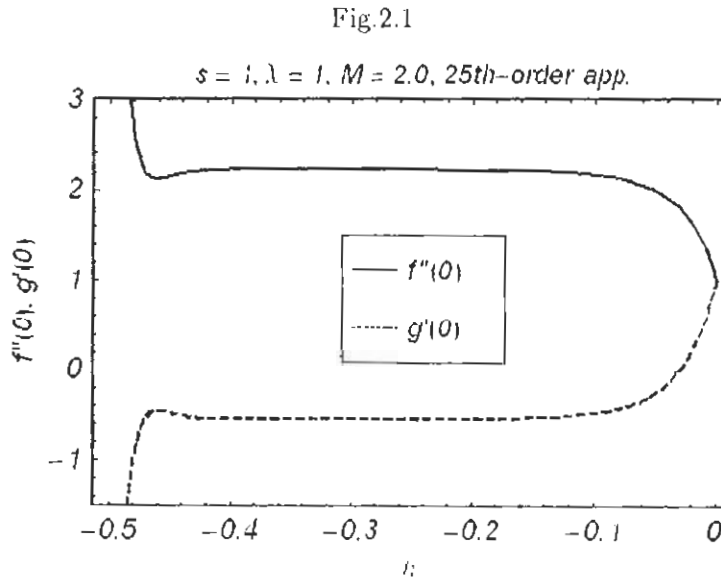


Fig. 2.1. \hbar -curves for 25th order of approximation.

2.4 Results and discussion

The graphs for the functions $f'(\eta)$ and $g(\eta)$ are drawn against η for different values of the parameters M , s and λ . In all cases, panel (a) displays the function f' and (b) shows the function g . It is depicted from Fig. 2.2 (a) that the velocity f' increases and boundary layer thickness decreases by increasing the suction parameter s . This is in accordance with the fact that the suction controls the boundary layer thickness. The effect of s on the velocity g

is similar to that of f' but in this case boundary layer thickness increases as shown in Fig. 2.2 (b). Figure. 2.3(a,b) elucidates that the effect of Hartman number is similar to that of the suction parameter. The effect of rotation parameter is quite opposite when compared with suction parameter and Hartman number as shown in Fig. 2.4(a,b).

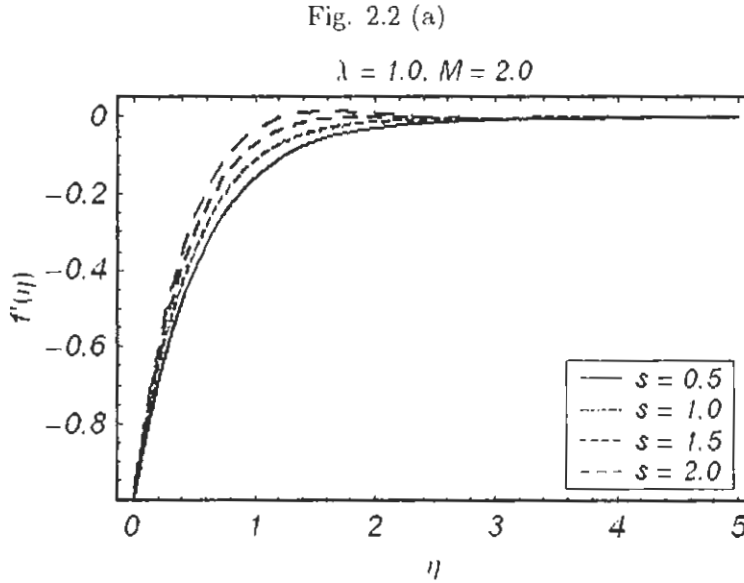


Fig. 2.2(a). Variations of f' by increasing suction parameter s .

Fig. 2.2 (b)

$\lambda = 1.0, M = 2.0$

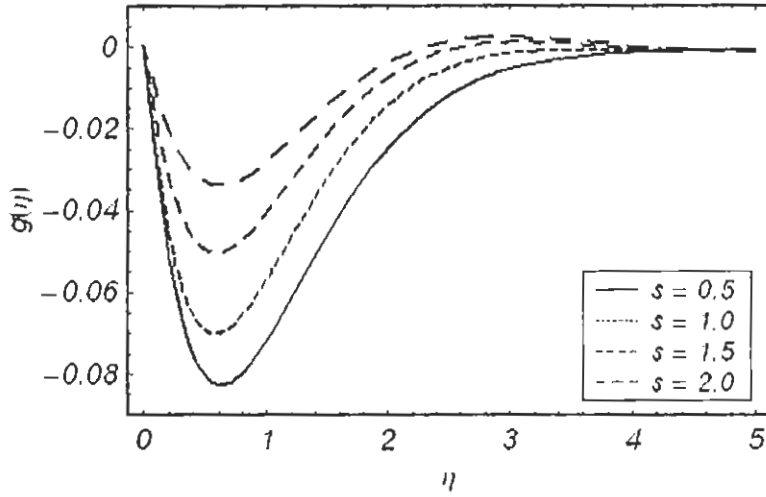


Fig. 2.2(b). Variations of g by increasing suction parameter s .

Fig. 2.3 (a)

$s = 1, \lambda = 1.0$

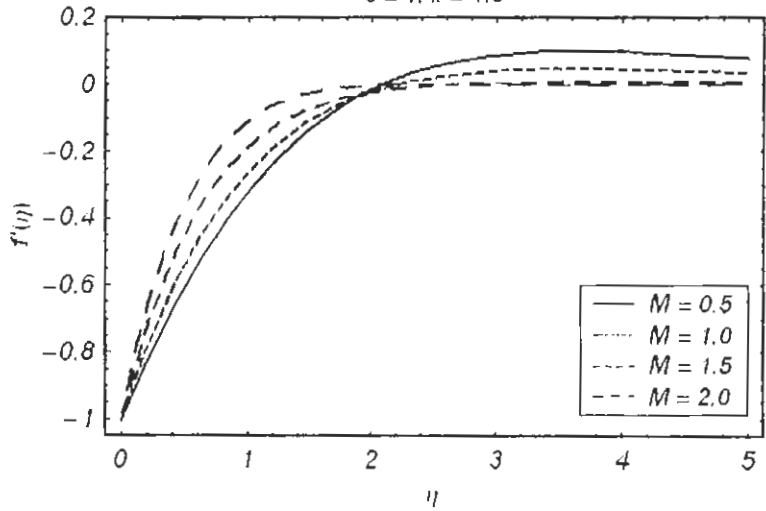


Fig. 2.3 (a). Variations of f' by increasing Hartman number M .

Fig. 2.3 (b)

$$s = 1, \lambda = 1.0$$

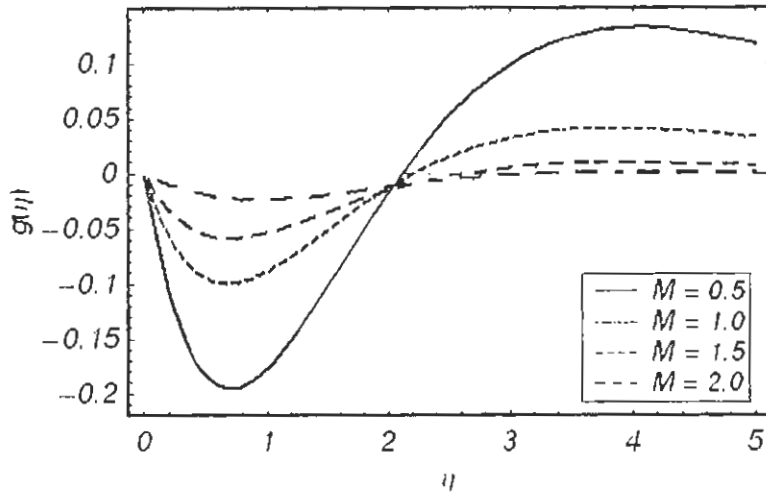


Fig. 2.3 (b). Variations of g by increasing Hartman number M .

Fig. 2.4 (a)

$$s = 1, M = 2.0$$

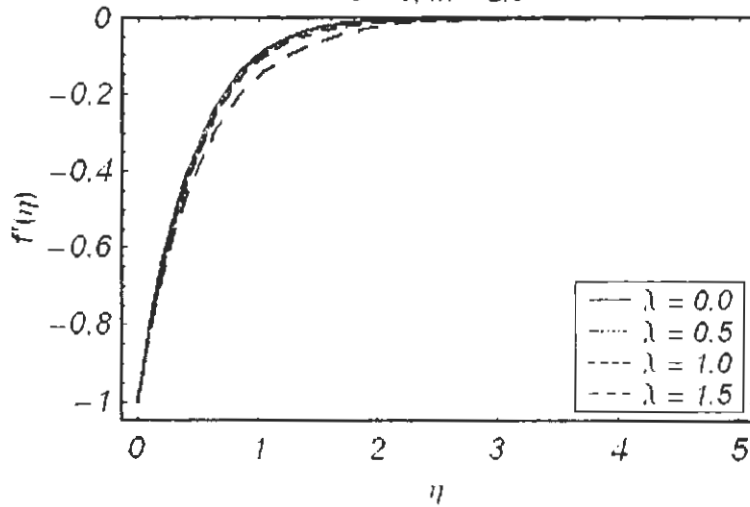


Fig. 2.4 (a). Variations of f' by increasing rotation parameter λ .

Fig.2.4(b)

$s = 1, M = 2.0$

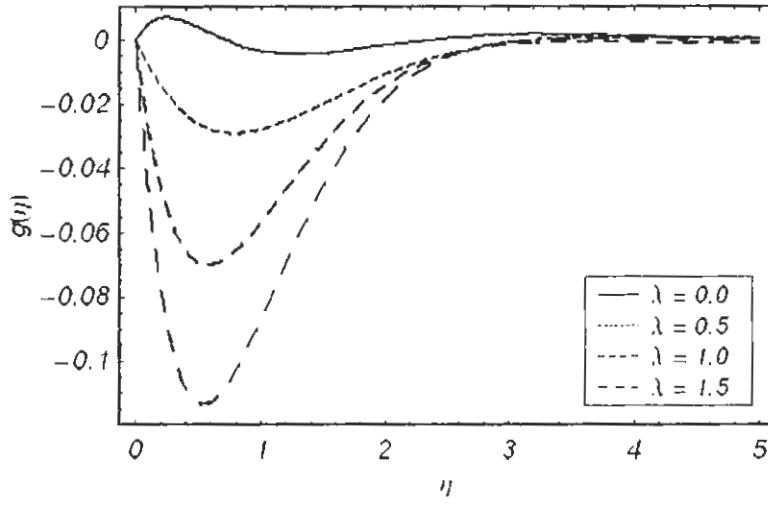


Fig. 2.4 (b). Variations of g by increasing rotation parameter λ .

Chapter 3

Three-dimensional rotating flow induced by a shrinking sheet for suction

The purpose of this chapter is to discuss the three dimensional flow analysis in a rotating frame. The flow between the two plates is engendered by a porous shrinking surface. A homotopy analysis method (HAM) is used to arrive at the similarity solutions of non-linear ordinary differential system. Convergence of the obtained solutions is ensured through proper choice of an auxiliary parameter. Graphs are sketched and discussed for various emerging parameters on the velocity field. Besides that the variations of the wall shear stress are also tabulated and analyzed. Comparison is made amongst the influences of various sundry parameters.

3.1 Description of the problem

Let us consider the steady, incompressible and three-dimensional flow of an electrically conducting viscous fluid between two horizontal parallel plates at $y = \pm h$. Both the fluid and the plates rotate in uniform with a constant angular velocity $\Omega = \Omega \hat{j}$, where \hat{j} is a unit vector in the y -direction. The plate $y = +h$ is rigid and stationary. The flow in the fluid system is generated by shrinking of a porous plate at $y = -h$. The geometry of the problem is shown in

Fig. 1. Making use of the Eqs. (1.3), (1.7) and (1.14) the governing equations are

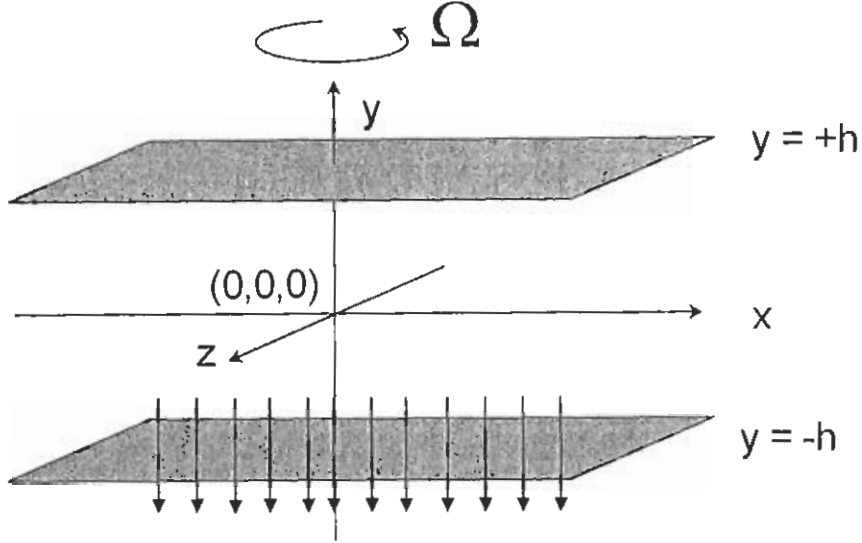


Fig. 3.1. Configuration of the flow.

$$\frac{\partial u}{\partial x} + \frac{\partial v}{\partial y} = 0, \quad (3.1)$$

$$u \frac{\partial u}{\partial x} + v \frac{\partial u}{\partial y} + 2\Omega w = -\frac{1}{\rho} \frac{\partial p^*}{\partial x} + \nu \left[\frac{\partial^2 u}{\partial x^2} + \frac{\partial^2 u}{\partial y^2} \right] - \frac{\sigma B_0^2}{\rho} u, \quad (3.2)$$

$$u \frac{\partial v}{\partial y} = -\frac{1}{\rho} \frac{\partial p^*}{\partial y} + \nu \left[\frac{\partial^2 v}{\partial x^2} + \frac{\partial^2 v}{\partial y^2} \right], \quad (3.3)$$

$$u \frac{\partial w}{\partial x} + v \frac{\partial w}{\partial y} - 2\Omega u = \nu \left[\frac{\partial^2 w}{\partial x^2} + \frac{\partial^2 w}{\partial y^2} \right] - \frac{\sigma B_0^2}{\rho} w. \quad (3.4)$$

The boundary conditions for the problem under consideration are

$$\begin{aligned} u &= -ax, & v &= -V, & w &= 0 & \text{at } y &= -h, \\ u &= 0, & v &= 0, & w &= 0 & \text{at } y &= +h \end{aligned} \quad (3.5)$$

in which u , v and w are the velocity components in x -, y - and z -directions respectively, ρ the density, ν the kinematic viscosity, σ the electrical conductivity, B_0 the magnetic induction, p^*

the modified pressure, $a > 0$ the shrinking constant and $V > 0$ the suction velocity.

Using the following definitions

$$\eta = \frac{y}{h}, \quad u = -axf'(\eta), \quad v = ahf(\eta), \quad w = axg(\eta) \quad (3.6)$$

the incompressibility condition (3.1) is automatically satisfied and Eqs. (3.2) – (3.4) after eliminating the modified pressure become

$$f'''' - M^2 f' - 2K^2 g' - R(f' f'' - f f''') = 0, \quad (3.7)$$

$$g'' - M^2 g + 2K^2 f' - R(f' g - f g') = 0, \quad (3.8)$$

where primes signify the differentiation with respect to η .

The boundary conditions now transform into the following conditions:

$$\begin{aligned} f &= \lambda, & f' &= -1, & g &= 1 & \text{at } \eta &= -1, \\ f &= 0, & f' &= 0, & g &= 0 & \text{at } \eta &= 1, \end{aligned} \quad (3.9)$$

in which the suction parameter λ , the viscosity parameter R , the Hartman number M and the rotation parameter K are

$$\lambda = -\frac{V}{ah}, \quad R = \frac{ah^2}{\nu}, \quad M^2 = \frac{\sigma B_0^2 h^2}{\rho\nu}, \quad K^2 = \frac{\Omega h^2}{\nu}.$$

In the next section we will solve the non-linear system consisting of Eqs. (3.7) – (3.9) by HAM.

3.2 Analytic solution

For the HAM solution of Eqs. (3.7) – (3.9), the initial approximations of f and g and auxiliary operators \mathcal{L}_3 and \mathcal{L}_4 are

$$f_0(\eta) = \left(\frac{\lambda}{2} - \frac{1}{4}\right) + \left(\frac{1-3\lambda}{4}\right)\eta + \frac{\eta^2}{4} + \frac{\lambda-1}{4}\eta^3, \quad (3.10)$$

$$g_0(\eta) = 1 - \eta^2, \quad (3.11)$$

$$\mathcal{L}_3(f) = \frac{d^4 f}{d\eta^4}, \quad (3.12)$$

$$\mathcal{L}_4(f) = \frac{d^2 f}{d\eta^2}. \quad (3.13)$$

It is easy to check that these operators satisfy the following equations:

$$\mathcal{L}_3 [C_6\eta^3 + C_7\eta^2 + C_8\eta + C_9] = 0, \quad (3.14)$$

$$\mathcal{L}_4 [C_{10}\eta + C_{11}] = 0, \quad (3.15)$$

where C_i ($i = 6 - 11$) are arbitrary constants. On the basis of Eqs. (3.7) and (3.8), we introduce the following non-linear operator \mathcal{N}_3 and \mathcal{N}_4 :

$$\begin{aligned} \mathcal{N}_3 [\hat{f}(\eta; q), \hat{g}(\eta; q)] &= \frac{\partial^4 \hat{f}(\eta; q)}{\partial \eta^4} - M^2 \frac{\partial^2 \hat{f}(\eta; q)}{\partial \eta^2} - 2K^2 \frac{\partial \hat{g}(\eta; q)}{\partial \eta} \\ &\quad - R \left(\frac{\partial \hat{f}(\eta; q)}{\partial \eta} \frac{\partial^2 \hat{f}(\eta; q)}{\partial \eta^2} - \hat{f}(\eta; q) \frac{\partial^3 \hat{f}(\eta; q)}{\partial \eta^3} \right), \end{aligned} \quad (3.16)$$

$$\begin{aligned} \mathcal{N}_4 [\hat{g}(\eta; q), \hat{f}(\eta; q)] &= \frac{\partial^2 \hat{g}(\eta; q)}{\partial \eta^2} - M^2 \hat{g}(\eta; q) + 2K^2 \frac{\partial \hat{f}(\eta; q)}{\partial \eta} \\ &\quad - R \left(\frac{\partial \hat{f}(\eta; q)}{\partial \eta} \hat{g}(\eta; q) - \hat{f}(\eta; q) \frac{\partial \hat{g}(\eta; q)}{\partial \eta} \right), \end{aligned} \quad (3.17)$$

where $\hat{f}(\eta; q)$ and $\hat{g}(\eta; q)$ are the kind of mapping functions for $f(\eta)$ and $g(\eta)$ with q serving as an embedding parameter varying in the range $[0, 1]$. Using these operators, we construct the following so-called zero order deformation problems:

Zeroth-order deformation problems

$$(1 - q) \mathcal{L}_3 [\hat{f}(\eta; q) - f_0(\eta y)] = q \hbar_1 \mathcal{N}_3 [\hat{f}(\eta; q)], \quad (3.18)$$

$$\hat{f}(-1; q) = \lambda, \quad \hat{f}'(-1; q) = -1, \quad \hat{f}(1; q) = 0, \quad \hat{f}'(1; q) = 0, \quad (3.19)$$

$$(1 - q) \mathcal{L}_4 [\hat{g}(\eta; q) - g_0(\eta)] = q \hbar_2 \mathcal{N}_4 [\hat{g}(\eta; q), \hat{f}(\eta; q)], \quad (3.20)$$

$$\widehat{g}(-1; q) = 0, \quad \widehat{g}(1; q) = 0, \quad (3.21)$$

where h_1 and h_2 are the auxiliary non-zero parameters. Upon making use of the similar procedure as in the previous chapter, we get the following m th order deformation problems:

The m th-order deformation problems

$$\mathcal{L}_3 [f_m(\eta) - \chi_m f_{m-1}(\eta)] = \hbar_1 \mathcal{R}_{1m}(\eta), \quad (3.22)$$

$$f_m(-1) = f'_m(-1) = f_m(1) = f'_m(1) = 0, \quad (3.23)$$

$$\mathcal{L}_4 [g_m(\eta) - \chi_m g_{m-1}(\eta)] = \hbar_2 \mathcal{R}_{2m}(\eta), \quad (3.24)$$

$$g_m(-1) = g_m(1) = 0, \quad (3.25)$$

$$\mathcal{R}_{1m}(y) = f_{m-1}'''' - M^2 f_{m-1}'' - 2K^2 g'_{m-1} + R \sum_{k=0}^{m-1} [f'_{m-1-k} f''_k - f_{m-1-k} f_k'''], \quad (3.26)$$

$$\mathcal{R}_{2m}(y) = g_{m-1}'' - M^2 g_{m-1} + 2K^2 f'_{m-1} - R \sum_{k=0}^{m-1} [g_{m-1-k} f'_k - g'_{m-1-k} f_k], \quad (3.27)$$

where χ_m is defined in Eq. (1.40).

With the help of MATHEMATICA, the solution of Eqs. (3.22) – (3.25) can be expressed in the form

$$f(\eta) = \sum_{m=0}^{\infty} f_m(\eta) = \lim_{M \rightarrow \infty} \left[\sum_{n=1}^{4M+3} \left(\sum_{m=n-1}^{4M+2} a_{m,n} \eta^n \right) \right], \quad (3.28)$$

$$g(\eta) = \sum_{m=0}^{\infty} g_m(\eta) = \lim_{M \rightarrow \infty} \left[\sum_{n=1}^{4M+2} \left(\sum_{m=n-1}^{4M+1} b_{m,n} \eta^n \right) \right], \quad (3.29)$$

where the coefficients $a_{m,n}$, $b_{m,n}$ of $f(\eta)$ and $g(\eta)$ are obtained as follows

$$a_{m,0} = \chi_m \chi_{4m+1} a_{m-1,0} - \frac{1}{4} \sum_{n=0}^{4m+3} \frac{\Delta_{m,n} [1 + (-1)^n]}{(n+1)(n+2)(n+3)(n+4)},$$

$$a_{m,1} = \chi_m \chi_{4m} a_{m-1,1} + \frac{1}{2} \sum_{n=0}^{4m+3} \frac{\Delta_{m,n} [(-1)^n - \frac{3}{2} ((n+3)(-1)^n + 1)]}{(n+1)(n+2)(n+3)(n+4)},$$

$$\begin{aligned}
a_{m,2} &= \chi_m \chi_{4m-1} a_{m-1,2} - \frac{1}{4} \sum_{n=0}^{4m+3} \frac{\Delta_{m,n} [1 + (-1)^n]}{(n+1)(n+2)(n+3)(n+4)}, \\
a_{m,3} &= \chi_m \chi_{4m-2} a_{m-1,3} - \frac{1}{4} \sum_{n=0}^{4m+3} \frac{\Delta_{m,n} [1 + (-1)^n]}{(n+1)(n+2)(n+3)(n+4)}, \\
a_{m,n} &= \chi_m \chi_{4m-n+1} a_{m-1,n} + \sum_{n=4}^{4m+3} \frac{\Delta_{m,n-4}}{n(n-1)(n-2)(n-3)}, \quad n \geq 4, \\
b_{m,0} &= \chi_m \chi_{4m} b_{m-1,0} - \frac{1}{2} \sum_{n=0}^{4m+2} \frac{\Gamma_{m,n} [1 + (-1)^n]}{(n+1)(n+2)}, \\
b_{m,1} &= \chi_m \chi_{4m-1} b_{m-1,1} - \frac{1}{2} \sum_{n=0}^{4m+2} \frac{\Gamma_{m,n} [1 + (-1)^n]}{(n+1)(n+2)}, \\
b_{m,n} &= \chi_m \chi_{4m-n} b_{m-1,n} + \sum_{n=0}^{4m+2} \frac{\Gamma_{m,n-2}}{n(n-1)}, \quad n \geq 2,
\end{aligned}$$

$$\Delta_{m,n} = \hbar_1 [\chi_{4m-n+1} (f_{m-1,n} - M^2 d_{m-1,n}) - 2K^2 \chi_{4m-n} g_{m-1,n}] + R \chi_{4m-n+4} (\alpha_{m,n} - \beta_{m,n}), \quad (3.30)$$

$$\Gamma_{m,n} = \hbar_2 [\chi_{4m-n} (h_{m-1,n} - M^2 b_{m-1,n}) + 2K^2 \chi_{4m-n+1} c_{m-1,n} - R \chi_{4m-n+3} (\gamma_{m,n} - \delta_{m,n})]. \quad (3.31)$$

$$\begin{aligned}
\alpha_{m,n} &= \sum_{k=0}^{m-1} \sum_{j=\max\{0, n-4m+4k+1\}}^{\min\{n, 4k+3\}} d_{k,j} c_{m-1-k, n-j}, & \beta_{m,n} &= \sum_{k=0}^{m-1} \sum_{j=\max\{0, n-4m+4k+1\}}^{\min\{n, 4k+3\}} a_{k,j} e_{m-1-k, n-j}, \\
\gamma_{m,n} &= \sum_{k=0}^{m-1} \sum_{j=\max\{0, n-4m+4k+1\}}^{\min\{n, 4k+3\}} c_{k,j} g_{m-1-k, n-j}, & \delta_{m,n} &= \sum_{k=0}^{m-1} \sum_{j=\max\{0, n-4m+4k+1\}}^{\min\{n, 4k+3\}} a_{k,j} h_{m-1-k, n-j},
\end{aligned}$$

$$\begin{aligned}
c_{m,n} &= (n+1) a_{m, n+1}, & d_{m,n} &= (n+1) c_{m, n+1}, & e_{m,n} &= (n+1) d_{m, n+1}, \\
f_{m,n} &= (n+1) e_{m, n+1}, & g_{m,n} &= (n+1) b_{m, n+1}, & h_{m,n} &= (n+1) g_{m, n+1},
\end{aligned} \quad (3.32)$$

$$\begin{aligned}
a_{0,0} &= \frac{2\lambda - 1}{4}, & a_{0,1} &= \frac{1 - 3\lambda}{4}, & a_{0,2} &= \frac{1}{4}, \\
a_{0,3} &= \frac{\lambda - 1}{4}, & b_{0,0} &= 1, & b_{0,1} &= 0, & b_{0,2} &= -1.
\end{aligned} \quad (3.33)$$

3.3 Convergence of the HAM solution

Equations (3.28) and (3.29) present the series solutions of the considered flow problem. Here the values of h_1 and h_2 control the convergence region and rate of approximations of the series solutions (3.28) and (3.29). In order to see that whether the series given by Eqs. (3.28) and (3.29) are convergent, we draw h -curves for 25th-order approximation in Fig. 3.2 by taking $h_1 = h_2 = h$. Fig. 3.2 indicates that the range for the admissible values of h is $-1.4 \leq h \leq -0.1$. The series (3.28) and (3.29) converge in the whole region of η when $h = -0.8$. Table 3.1 shows the convergence of $f''(0)$ and $-g'(0)$ by increasing order of approximations.

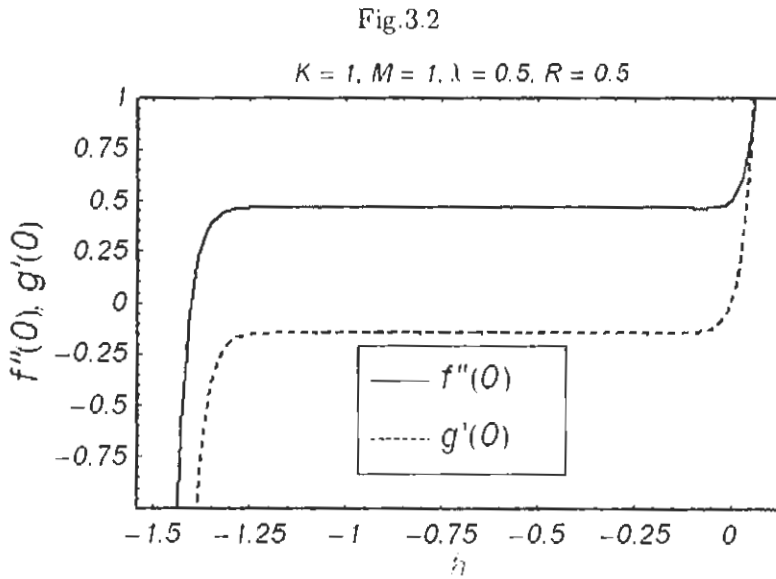


Fig. 3.2. h -curves for the 25th-order of approximation.

order of approximations	$f''(0)$	$-g'(0)$
1	0.440000	0.066666
3	0.433087	0.035714
4	0.432737	0.035382
10	0.432728	0.035386
15	0.432728	0.035386
20	0.432728	0.035386
30	0.432728	0.035386

Table. 3.1. Convergence of HAM solutions for increasing order of approximations.

3.4 Results and discussion

This section looks at the effects of various pertinent parameters on f , f' and g . For this purpose, Figs. 3.3(a, b) – 3.8(a, b) have been plotted for suction parameter λ , the Hartman number M , rotation parameter K and viscosity parameter R . Table 3.2 is prepared for the variations of λ , M and K on the wall shear stress $f''(0)$ and $-g'(0)$.

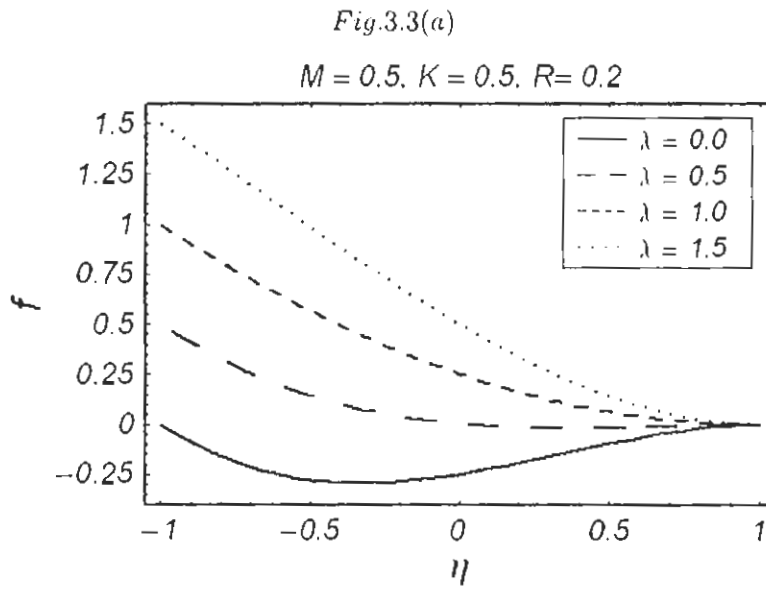


Fig. 3.3 (a). Influence of λ on f at $h = -0.8$.

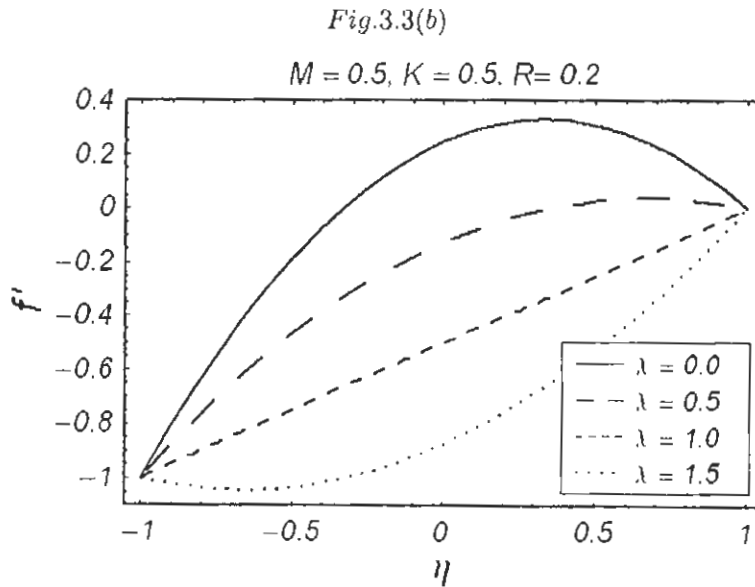


Fig. 3.3 (b). Influence of λ on f' at $h = -0.8$.

Fig.3.4(a)

$\lambda = 0.5, K = 0.5, R = 0.5$

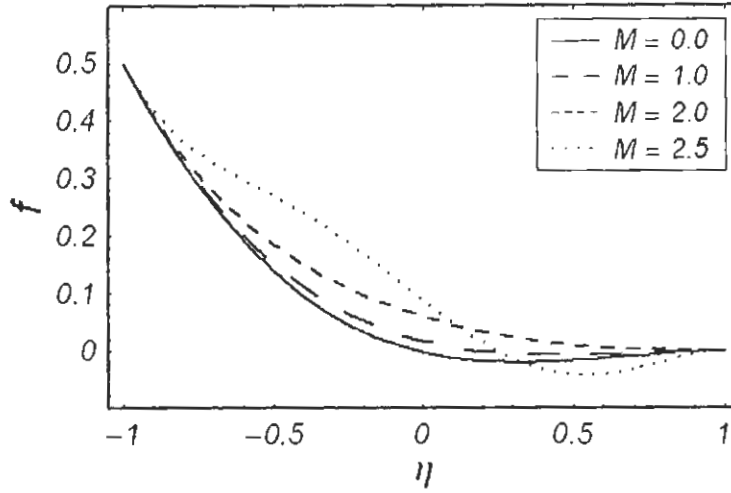


Fig. 3.4 (a). Influence of M on f at $h = -0.8$.

Fig.3.4(b)

$\lambda = 0.5, K = 0.5, R = 0.5$

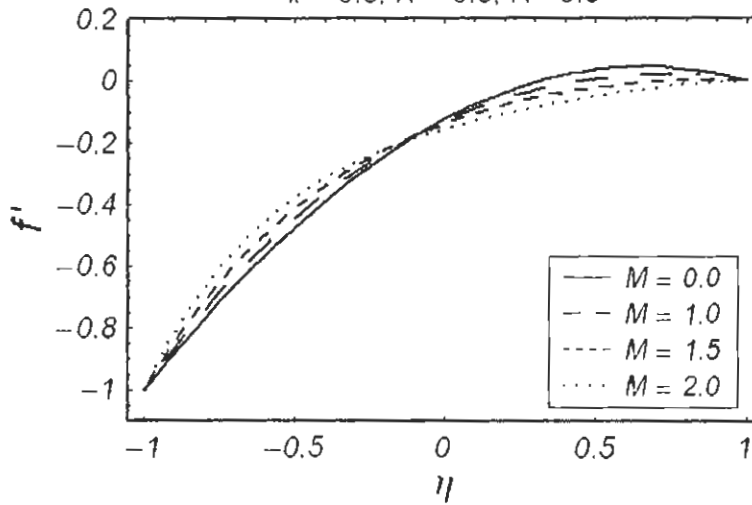


Fig. 3.4 (b). Influence of M on f' at $h = -0.8$.

Fig. 3.5(a)

$\lambda = 0.5, M = 0.5, R = 0.5$

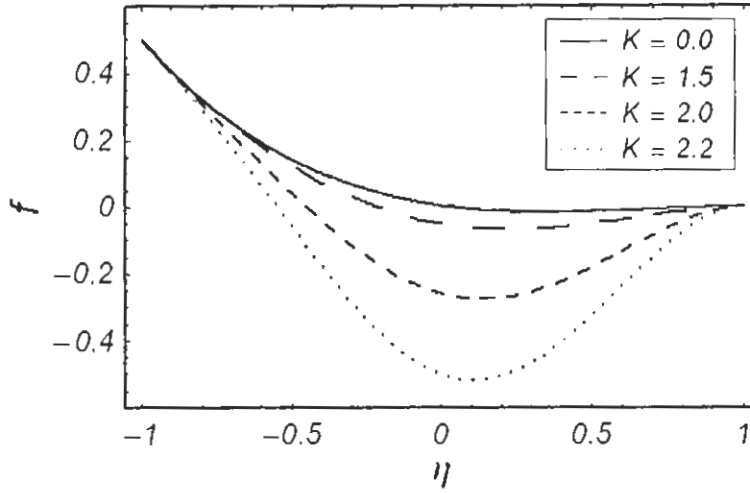


Fig. 3.5 (a). Influence of K on f at $h = -0.8$.

Fig. 3.5(b)

$\lambda = 0.5, M = 0.5, R = 0.5$

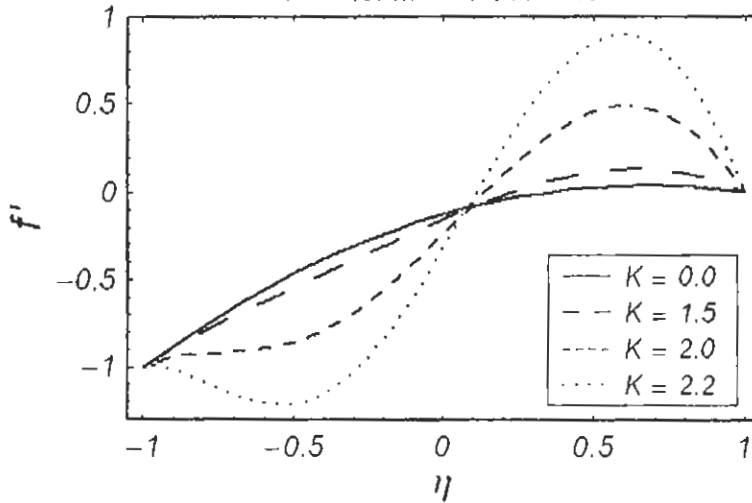


Fig. 3.5 (b). Influence of K on f' at $h = -0.8$.

Fig. 3.6(a)

$\lambda = 0.5, M = 0.3, K = 1.0$

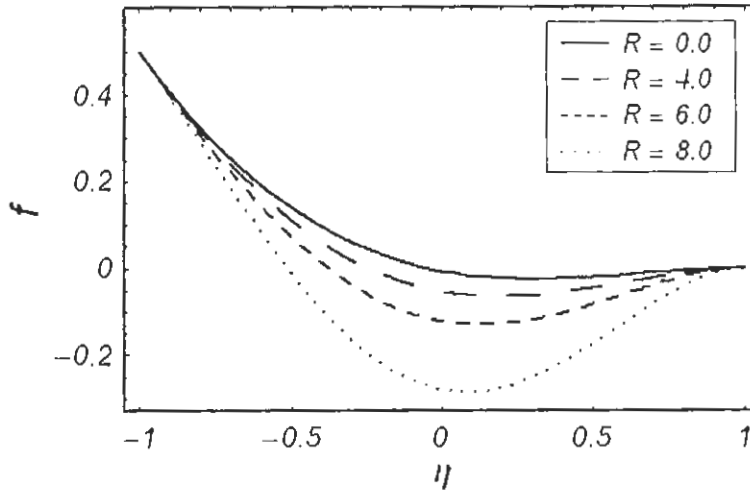


Fig. 3.6 (a). Influence of R on f at $h = -0.8$.

Fig. 3.6(b)

$\lambda = 0.5, M = 0.3, K = 1.0$

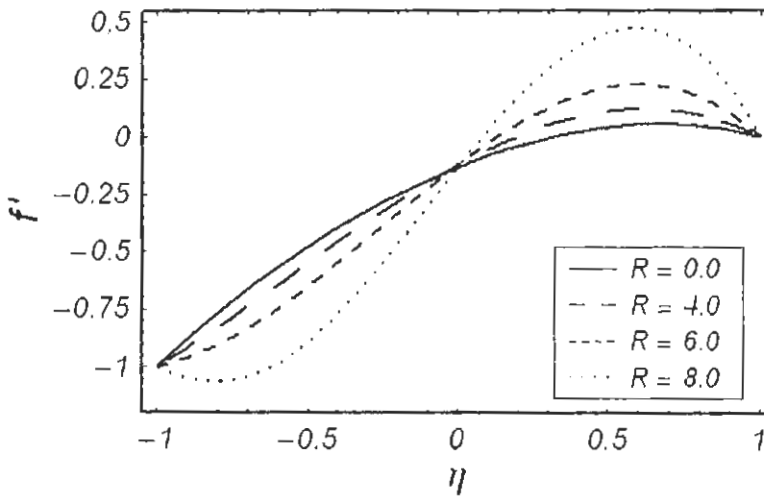


Fig. 3.6 (b). Influence of R on f' at $h = -0.8$.

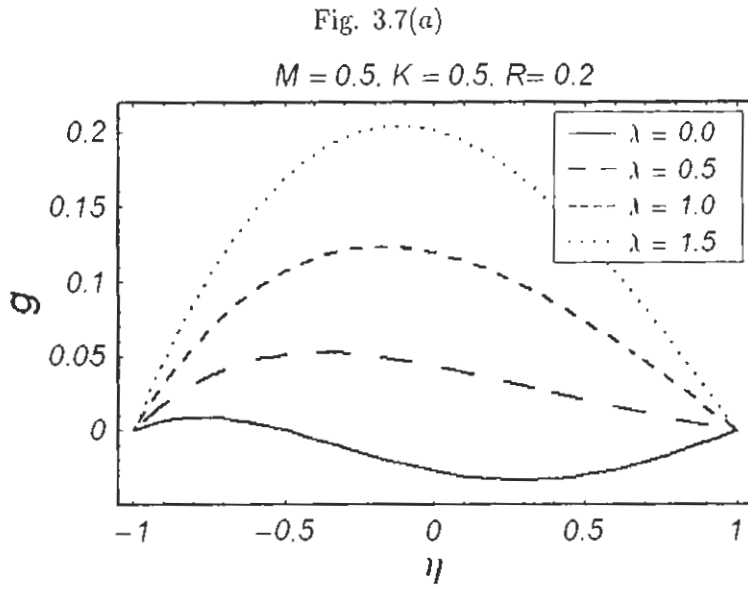


Fig. 3.7 (a). Influence of λ on g at $\hbar = -0.8$.

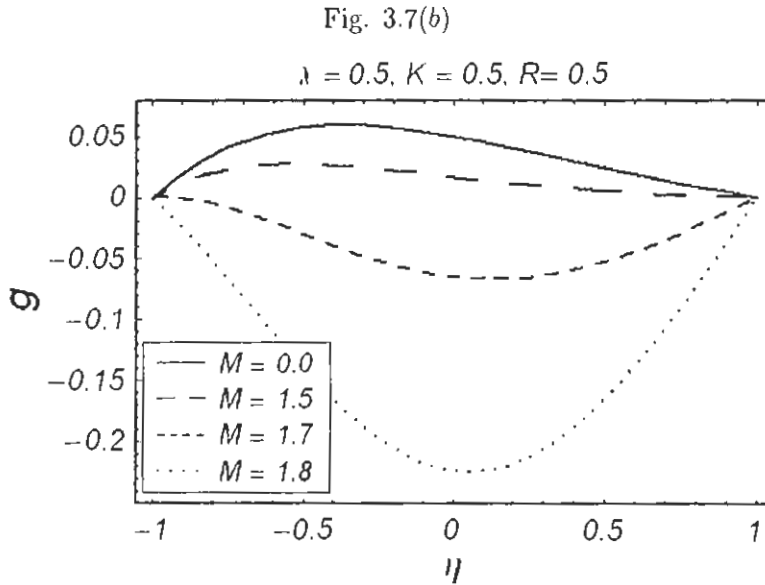


Fig. 3.7 (b). Influence of M on g at $\hbar = -0.8$.

Fig. 3.8(a)

$\lambda = 0.5, M = 0.5, R = 0.5$

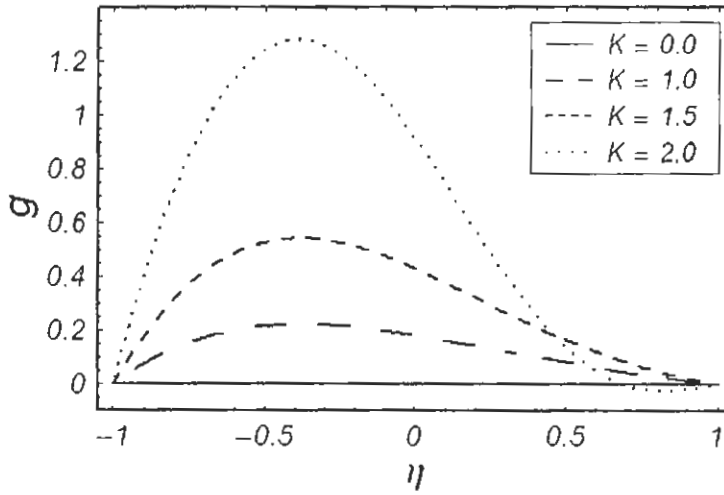


Fig. 3.8 (a). Influence of K on g at $h = -0.8$.

Fig. 3.8(b)

$\lambda = 0.5, M = 0.3, K = 1.0$

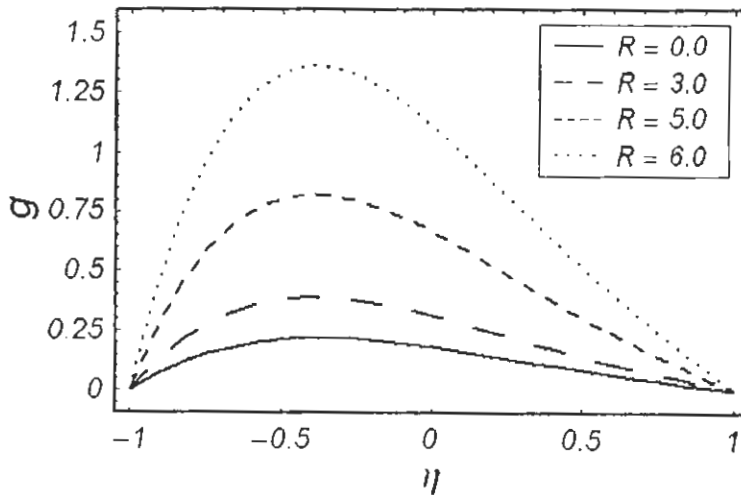


Fig. 3.8 (b). Influence of R on g at $h = -0.8$.

λ	M	K	R	$f''(0)$	$-g'(0)$
0.0	0.5	0.5	0.2	0.492430	0.040333
0.2				0.488033	0.040043
0.5				0.485111	0.040565
0.7				0.485640	0.041582
1.0				0.490199	0.044167
1.5				0.507998	0.051499
2.0				0.538803	0.062959
3.0				0.640577	0.100099
1.0	0.0			0.511361	0.047207
	0.5			0.490199	0.044167
	0.7			0.471027	0.041531
	1.0			0.433631	0.036672
	2.0			0.279041	0.019667
	0.5	0.0		0.487577	0.000000
		0.5		0.490199	0.044167
		0.7		0.497729	0.087368
		1.0		0.531335	0.185574
		1.5		0.759040	0.527306

Table. 3.2. Variations of wall shear stresses $f''(0)$ and $-g'(0)$.

Figs. 3.3(a) – 3.6(b) have been plotted for the effects of λ , M , K and R on the velocity components f and f' . Figs. 3.3(a) and 3.3(b) describe the variation of λ on f and f' , respectively. From Fig. 3.3(a) it is found that f increases as λ increases and f is maximum at the lower plate (shrinking sheet). It is evident from Fig. 3.3(b) that f' decreases when λ increases and f' has large values at the center of the channel. Figs. 3.4(a) and 3.4(b) illustrate the effects of M on f and f' . Fig. 3.4(a) shows that f is an increasing function of M . It is noted from Fig. 3.4(b) that initially f' increases but after the center of the channel it decreases as M increases. Both f and f' show fluctuations when $M > 2$. Figs. 3.5(a) and 3.5(b) show the effects of K on f and f' . It is noted that f is a decreasing function of K and the velocity f is maximum at the

center of the channel. Fig. 3.5(b) indicates that f' increases near the plates and decreases at the center of channel when K increases. Figs. 3.6(a) and 3.6(b) depict the effects of viscosity parameter R on f and f' . It is observed from these Figs. that both f and f' have similar results when compared with Figs. 3.5(a) and 3.5(b), but this change is larger in case of rotation K .

In order to see the effects of λ , M , K and R on g , the Figs. 3.7(a) – 3.8(b) are made. Fig. 3.7(a) elucidates the effects of λ on g . It is found that g is an increasing function of λ but this increment is larger at the centre of the channel as compared with at the plates. Fig. 3.7(b) displays the effects of M on g . From this Fig. it is evident that g has quite opposite behavior when compared with λ . Fig. 3.8(a) shows the effects of rotation K on g . It is noted that g increases with K and near the shrinking sheet (lower plate $\eta = -1$) it has maximum values. Fig. 3.8(b) illustrates the effects of R on g . Fig. 3.8(b) shows that g has similar behavior for large R when compared with the case of K . However this change is slightly larger in case of R .

In order to see the variations of wall shear stress $f''(0)$ and $-g'(0)$ for different values of λ , M , K and R , we prepared Table 3.2. It is observed that $f''(0)$ initially decreases by increasing λ but $f''(0)$ increases after $\lambda = 0.5$. However $-g'(0)$ increases when λ increases. The magnitude of both $f''(0)$ and $-g'(0)$ decreases when M increases and have quite opposite results for large K .

Chapter 4

Homotopy analysis for the rotating flow over a non-linear stretching surface

The object of this chapter is to investigate the steady, rotating flow of an incompressible viscous fluid due to the non-linear stretching of a sheet. An electrically conducting fluid fills the porous half-space. The momentum equation leads to a non-linear boundary value problem by means of an exact similarity transformations. Analytic solutions of the resulting problem is provided using the homotopy analysis method (HAM). Expressions of velocity components are developed and discussed. A comparison is also made with the existing result and an excellent agreement is noted.

4.1 Problem formulation

We consider the magnetohydrodynamic (MHD) flow induced in a semi-infinite expanse ($z > 0$). An incompressible viscous fluid filling the half space is bounded by a stretching surface (at $z = 0$). The fluid is electrically conducting under the action of a uniform external applied magnetic field \mathbf{B}_0 normal to the stretching surface i.e. along the z -axis. Let (u, v, w) be the velocity components in the directions of the Cartesian coordinates (x, y, z) respectively and the system rotates about the z -axis.

The equations which govern the MHD rotating flow are Eq. (1.7) and the following equations:

$$\rho[(\mathbf{V} \cdot \nabla)\mathbf{V} + 2\boldsymbol{\Omega} \times \mathbf{V} + \boldsymbol{\Omega} \times (\boldsymbol{\Omega} \times \mathbf{r})] = \nabla \cdot \boldsymbol{\tau} + \mathbf{J} \times \mathbf{B} - \frac{\phi\mu}{k}\mathbf{V}, \quad (4.1)$$

in which $\mathbf{V} = (u, v, w)$ is the velocity vector, $\boldsymbol{\tau}$ is the Cauchy stress tensor, ρ is the density, ϕ and k are the porosity and permeability of the porous medium, respectively. \mathbf{J} is the current density, \mathbf{B} is the total magnetic field so that $\mathbf{B} = \mathbf{B}_0 + \mathbf{b}$, \mathbf{b} is the induced magnetic field. In absence of displacement currents, the Maxwell equations and generalized Ohms' law are

$$\nabla \cdot \mathbf{B} = 0, \quad \nabla \times \mathbf{B} = \mu_m \mathbf{J}, \quad \nabla \times \mathbf{E} = 0. \quad (4.2)$$

$$\mathbf{J} = \sigma(\mathbf{E} + \mathbf{V} \times \mathbf{B}), \quad (4.3)$$

where μ_m is the magnetic permeability, \mathbf{E} is the electric field and σ is the electrical conductivity. In the present analysis, we make the following assumptions:

- The quantities ρ , μ_m and σ are constant.
- The magnetic field \mathbf{B} is perpendicular to the velocity field \mathbf{V} . The induced magnetic field is negligible. This assumption is realistic when the magnetic Reynolds number is small [2].
- No external electric field is applied and the effect of polarization of the ionized fluid is negligible. We also assume that the electric field $\mathbf{E} = \mathbf{0}$. In view of above considerations, the Lorentz force $\mathbf{J} \times \mathbf{B}$ takes the following form:

$$\mathbf{J} \times \mathbf{B} = -\sigma B_0^2(u, v, 0). \quad (4.4)$$

For an incompressible steady MHD rotating flow of a viscous fluid in a porous medium, Eqs. (1.3), (1.7), (4.1) and (4.4) yield

$$\frac{\partial u}{\partial x} + \frac{\partial v}{\partial y} + \frac{\partial w}{\partial z} = 0. \quad (4.5)$$

$$\left(u \frac{\partial}{\partial x} + v \frac{\partial}{\partial y} + w \frac{\partial}{\partial z}\right) u - 2\Omega v = -\frac{1}{\rho} \frac{\partial \bar{p}}{\partial x} + \nu \left(\frac{\partial^2}{\partial x^2} + \frac{\partial^2}{\partial y^2} + \frac{\partial^2}{\partial z^2}\right) u - \frac{\sigma B_0^2}{\rho} u - \frac{\phi \nu}{k} u, \quad (4.6)$$

$$\left(u \frac{\partial}{\partial x} + v \frac{\partial}{\partial y} + w \frac{\partial}{\partial z}\right) v + 2\Omega u = -\frac{1}{\rho} \frac{\partial \bar{p}}{\partial y} + \nu \left(\frac{\partial^2}{\partial x^2} + \frac{\partial^2}{\partial y^2} + \frac{\partial^2}{\partial z^2}\right) v - \frac{\sigma B_0^2}{\rho} v - \frac{\phi \nu}{k} v, \quad (4.7)$$

$$\left(u \frac{\partial}{\partial x} + v \frac{\partial}{\partial y} + w \frac{\partial}{\partial z}\right) w = -\frac{1}{\rho} \frac{\partial \bar{p}}{\partial z} + \nu \left(\frac{\partial^2}{\partial x^2} + \frac{\partial^2}{\partial y^2} + \frac{\partial^2}{\partial z^2}\right) w - \frac{\phi \nu}{k} w, \quad (4.8)$$

where ν is the kinematic viscosity and \bar{p} is the modified pressure including the centrifugal term.

The boundary conditions for the flow induced by the non-linear stretching are

$$u = cx^b, \quad v = 0, \quad w = 0 \quad \text{at } z = 0, \quad (4.9)$$

$$u \rightarrow 0, \quad v \rightarrow 0, \quad \text{as } z \rightarrow \infty, \quad (4.10)$$

where c and b are constants. Based use of the following transformations

$$\begin{aligned} u &= cx^b f'(\eta), \quad v = cx^b g(\eta), \quad \eta = \sqrt{\frac{c(b+1)}{2\nu}} x^{\frac{b-1}{2}} z, \\ w &= -\sqrt{\frac{c\nu(b+1)}{2}} x^{\frac{b-1}{2}} \left[f(\eta) + \frac{b-1}{b+1} \eta f'(\eta) \right] \end{aligned} \quad (4.11)$$

Eq. (4.5) is identically satisfied and Eqs. (4.6) – (4.8) reduce to

$$f'''(\eta) - \frac{2b}{b+1} f'^2(\eta) + f(\eta) f''(\eta) + \frac{4\lambda}{b+1} g(\eta) - M^2 f'(\eta) - \vartheta f'(\eta) = 0, \quad (4.12)$$

$$g''(\eta) - \frac{2b}{b+1} g(\eta) f'(\eta) + g'(\eta) f(\eta) - \frac{4\lambda}{b+1} f'(\eta) - M^2 g(\eta) - \vartheta g(\eta) = 0, \quad (4.13)$$

with the boundary conditions

$$f(0) = 0, \quad f'(0) = 1, \quad g(0) = 0, \quad (4.14)$$

$$f' \rightarrow 0, \quad g \rightarrow 0 \quad \text{as } \eta \rightarrow \infty, \quad (4.15)$$

where primes indicate differentiation with respect to η and

$$M^2 = \frac{2\sigma B_0^2}{c\rho(b+1)x^{b-1}}, \quad \lambda = \frac{\Omega}{cx^{b-1}}, \quad \vartheta = \frac{2\nu\phi}{ck(b+1)x^{b-1}}, \quad (4.16)$$

in which M is the local Hartman number, λ is local rotation parameter and ϑ is the local porosity parameter. The shear stress at the surface in x and y directions are

$$\tau_{xz} = c\mu \sqrt{\frac{c(b+1)}{2\nu}} x^{\frac{3b-1}{2}} f''(0), \quad (4.17)$$

$$\tau_{yz} = c\mu \sqrt{\frac{c(b+1)}{2\nu}} x^{\frac{3b-1}{2}} g'(0). \quad (4.18)$$

We now proceed to find an analytic solution of the problem consisting of Eqs. (4.12) – (4.15) in the next section by means of homotopy analysis method (HAM).

4.2 HAM solution of the problem

Here we choose the initial approximations

$$f_0(\eta) = 1 - e^{-\eta}, \quad g_0(\eta) = \eta e^{-\eta} \quad (4.19)$$

and the auxiliary linear operators are defined in equation (2.10) which satisfies the condition (2.11). Denoting $q \in [0, 1]$ the embedding parameter and \hbar_3, \hbar_4 the nonzero auxiliary parameters, we have the following zeroth order problem:

$$(1 - q) \mathcal{L}_1 [F(\eta, q) - f_0(\eta)] = q\hbar_3 \mathcal{N}_5 [F(\eta, q), G(\eta, q)], \quad (4.20)$$

$$(1 - q) \mathcal{L}_2 [G(\eta, q) - g_0(\eta)] = q\hbar_4 \mathcal{N}_6 [F(\eta, q), G(\eta, q)]. \quad (4.21)$$

$$F(0, q) = 0, \quad F'(0, q) = 0, \quad F'(\infty, q) = 0, \quad G(0, q) = 0 \text{ and } G(\infty, q) = 0. \quad (4.22)$$

In above equations

$$\begin{aligned} \mathcal{N}_5 [F(\eta, q), G(\eta, q)] = & \frac{\partial^3 F(\eta, q)}{\partial \eta^3} - \frac{2b}{b+1} \left(\frac{\partial F(\eta, q)}{\partial \eta} \right)^2 + F(\eta, q) \frac{\partial^2 F(\eta, q)}{\partial \eta^2} + \frac{4\lambda}{b+1} G(\eta, q) \\ & - M^2 \frac{\partial F(\eta, q)}{\partial \eta} - \vartheta \frac{\partial F(\eta, q)}{\partial \eta}, \end{aligned} \quad (4.23)$$

$$\begin{aligned} \mathcal{N}_6 [F(\eta, q), G(\eta, q)] = & \frac{\partial^2 G(\eta, q)}{\partial \eta^2} - \frac{2b}{b+1} G(\eta, q) \frac{\partial F(\eta, q)}{\partial \eta} + F(\eta, q) \frac{\partial G(\eta, q)}{\partial \eta} - \frac{4\lambda}{b+1} \frac{\partial F(\eta, q)}{\partial \eta} \\ & - M^2 G(\eta, q) - \vartheta G(\eta, q). \end{aligned} \quad (4.24)$$

For $q = 0$ and $q = 1$, one gets

$$F(\eta, 0) = f_0(\eta), \quad G(\eta, 0) = g_0(\eta) \quad \text{and} \quad F(\eta, 1) = f(\eta), \quad G(\eta, 1) = g(\eta). \quad (4.25)$$

When q increases from 0 to 1, then $F(\eta, q), G(\eta, q)$ varies from the initial guesses $f_0(\eta), g_0(\eta)$ to the solution $f(\eta), g(\eta)$. The problems at the m th order deformation problem are

$$\mathcal{L}_1 [f_m(\eta) - \chi_m f_{m-1}(\eta)] = \hbar_3 \mathcal{R}_3(\eta), \quad (4.26)$$

$$\mathcal{L}_2 [g_m(\eta) - \chi_m g_{m-1}(\eta)] = \hbar_4 \mathcal{R}_4(\eta), \quad (4.27)$$

$$f_m(0) = 0, \quad f'_m(0) = 0, \quad g_m(0) = 0, \quad f'_m(\infty) \rightarrow 0 \quad \text{and} \quad g_m(\infty) \rightarrow 0. \quad (4.28)$$

in which

$$\begin{aligned} \mathcal{R}_3(\eta) = & \frac{d^3 f_{m-1}}{d\eta^3} - \frac{2b}{b+1} \sum_{k=0}^{m-1} \frac{df_{m-1-k}}{d\eta} \frac{df_k}{d\eta} + \sum_{k=0}^{m-1} f_{m-1-k} \frac{d^2 f_k}{d\eta^2} \\ & + \frac{4\lambda}{n+1} g_{m-1} - M^2 \frac{df_{m-1}}{d\eta} - \vartheta \frac{df_{m-1}}{d\eta}, \end{aligned} \quad (4.29)$$

$$\begin{aligned} \mathcal{R}_4(\eta) = & \frac{d^2 g_{m-1}}{d\eta^2} - \frac{2b}{b+1} \sum_{k=0}^{m-1} g_{m-1-k} \frac{df_k}{d\eta} + \sum_{k=0}^{m-1} f_{m-1-k} \frac{dg_k}{d\eta} \\ & - \frac{4\lambda}{b+1} \frac{df_{m-1}}{d\eta} - M^2 g_{m-1} - \vartheta g_{m-1}, \end{aligned} \quad (4.30)$$

where χ_m is defined in Eq. (1.40). In order to solve the above equations upto first few order of approximations, the symbolic computation software MATHEMATICA is used and obtain the following series solutions:

$$f_m(\eta) = \sum_{n=0}^{m+1} \sum_{q=0}^{m+1-n} a_{m,n}^q \eta^q e^{-n\eta}, \quad g_m(\eta) = \sum_{n=0}^{m+1} \sum_{q=0}^{m+1-n} b_{m,n}^q \eta^q e^{-n\eta}, \quad m \geq 0. \quad (4.31)$$

Inserting Eq. (4.31) into Eqs. (4.26) and (4.27) we get the following recurrence formulas for the coefficients $a_{m,n}^q$ and $b_{m,n}^q$ of $f_m(z)$ and $g_m(z)$ as follows for $m \geq 1$, $0 \leq n \leq m+1$

$$a_{m,0}^0 = \chi_m \chi_{m+2} a_{m-1,0}^0 - \sum_{q=0}^m \Delta_{m,0}^q \mu_{1,1}^q - \sum_{n=2}^{m+1} \sum_{q=0}^{m+1-n} \Delta_{m,n}^q (\mu_{n,1}^q - (n-1)\mu_{n,0}^q), \quad (4.32)$$

$$a_{m,1}^0 = \chi_m \chi_{m+1} a_{m-1,1}^0 - \sum_{q=0}^m \Delta_{m,1}^q \mu_{1,1}^q + \sum_{n=2}^{m+1} \sum_{q=0}^{m+1-n} \Delta_{m,n}^q (\mu_{n,1}^q - n\mu_{n,0}^q), \quad (4.33)$$

$$\begin{aligned} a_{m,n}^k &= \chi_m \chi_{m+2-n} \lambda_{m+2-n-k} a_{m-1,n}^k + \sum_{q=0}^{m+1-n} \Delta_{m,n}^q \mu_{n,k}^q \\ &\quad - \sum_{n=2}^{m+1} \sum_{q=0}^{m+1-n} \Delta_{m,n}^q (\mu_{n,1}^q - (n-1)\mu_{n,0}^q), \end{aligned} \quad (4.34)$$

$1 \leq n \leq m+1, \quad 1 \leq k \leq m+1-n,$

$$b_{m,1}^0 = \chi_m \chi_{m+1} b_{m-1,1}^0 - \sum_{n=2}^{m+1} \sum_{q=0}^{m+1-n} \Gamma_{m,n}^q \mu_{n,0}^q, \quad (4.35)$$

$$\begin{aligned} b_{m,n}^k &= \chi_m \chi_{m+2-n} \chi_{m+2-n-k} b_{m-1,n}^k + \sum_{q=0}^{m+1-n} \Gamma_{m,n}^q \mu_{n,k}^q, \\ 1 &\leq n \leq m+1, \quad 0 \leq k \leq 2n, \end{aligned} \quad (4.36)$$

$$\Delta_{m,n}^q = h_3 \left[\begin{aligned} &\chi_{m+2-n} \chi_{m+2-n-q} \left\{ a 3_{m-1,n}^q + \frac{4\lambda}{b+1} b_{m-1,n}^q - (M^2 + \vartheta) a 1_{m-1,n}^q \right\} \\ &\quad + \left\{ \beta_{m,n}^q - \frac{2b}{b+1} \alpha_{m,n}^q \right\} \end{aligned} \right], \quad (4.37)$$

$$\Gamma_{m,n}^q = h_4 \left[\begin{aligned} &\chi_{m+2-n} \chi_{m+2-n-q} \left\{ b 2_{m-1,n}^q - \frac{4\lambda}{b+1} a 1_{m-1,n}^q - (M^2 + \vartheta) b_{m-1,n}^q \right\} \\ &\quad + \left\{ \gamma_{m,n}^q - \frac{2b}{b+1} \delta_{m,n}^q \right\} \end{aligned} \right]. \quad (4.38)$$

Here the coefficients $\alpha_{m,n}^q$, $\beta_{m,n}^q$, $\gamma_{m,n}^q$ and $\delta_{m,n}^q$ where $m \geq 1$, $0 \leq n \leq m+1$ are

$$\alpha_{m,n}^q = \sum_{k=0}^{m-1} \sum_{i=\max\{0, n+k-m\}}^{\min\{n, k+1\}} \sum_{j=\max\{0, q+1+n-i-2(m-k)\}}^{\min\{q, 2k+1-i\}} a 1_{m-1-k, n-i}^{q-j} a 1_{k,i}^j, \quad (4.39)$$

$$\beta_{m,n}^q = \sum_{k=0}^{m-1} \sum_{i=\max\{0,n+k-m\}}^{\min\{n,k+1\}} \sum_{j=\max\{0,q+1+n-i-2(m-k)\}}^{\min\{q,2k+1-i\}} \alpha_{m-1-k,n-i}^{q-j} \alpha_{k,i}^j, \quad (4.40)$$

$$\gamma_{m,n}^q = \sum_{k=0}^{m-1} \sum_{i=\max\{0,n+k-m\}}^{\min\{n,k+1\}} \sum_{j=\max\{0,q+1+n-i-2(m-k)\}}^{\min\{q,2k+1-i\}} \alpha_{m-1-k,n-i}^{q-j} b_{k,i}^j, \quad (4.41)$$

$$\delta_{m,n}^q = \sum_{k=0}^{m-1} \sum_{i=\max\{0,n+k-m\}}^{\min\{n,k+1\}} \sum_{j=\max\{0,q+1+n-i-2(m-k)\}}^{\min\{q,2k+1-i\}} \alpha_{m-1-k,n-i}^{q-j} b_{k,i}^j, \quad (4.42)$$

$$a1_{m,n}^q = (q+1) a_{m,n}^{q+1} - n a_{m,n}^q, \quad a2_{m,n}^q = (q+1) a1_{m,n}^{q+1} - n a1_{m,n}^q, \quad (4.43)$$

$$a3_{m,n}^q = (q+1) a2_{m,n}^{q+1} - n a2_{m,n}^q, \quad (4.44)$$

$$b1_{m,n}^q = (q+1) b_{m,n}^{q+1} - n b_{m,n}^q, \quad b2_{m,n}^q = (q+1) b1_{m,n}^{q+1} - n b1_{m,n}^q, \quad (4.45)$$

where $\mu_{1,k}^q$, $\mu_{n,k}^q$, $\mu1_{1,k}^q$ and $\mu1_{n,k}^q$ are given in Eqs. (2.50), (2.54), (2.57) and (2.59). With the above recurrence formulas, we can calculate all the coefficients $a_{m,n}^q$ and $b_{m,n}^q$ using only the first few

$$a_{0,0}^0 = 1, \quad a_{0,1}^0 = -1, \quad b_{0,1}^1 = 1 \quad (4.46)$$

given by the initial guess approximations for the solutions $f(\eta)$ and $g(\eta)$ in Eq. (4.19). The corresponding M th-order approximations of Eqs. (4.20) – (4.22) are

$$\sum_{m=0}^M f_m(\eta) = \sum_{m=0}^M a_{m,0}^0 + \sum_{n=1}^{M+1} e^{-n\eta} \left(\sum_{m=n-1}^M \sum_{q=0}^{m+1-n} a_{m,n}^q \eta^q \right), \quad (4.47)$$

$$\sum_{m=0}^M g_m(\eta) = \sum_{m=0}^M b_{m,0}^0 + \sum_{n=1}^{M+1} e^{-n\eta} \left(\sum_{m=n-1}^M \sum_{q=0}^{m+1-n} b_{m,n}^q \eta^q \right) \quad (4.48)$$

and thus the explicit analytic solutions are

$$f(\eta) = \sum_{m=0}^{\infty} f_m(\eta) = \lim_{M \rightarrow \infty} \left[\sum_{m=0}^M a_{m,0}^0 + \sum_{n=1}^{M+1} e^{-n\eta} \left(\sum_{m=n-1}^M \sum_{q=0}^{m+1-n} a_{m,n}^q \eta^q \right) \right], \quad (4.49)$$

$$g(\eta) = \sum_{m=0}^{\infty} g_m(\eta) = \lim_{M \rightarrow \infty} \left[\sum_{m=0}^M b_{m,0}^0 + \sum_{n=1}^{M+1} e^{-n\eta} \left(\sum_{m=n-1}^M \sum_{q=0}^{m+1-n} b_{m,n}^q \eta^q \right) \right]. \quad (4.50)$$

4.3 Convergence of the analytic solution

The explicit analytic solutions in Eqs. (4.49) and (4.50) contains \hbar_3 and \hbar_4 which give the convergence region and rate of approximation for the HAM solution. The reader is referred to [95] (pp. 31–33) for the detailed discussion regarding the role of auxiliary parameters on the convergence region. Also a theorem similar to the convergence theorem 2.1 (pp. 18 and 19 of reference [95]) can easily be proved for the problem under consideration. In Fig. 4.1(a, b), the \hbar -curves are plotted for 5th and 15th order of approximations for the dimensionless velocity components f' and g when $b = 0.1$, $\lambda = 0.1$, $M = 0.5$ and $\vartheta = 0.5$. From Fig. 4.1(a), we note that the range for the admissible values of \hbar_3 is $-1.7 \leq \hbar_3 \leq -0.4$ as shown by the 15th order of approximations. Fig. 4.1(b) shows that the range for the admissible values of \hbar_4 is also $-1.5 \leq \hbar_4 \leq -0.4$. It can be further observed from Fig. 4.1(a, b) that the range for the admissible values of \hbar_3 and \hbar_4 increases with increase of the order of approximations. As pointed out by Liao [95] we can select any value of \hbar_i ($i = 3, 4$) from the admissible range of \hbar_i ($i = 3, 4$) for which we can get convergent solution. Table 4.1 shows that the value of $\hbar_3 = \hbar_4 = -1$ leads to the divergent solution when $b = 7$, $M = 0.5$, $\lambda = 0.1$, $\vartheta = 0.5$. Similarly we determined that the solution diverge for the values of \hbar_3 and \hbar_4 when $b = 1.5$, $M = 1.5$, $\lambda = 0.1$, $\vartheta = 0.0, 0.2, 0.5, 0.7, 1.0$ and $b = 1.5$, $M = 1.5$, $\lambda = 0.0, 0.2, 0.5, 0.7, 1.0$, $\vartheta = 0.1$. However when $\hbar_3 = \hbar_4 = -0.75$ the series solution converges for all different values of the pertinent parameters. Table 4.2 shows the $\{m, m\}$ homotopy-Padé approximation when $b = 7$, $M = 0.5$, $\lambda = 0.1$, $\vartheta = 0.5$. Comparison of HAM solution at $\hbar_3 = \hbar_4 = -0.75$ of Table 4.1 alongwith the homotopy-Padé approximation of Table 4.2 makes sure that the homotopy-Padé approximation converges rapidly. Our calculations result that the series solutions in Eqs. (4.49) and (4.50) converge in the whole region of η when $\hbar_3 = \hbar_4 = \hbar = -0.75$.

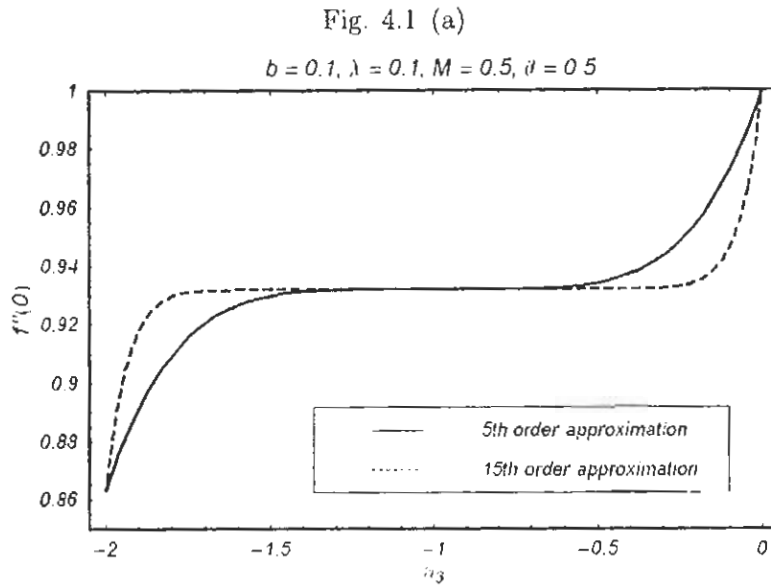


Fig. 4.1 (a). h -curves are plotted for 5th and 15th order of approximations for $f''(0)$.

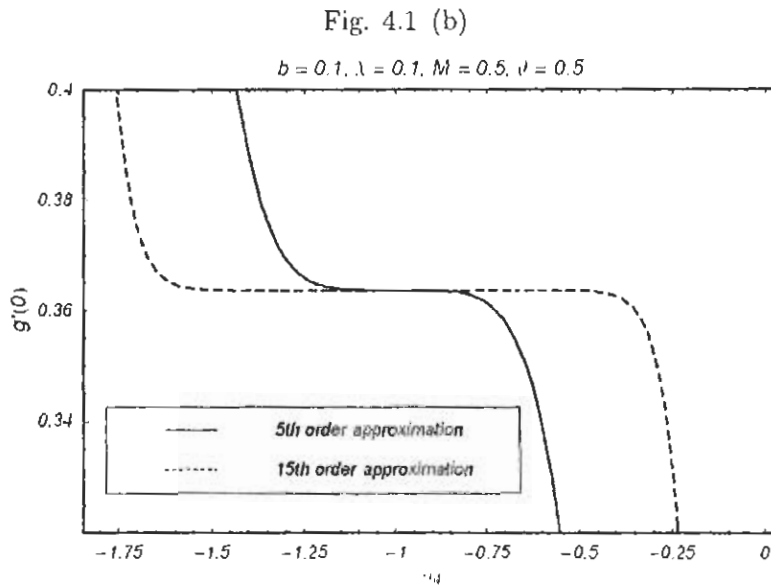


Fig. 4.1 (b). h -curves are plotted for 5th and 15th order of approximations for $g'(0)$.

Order of approximation	$\hbar = -1$		$\hbar = -0.75$	
	$-f''(0)$	$-g'(0)$	$-f''(0)$	$-g'(0)$
5	1.5386262	0.0705967	1.4975180	0.0195061
10	1.4379532	-0.0544487	1.4963156	0.0191512
15	1.622488	0.1779839	1.4964375	0.0193187
20	1.1831901	-0.3836943	1.4964231	0.0193002
25	2.3703257	1.155657	1.4964251	0.0193029
30	-1.0976900	-3.367249	1.4964248	0.0193024
35	9.5336308	10.542240	1.4964249	0.0193025
40	-24.196985	-33.695670	1.4964249	0.0193025

Table 4.1. The HAM approximations of $-f''(0)$ and $-g'(0)$ at $\hbar = -1$ and $\hbar = -0.75$ when $b = 7$, $M = 0.5$, $\lambda = 0.1$, $\vartheta = 0.5$.

Homotopy-Padé approximation		
$[m, m]$	$-f''(0)$	$-g'(0)$
[5, 5]	1.4964237	0.0192999
[10, 10]	1.4964249	0.0193025
[15, 15]	1.4964249	0.0193025
[20, 20]	1.4964249	0.0193025

Table 4.2. The $[m, m]$ homotopy-Padé approximations of $-f''(0)$ and $-g'(0)$ for $b = 7$, $M = 0.5$, $\lambda = 0.1$ and $\vartheta = 0.5$.

b	Cortell's [90] solution	homotopy-Padé approximation
0.0	0.627547	0.62755488
0.2	0.766758	0.76683734
0.5	0.889477	0.88954392
0.75	0.953786	0.95395659
1.0	1.0	1.0
1.5	1.061587	1.0616009
3.0	1.148588	1.1485932
7.0	1.216847	1.2168503
10.0	1.234875	1.2348745
20.0	1.257418	1.2574235
100.0	1.276768	1.2767735

Table 4.3. The comparison of Cortell's solution [90] with $[20, 20]$ homotopy-Padé approximations of the present work for different values of the non-linear stretching parameter b when $M = \lambda = \vartheta = 0$.

4.4 Results and discussion

This section includes the graphs of $f'(\eta)$ and $g(\eta)$ for 15th order approximations. These graphs illustrate the variation of the parameters b , M , λ and ϑ . Such variations can be seen through Figs. 4.2(a) – 4.5(b).

Fig. 4.2 (a)

$M = 0.5, \lambda = 0.5, \nu = 0.2, \eta = -0.75$

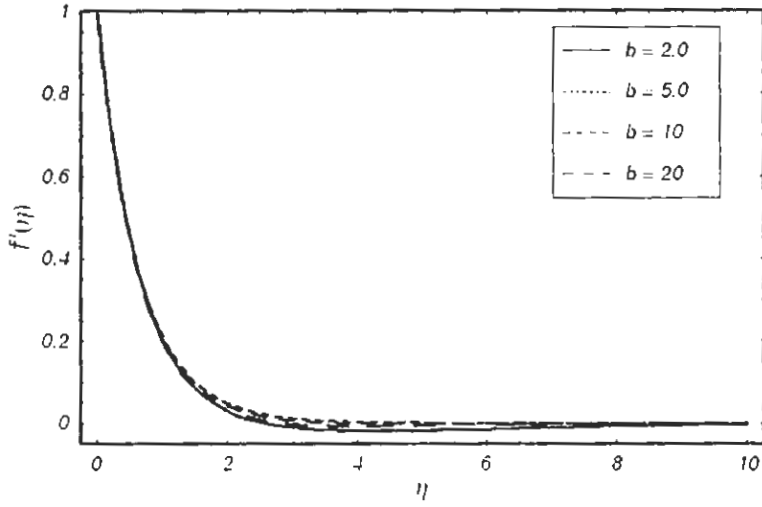


Fig. 4.2 (a). Variations of f' with the increase in b .

Fig. 4.2 (b)

$M = 0.2, \lambda = 0.5, \nu = 0.2, \eta = -0.75$

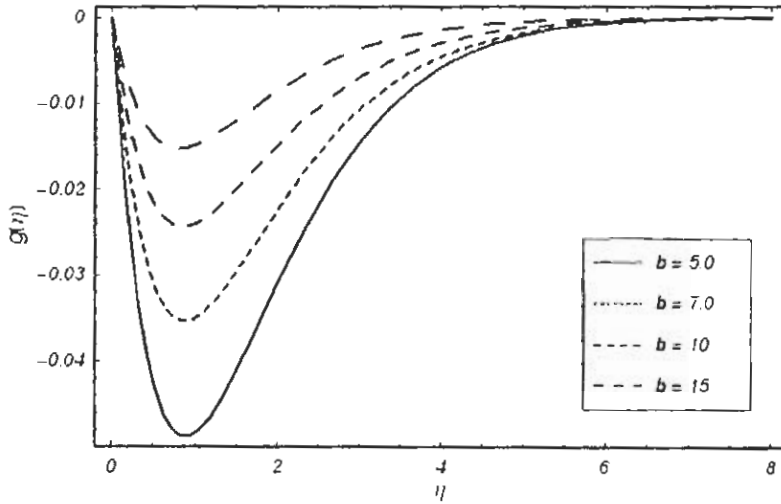


Fig. 4.2 (b). Variations of g with the increase in b .

Fig. 4.3 (a)

$b = 5.0, \lambda = 0.5, \nu = 0.2, \beta = -0.75$

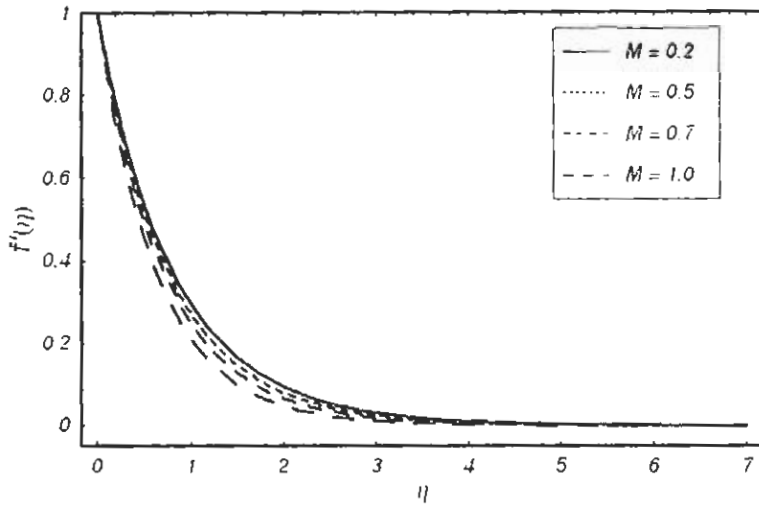


Fig. 4.3 (a). Variations of f' with the increase in M .

Fig. 4.3 (b)

$b = 5.0, \lambda = 0.5, \nu = 0.2, \beta = -0.75$

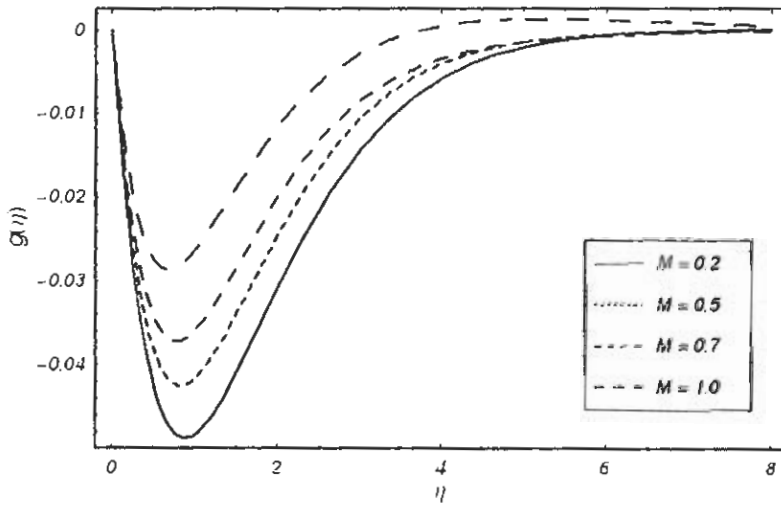


Fig. 4.3 (b). Variations of g with the increase in M .

Fig. 4.4 (a)

$b = 5.0, M = 0.2, d = 0.2, \eta = -0.75$

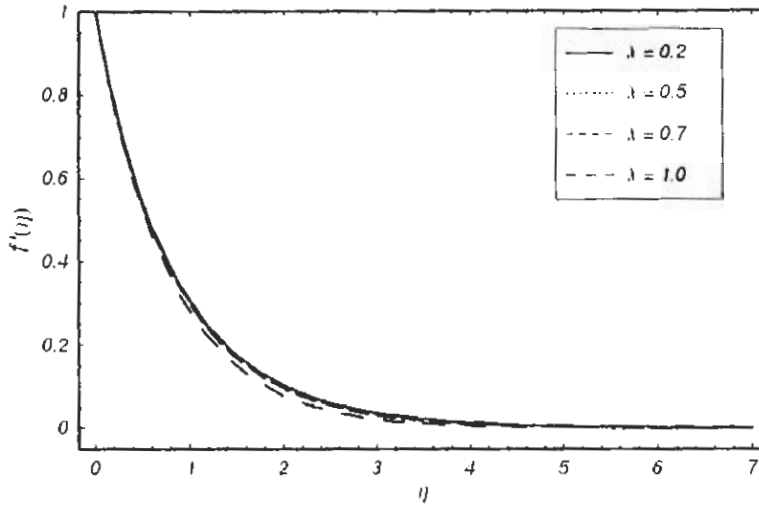


Fig. 4.4 (a). Variations of f' with the increase in λ .

Fig. 4.4 (b)

$b = 5.0, M = 0.5, d = 0.2, \eta = -0.75$

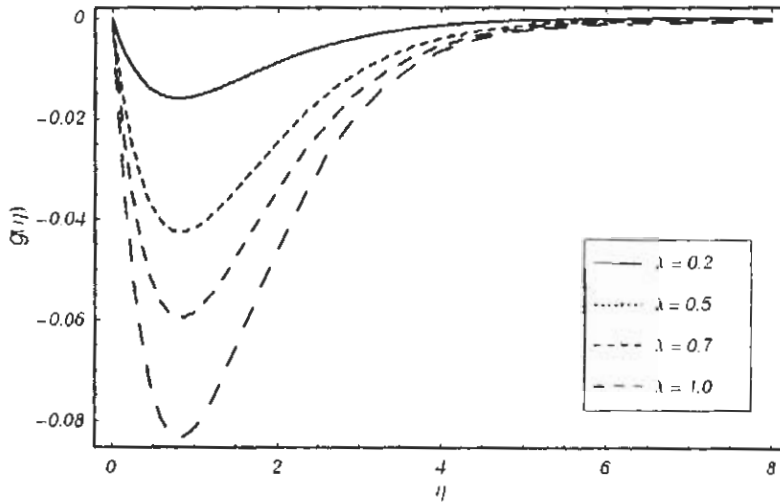


Fig. 4.4 (b). Variations of g with the increase in λ .

Fig. 4.5 (a)

$b = 5.0, M = 0.2, \lambda = 0.5, \eta = -0.75$

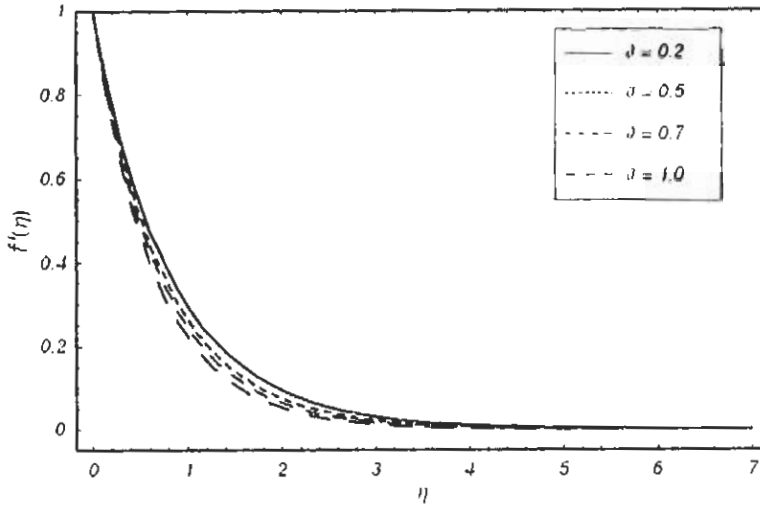


Fig. 4.5 (a). Variation of f' with the increase in ϑ .

Fig. 4.5 (b)

$b = 5.0, M = 0.2, \lambda = 0.2, \eta = -0.75$

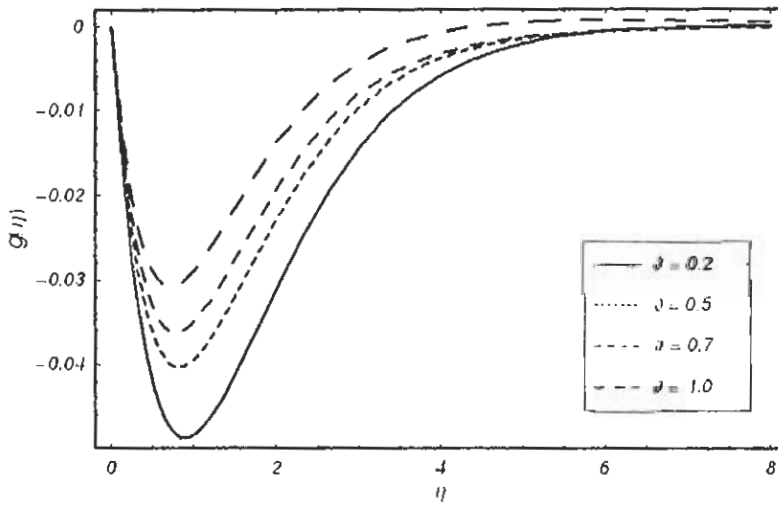


Fig. 4.5 (b). Variation of g with the increase in ϑ .

Fig. 4.2 (a) and 4.2 (b) shows that there is very small change in f' by increasing b . However there is a significant change in g when b is changed and M , λ and ϑ are fixed. This Fig. indicates that the magnitude of g increases by increasing b . The effect of Hartman number M on f' and g are shown in the Fig. 4.3(a) and 4.3 (b). Here the used values of the Hartman number are $M = 0.2, 0.5, 0.7$ and 1 . The effect of M on f' and g is significant. We conclude that an increase in M leads to an increase in f' and decrease in g . The variation of λ on f' and g is shown in Fig. 4.4(a) and 4.4 (b). These Figs. show that f' decreases. The behavior of λ on the magnitude of g is quite opposite to that of f' . Fig 4.5(a) and 4.5 (b) depicts the effects of the porosity parameter ϑ on f' and g . It is found that the effect of the porosity parameter on f' and g is similar to that of the Hartman number M .

In order to see the effect of different parameters b , M , ϑ and λ on the wall shear stress $-f''(0)$ and $-g'(0)$, Table 4.4 is constructed. It is observed that $-f''(0)$ increases with an increase in the non-linearity of the stretching b . However $-g'(0)$ decreases with an increase in b . The increase of Hartman number increases $-f''(0)$ and $-g'(0)$. Similarly the increase in porosity ϑ and rotation λ causes an increase in $-f''(0)$. On the other hand increase in porosity decreases $-g'(0)$ but an increase in λ increases $-g'(0)$.

b	M	ϑ	λ	$-f''(0)$	$-g'(0)$
0.0				1.069949	0.194189
0.2				1.159419	0.153881
0.5				1.244544	0.1174821
0.75				1.291418	0.0981848
1.0				1.3257934	0.0843510
1.5				1.3728528	0.0658266
3.0				1.4412643	0.0397066
7.0				1.4964249	0.01930255
10.0				1.5111942	0.0139339
1.5	0.0			1.2787653	0.0723894
	0.2			1.2942709	0.0712026
	0.5			1.3728525	0.0658266
	0.7			1.4575394	0.0609834
	1.0			1.6229786	0.0534946
	1.5	0.0		1.8395130	0.0462558
		0.2		1.8930839	0.0447767
		0.5		1.9707145	0.0428031
		0.7		2.0208135	0.0416243
		1.0		2.0937172	0.0400261
		0.2	0.2	1.8947351	0.0894639
			0.5	1.9060671	0.2221391
			0.7	1.9185639	0.3086837
			1.0	1.9437001	0.4344984
			1.5	1.987963	0.6315092

Table 4.4. The $[20, 20]$ homotopy-Padé approximations of $-f''(0)$ and $-g'(0)$ for different values of the parameters b , M , λ and ϑ .

Chapter 5

MHD rotating flow of a second grade fluid over a shrinking surface

The aim of present chapter is to extend the analysis of chapter two for a simplest subclass of a viscoelastic fluid namely the second grade fluid. The flow equations are first modeled and then reduced into ordinary differential equations. Series solution of the arising equation is calculated using HAM. Besides that the displayed graphical results show the variations of the pertinent parameters. In addition, a comparison between the solutions of viscous and second grade fluids is made.

5.1 Mathematical formulation

Here, the physical model of the flow problem is similar to that of chapter two except that second grade fluid replaces the viscous fluid. The corresponding expression of Cauchy stress tensor in a second grade fluid is given in Eq. (1.12). Employing Eq. (1.12), the continuity and momentum equations are

$$\frac{\partial u}{\partial x} + \frac{\partial w}{\partial z} = 0, \quad (5.1)$$

$$u \frac{\partial u}{\partial x} + w \frac{\partial u}{\partial z} - 2\Omega v = \frac{1}{\rho} \left[\frac{\partial T_{xx}}{\partial x} + \frac{\partial T_{xz}}{\partial z} \right] - \frac{\sigma B_0^2}{\rho} u, \quad (5.2)$$

$$u \frac{\partial v}{\partial x} + w \frac{\partial v}{\partial z} + 2\Omega u = \frac{1}{\rho} \left[\frac{\partial T_{yx}}{\partial x} + \frac{\partial T_{yz}}{\partial z} \right] - \frac{\sigma B_0^2}{\rho} v, \quad (5.3)$$

where asterisk has been suppressed for simplicity. In the next section we will obtain the solution of above equations subject to the boundary conditions in Eq. (2.8).

5.2 Solution by homotopy analysis method

In order to provide the HAM solution, we choose the initial approximations and operators given in Eqs. (2.9)-(2.11). The resulting problem at the zeroth order is of the following form

$$(1 - q) \mathcal{L}_1 [F(\eta, q) - f_0(\eta)] = q \hbar_5 \mathcal{N}_7 [F(\eta, q), G(\eta, q)], \quad (5.15)$$

$$(1 - q) \mathcal{L}_2 [G(\eta, q) - g_0(\eta)] = q \hbar_6 \mathcal{N}_8 [F(\eta, q), G(\eta, q)], \quad (5.16)$$

$$F(0, q) = s, \quad F'(\infty, q) = -1, \quad F'(\infty, q) = 0, \quad G(0, q) = 0 \text{ and } G(\infty, q) = 0. \quad (5.17)$$

In above equations

$$\mathcal{N}_7 [F(\eta, q), G(\eta, q)] = \frac{\partial^3 F(\eta, q)}{\partial \eta^3} - \left(\frac{\partial F(\eta, q)}{\partial \eta} \right)^2 + F(\eta, q) \frac{\partial^2 F(\eta, q)}{\partial \eta^2} + 2\lambda G(\eta, q) - M^2 \frac{\partial F(\eta, q)}{\partial \eta} - \alpha_1 \left[\begin{aligned} & 2 \frac{\partial F(\eta, q)}{\partial \eta} \frac{\partial^2 F(\eta, q)}{\partial \eta^2} - \left(\frac{\partial^2 F(\eta, q)}{\partial \eta^2} \right)^2 + \left(\frac{\partial G(\eta, q)}{\partial \eta} \right)^2 \\ & + \frac{\partial^2 G(\eta, q)}{\partial \eta^2} G(\eta, q) + \frac{\partial^4 F(\eta, q)}{\partial \eta^4} F(\eta, q) \end{aligned} \right], \quad (5.18)$$

$$\mathcal{N}_8 [F(\eta, q), G(\eta, q)] = \frac{\partial^2 G(\eta, q)}{\partial \eta^2} - G(\eta, q) \frac{\partial F(\eta, q)}{\partial \eta} + F(\eta, q) \frac{\partial G(\eta, q)}{\partial \eta} - 2\lambda \frac{\partial F(\eta, q)}{\partial \eta} - M^2 G(\eta, q) + \alpha_1 \left[\begin{aligned} & 2 \frac{\partial G(\eta, q)}{\partial \eta} \frac{\partial^2 F(\eta, q)}{\partial \eta^2} \\ & - \frac{\partial F(\eta, q)}{\partial \eta} \frac{\partial^2 F(\eta, q)}{\partial \eta^2} - \frac{\partial^3 G(\eta, q)}{\partial \eta^3} F(\eta, q) \end{aligned} \right]. \quad (5.19)$$

Obviously, when $q = 0$ and $q = 1$, Eqs. (5.18) and (5.19) satisfy Eq. (2.17). Expanding F in Taylor's series with respect to q , we have

$$F(\eta, q) = f_0(\eta) + \sum_{m=1}^{\infty} f_m(\eta) q^m, \quad G(\eta, q) = g_0(\eta) + \sum_{m=1}^{\infty} g_m(\eta) q^m, \quad (5.20)$$

$$f_m(\eta) = \frac{1}{m!} \left. \frac{\partial^m F(\eta, q)}{\partial q^m} \right|_{q=0}, \quad g_m(\eta) = \frac{1}{m!} \left. \frac{\partial^m G(\eta, q)}{\partial q^m} \right|_{q=0}. \quad (5.21)$$

Note that Eq. (5.20) contains the auxiliary parameters \hbar_5 and \hbar_6 . Assuming the solution in Eq. (5.20) that \hbar_5 and \hbar_6 are chosen so that the Eqs. (5.20) are convergent at $q = 1$, we have,

using Eq. (2.17), the solution series

$$f(\eta) = f_0(\eta) + \sum_{m=1}^{\infty} f_m(\eta), \quad g(\eta) = g_0(\eta) + \sum_{m=1}^{\infty} g_m(\eta). \quad (5.22)$$

The m th order deformation problems are

$$\mathcal{L}_1 [f_m(\eta) - \chi_m f_{m-1}(\eta)] = \hbar_5 \mathcal{R}5_m(\eta), \quad (5.23)$$

$$\mathcal{L}_2 [g_m(\eta) - \chi_m g_{m-1}(\eta)] = \hbar_6 \mathcal{R}6_m(\eta). \quad (5.24)$$

$$f_m(0) = 0, \quad f'_m(0) = 0, \quad g_m(0) = 0, \quad f'_m(\infty) \rightarrow 0 \text{ and } g_m(\infty) \rightarrow 0 \quad (5.25)$$

in which

$$\begin{aligned} \mathcal{R}5_m(\eta) = & \frac{d^3 f_{m-1}}{d\eta^3} - \sum_{k=0}^{m-1} \frac{df_{m-1-k}}{d\eta} \frac{df_k}{d\eta} + \sum_{k=0}^{m-1} f_{m-1-k} \frac{d^2 f_k}{d\eta^2} + 2\lambda g_{m-1} - M^2 \frac{df_{m-1}}{d\eta} \\ & - \alpha_1 \sum_{k=0}^{m-1} \left[2 \frac{df_{m-1-k}}{d\eta} \frac{d^3 f_k}{d\eta^3} - \frac{d^2 f_{m-1-k}}{d\eta^2} \frac{d^2 f_k}{d\eta^2} + \frac{dg_{m-1-k}}{d\eta} \frac{dg_k}{d\eta} \right. \\ & \left. + \frac{d^2 g_{m-1-k}}{d\eta^2} g_k + \frac{d^3 f_{m-1-k}}{d\eta^3} f_k \right], \end{aligned} \quad (5.26)$$

$$\begin{aligned} \mathcal{R}6_m(\eta) = & \frac{d^2 g_{m-1}}{d\eta^2} - \sum_{k=0}^{m-1} g_{m-1-k} \frac{df_k}{d\eta} + \sum_{k=0}^{m-1} f_{m-1-k} \frac{dg_k}{d\eta} - 2\lambda \frac{df_{m-1}}{d\eta} - M^2 g_{m-1} \\ & + \alpha_1 \sum_{k=0}^{m-1} \left[2 \frac{dg_{m-1-k}}{d\eta} \frac{d^2 f_k}{d\eta^2} \right. \\ & \left. - \frac{df_{m-1-k}}{d\eta} \frac{d^2 g_k}{d\eta^2} - \frac{d^3 g_{m-1-k}}{d\eta^3} f_k \right], \end{aligned} \quad (5.27)$$

where χ_m is defined in Eq. (1.40). The solutions of above equations upto first few order of approximations can be obtained by means of the symbolic computation software MATHEMATICA. It is found that $f_m(\eta)$ and $g_m(\eta)$ are expressed by

$$f_m(\eta) = \sum_{n=0}^{m+1} \sum_{q=0}^{2m+1-n} a_{m,n}^q \eta^q e^{-n\eta}, \quad g_m(\eta) = \sum_{n=0}^{m+1} \sum_{q=0}^{2m+1-n} b_{m,n}^q \eta^q e^{-n\eta}, \quad m \geq 0. \quad (5.28)$$

Since recursive relations are useful for us to recognize the structure of the series solutions and to have an insight to the nature of the considered problem. Therefore, we put Eq. (5.28) into

Eqs. (5.23) and (5.24) and get the following recurrence formulas for the coefficients $a_{m,n}^q$ and $b_{m,n}^q$ of $f_m(z)$ and $g_m(z)$ as follows when $m \geq 1$, $0 \leq n \leq m+1$

$$\begin{aligned} a_{m,0}^0 &= \chi_m \chi_{m+2} \chi_{2m+1} a_{m-1,0}^0 - \sum_{q=0}^{2m} \Delta 1_{m,1}^q \mu_{1,1}^q \\ &\quad - \sum_{n=2}^{m+1} \sum_{q=0}^{2m+1-n} \Delta 1_{m,n}^q (\mu_{n,1}^q - (n-1)\mu_{n,0}^q), \end{aligned} \quad (5.29)$$

$$\begin{aligned} a_{m,1}^0 &= \lambda_m \chi_{m+1} \lambda_{2m} a_{m-1,1}^0 + \sum_{q=0}^{2m} \Delta 1_{m,1}^q \mu_{1,1}^q \\ &\quad + \sum_{n=2}^{m+1} \sum_{q=0}^{2m+1-n} \Delta 1_{m,n}^q (\mu_{m,n}^q - n\mu_{n,0}^q), \end{aligned} \quad (5.30)$$

$$b_{m,1}^0 = \chi_m \chi_{m+1} \chi_{2m} b_{m-1,1}^0 - \sum_{q=0}^{2m+1} \Delta 2_{m,0}^q \mu_{0,0}^q - \sum_{n=2}^{m+1} \sum_{q=0}^{2m+1-n} \Delta 2_{m,n}^q \mu_{n,0}^q, \quad (5.31)$$

$$a_{m,1}^k = \chi_m \chi_{m+1} \chi_{2m-k} a_{m-1,1}^k + \sum_{q=k-1}^{2m} \Delta 1_{m,1}^q \mu_{1,k}^q, \quad 0 \leq k \leq 2m, \quad (5.32)$$

$$b_{m,1}^k = \chi_m \chi_{m+1} \chi_{2m-k} b_{m-1,1}^k + \sum_{q=k-1}^{2m} \Delta 2_{m,1}^q \mu_{1,k}^q, \quad 0 \leq k \leq 2m, \quad (5.33)$$

$$\begin{aligned} a_{m,n}^k &= \chi_m \chi_{m+2-n} \chi_{2m+1-n-q} a_{m-1,n}^k + \sum_{q=k}^{2m+1-n} \Delta 1_{m,n}^q \mu_{n,k}^q, \\ 2 &\leq k \leq 2m+1-n, \quad 2 \leq n \leq m+1, \end{aligned} \quad (5.34)$$

$$\begin{aligned} b_{m,n}^k &= \chi_m \chi_{m+2-n} \chi_{2m+1-n-k} b_{m-1,n}^k + \sum_{q=k}^{2m+1-n} \Delta 2_{m,n}^q \mu_{n,k}^q, \\ 2 &\leq k \leq 2m+1-n, \quad 2 \leq n \leq m+1, \end{aligned} \quad (5.35)$$

$$\Delta 1_{m,n}^q = \hbar_5 \left[\begin{array}{c} \chi_{m+2-n} \chi_{2m+1-n-q} \left\{ a 3_{m-1,n}^q + 2\lambda b_{m-1,n}^q \right\} \\ + \chi_{2m+2-n-q} \left\{ \beta_{m,n}^q - \alpha_{m,n}^q - \alpha_1 \left(\begin{array}{c} 2\gamma_{m,n}^q - \delta_{m,n}^q \\ + \theta_{m,n}^q + \phi_{m,n}^q + \varphi_{m,n}^q \end{array} \right) \right\} \end{array} \right], \quad (5.36)$$

$$\Delta 2_{m,n}^q = \hbar_6 \left[\begin{array}{c} \chi_{m+2-n} \lambda_{2m+1-n-q} \left\{ b 2_{m-1,n}^q - 2\lambda b 1_{m-1,n}^q \right\} \\ + \chi_{2m+2-n-q} \left\{ \Theta_{m,n}^q - \Gamma_{m,n}^q + \alpha_1 \left(\begin{array}{c} 2\Sigma_{m,n}^q \\ -\Upsilon_{m,n}^q - \Psi_{m,n}^q \end{array} \right) \right\} \end{array} \right]. \quad (5.37)$$

Here $\alpha_{m,n}^q, \beta_{m,n}^q, \gamma_{m,n}^q, \theta_{m,n}^q, \phi_{m,n}^q, \varphi_{m,n}^q, \Gamma_{m,n}^q, \Theta_{m,n}^q, \Sigma_{m,n}^q, \Upsilon_{m,n}^q, \Psi_{m,n}^q$, for $m \geq 1, 0 \leq n \leq 2m+1$, are given by

$$\alpha_{m,n}^q = \sum_{k=0}^{m-1} \sum_{i=\max\{0,n+k-m\}}^{\min\{n,k+1\}} \sum_{j=\max\{0,q+1+n-i-2(m-k)\}}^{\min\{q,2k+1-i\}} a 1_{m-1-k,n-i}^{q-j} a 1_{k,i}^j, \quad (5.38)$$

$$\beta_{m,n}^q = \sum_{k=0}^{m-1} \sum_{i=\max\{0,n+k-m\}}^{\min\{n,k+1\}} \sum_{j=\max\{0,q+1+n-i-2(m-k)\}}^{\min\{q,2k+1-i\}} a_{m-1-k,n-i}^{q-j} a 2_{k,i}^j, \quad (5.39)$$

$$\gamma_{m,n}^q = \sum_{k=0}^{m-1} \sum_{i=\max\{0,n+k-m\}}^{\min\{n,k+1\}} \sum_{j=\max\{0,q+1+n-i-2(m-k)\}}^{\min\{q,2k+1-i\}} a 1_{m-1-k,n-i}^{q-j} a 3_{k,i}^j, \quad (5.40)$$

$$\theta_{m,n}^q = \sum_{k=0}^{m-1} \sum_{i=\max\{0,n+k-m\}}^{\min\{n,k+1\}} \sum_{j=\max\{0,q+1+n-i-2(m-k)\}}^{\min\{q,2k+1-i\}} b 1_{m-1-k,n-i}^{q-j} b 1_{k,i}^j, \quad (5.41)$$

$$\phi_{m,n}^q = \sum_{k=0}^{m-1} \sum_{i=\max\{0,n+k-m\}}^{\min\{n,k+1\}} \sum_{j=\max\{0,q+1+n-i-2(m-k)\}}^{\min\{q,2k+1-i\}} b_{m-1-k,n-i}^{q-j} b 2_{k,i}^j, \quad (5.42)$$

$$\varphi_{m,n}^q = \sum_{k=0}^{m-1} \sum_{i=\max\{0,n+k-m\}}^{\min\{n,k+1\}} \sum_{j=\max\{0,q+1+n-i-2(m-k)\}}^{\min\{q,2k+1-i\}} a_{m-1-k,n-i}^{q-j} a 4_{k,i}^j, \quad (5.43)$$

$$\Gamma_{m,n}^q = \sum_{k=0}^{m-1} \sum_{i=\max\{0,n+k-m\}}^{\min\{n,k+1\}} \sum_{j=\max\{0,q+1+n-i-2(m-k)\}}^{\min\{q,2k+1-i\}} b_{m-1-k,n-i}^{q-j} a 1_{k,i}^j, \quad (5.44)$$

$$\Theta_{m,n}^q = \sum_{k=0}^{m-1} \sum_{i=\max\{0,n+k-m\}}^{\min\{n,k+1\}} \sum_{j=\max\{0,q+1+n-i-2(m-k)\}}^{\min\{q,2k+1-i\}} b 1_{m-1-k,n-i}^{q-j} a_{k,i}^j, \quad (5.45)$$

$$\Sigma_{m,n}^q = \sum_{k=0}^{m-1} \sum_{i=\max\{0,n+k-m\}}^{\min\{n,k+1\}} \sum_{j=\max\{0,q+1+n-i-2(m-k)\}}^{\min\{q,2k+1-i\}} b1_{m-1-k,n-i}^{q-j} a2_{k,i}^j, \quad (5.46)$$

$$\Upsilon_{m,n}^q = \sum_{k=0}^{m-1} \sum_{i=\max\{0,n+k-m\}}^{\min\{n,k+1\}} \sum_{j=\max\{0,q+1+n-i-2(m-k)\}}^{\min\{q,2k+1-i\}} a1_{m-1-k,n-i}^{q-j} b2_{k,i}^j, \quad (5.47)$$

$$\Psi_{m,n}^q = \sum_{k=0}^{m-1} \sum_{i=\max\{0,n+k-m\}}^{\min\{n,k+1\}} \sum_{j=\max\{0,q+1+n-i-2(m-k)\}}^{\min\{q,2k+1-i\}} a3_{m-1-k,n-i}^{q-j} b_{k,i}^j, \quad (5.48)$$

$$a1_{m,n}^q = (q+1)a_{m,n}^{q+1} - na_{m,n}^q, \quad a2_{m,n}^q = (q+1)a1_{m,n}^{q+1} - na1_{m,n}^q, \quad (5.49)$$

$$a3_{m,n}^q = (q+1)a2_{m,n}^{q+1} - na2_{m,n}^q, \quad a4_{m,n}^q = (q+1)a3_{m,n}^{q+1} - na3_{m,n}^q, \quad (5.50)$$

$$b1_{m,n}^q = (q+1)b_{m,n}^{q+1} - nb_{m,n}^q, \quad b2_{m,n}^q = (q+1)b1_{m,n}^{q+1} - nb1_{m,n}^q, \quad (5.51)$$

$$b3_{m,n}^q = (q+1)b2_{m,n}^{q+1} - nb2_{m,n}^q, \quad (5.52)$$

where $\mu_{1,k}^q$, $\mu_{n,k}^q$, $\mu_{1,1,k}^q$ and $\mu_{1,n,k}^q$ are defined through Eqs. (2.50), (2.54), (2.57) and (2.59) respectively. Due to the above recurrence formulas, we can calculate all the coefficients $a_{m,n}^q$ and $b_{m,n}^q$ using only the first few defined in Eq. (2.76). The corresponding M th-order approximations of Eqs. (2.8), (5.13) and (5.14) are

$$\sum_{m=0}^M f_m(\eta) = \sum_{m=0}^M a_{m,0}^0 + \sum_{n=1}^{M+1} e^{-n\eta} \left(\sum_{m=n-1}^M \sum_{q=0}^{2m+1-n} a_{m,n}^q \eta^q \right), \quad (5.53)$$

$$\sum_{m=0}^M g_m(\eta) = \sum_{m=0}^M b_{m,0}^0 + \sum_{n=1}^{M+1} e^{-n\eta} \left(\sum_{m=n-1}^M \sum_{q=0}^{2m+1-n} b_{m,n}^q \eta^q \right). \quad (5.54)$$

The analytic solutions now are

$$f(\eta) = \sum_{m=0}^{\infty} f_m(\eta) = \lim_{M \rightarrow \infty} \left[\sum_{m=0}^M a_{m,0}^0 + \sum_{n=1}^{M+1} e^{-n\eta} \left(\sum_{m=n-1}^M \sum_{q=0}^{2m+1-n} a_{m,n}^q \eta^q \right) \right], \quad (5.55)$$

$$g(\eta) = \sum_{m=0}^{\infty} g_m(\eta) = \lim_{M \rightarrow \infty} \left[\sum_{m=0}^M b_{m,0}^0 + \sum_{n=1}^{M+1} e^{-n\eta} \left(\sum_{m=n-1}^M \sum_{q=0}^{2m+1-n} b_{m,n}^q \eta^q \right) \right]. \quad (5.56)$$

5.3 Convergence of the analytic solution

The explicit analytic solutions given in Eqs. (5.55) and (5.56) contain the auxiliary parameter \hbar_5 and \hbar_6 . The convergence region and rate of approximation for the HAM solution strongly depends upon these auxiliary parameters. The reader is referred to [95] (pages 31 – 33) for the detailed discussion regarding the role of auxiliary parameters on the convergence region. Also a theorem similar to the convergence theorem 2.1 (pages 18 and 19) of reference [95] can easily be proved for the problem under consideration. As suggested by Liao [95], the region of the \hbar -curve having slope zero is the valid region. Thus the value of \hbar that lies inside the valid region always give the convergent series solution. The \hbar -curves for f and g are plotted for 15th order of approximation by taking two different values of α_1 , M , s and λ (Fig. 5.1). Fig. 5.1(a) shows that the range for the admissible values of \hbar_5 is $-1.7 \leq \hbar_5 \leq -0.2$ when $\alpha_1 = 0$, $M = 0$, $s = 0.1$ and $\lambda = 0.1$. For $\alpha_1 = 0.1$, $M = 0.1$, $s = 0.3$ and $\lambda = 0.3$; the admissible range is $-0.8 \leq \hbar_5 \leq -0.2$. Fig. 5.1(b) indicates that the range for the admissible values of \hbar_6 is $-1.6 \leq \hbar_6 \leq -0.2$ for $\alpha_1 = 0$, $M = 0$, $s = 0.1$ and $\lambda = 0.1$ and for $\alpha_1 = 0.1$, $M = 0.1$, $s = 0.3$ and $\lambda = 0.3$ it is $-0.8 \leq \hbar_6 \leq -0.2$. Our calculations depict that series given in Eqs. (5.55) and (5.56) converge in the whole region of η when $\hbar_5 = \hbar_6 = \hbar = -0.5$.

Fig. 5.1 (a)

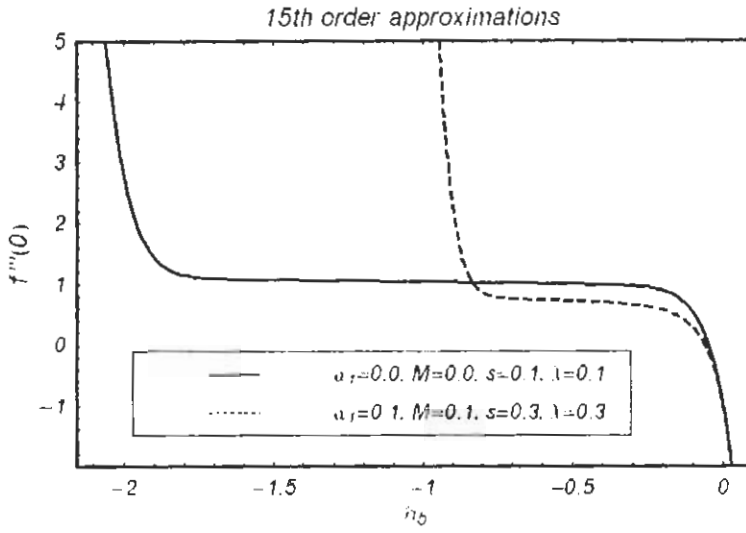


Fig. 5.1 (a). h -curves are plotted for 15th order of approximation for $f'''(0)$.

Fig. 5.1 (b)

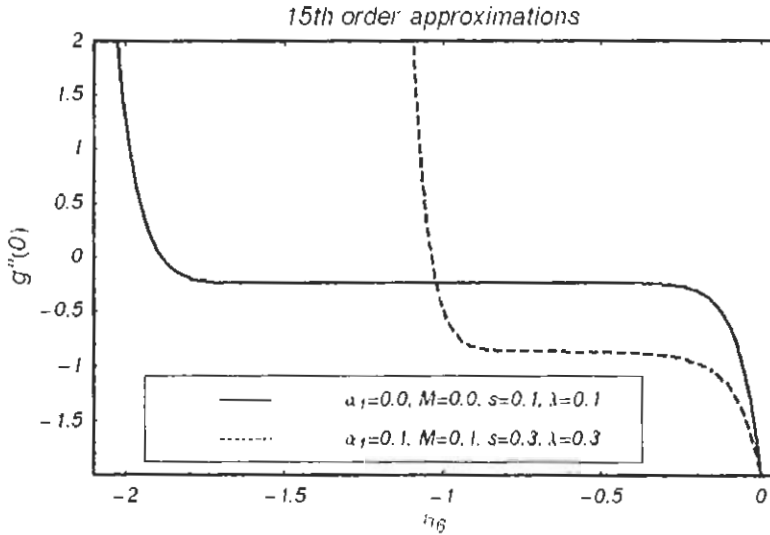


Fig. 5.1 (b). h -curves are plotted for 15th order of approximation for $g''(0)$.

5.4 Results and discussion

Shrinking flow of MHD second grade fluid in a rotating frame is studied analytically. Computations are carried out for a wide range of physical parameters of the problem and the graphical results are presented to illustrate the effects of various controlling parameters including second grade parameter (α_1), shrinking parameter (s), rotation (λ) and the Hartman number (M) when $h_5 = h_6 = \bar{h}$.

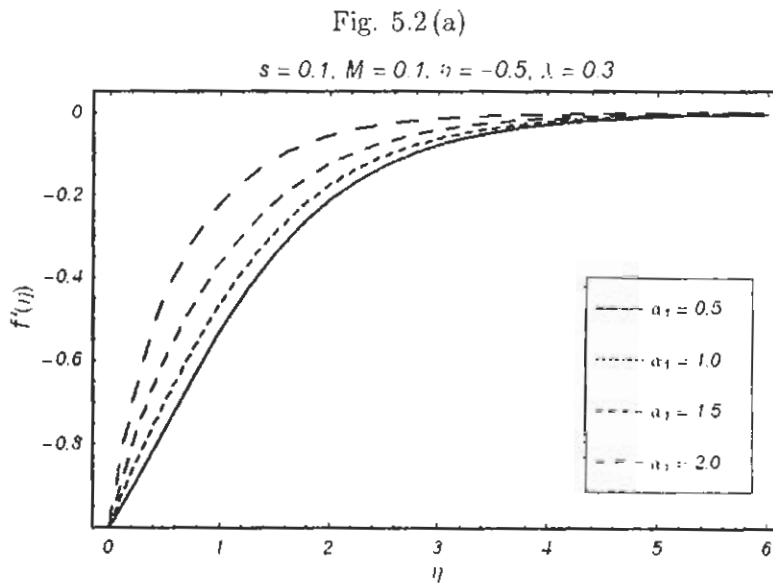


Fig. 5.2 (a). Variations of f' with an increase in α_1 .

Fig. 5.2 (b)

$s = 0.5, M = 0.1, \eta = -0.5, \lambda = 0.3$

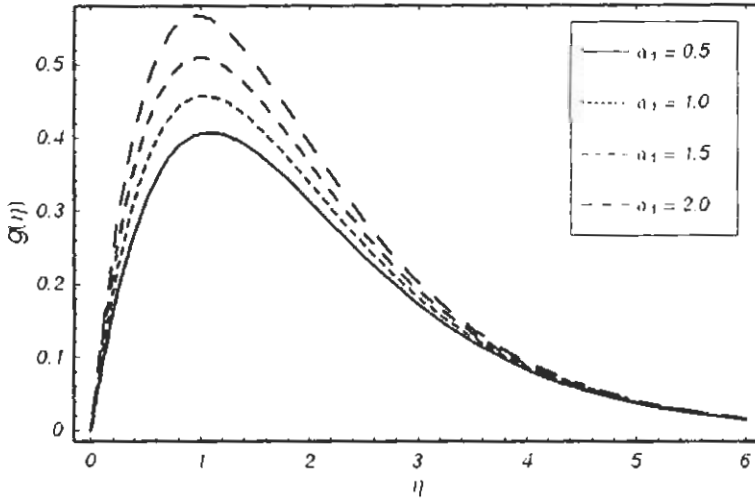


Fig. 5.2 (b). Variations of g with an increase in α_1 .

Fig. 5.3 (a)

$\alpha_1 = 0.5, M = 0.1, \eta = -0.5, \lambda = 0.3$

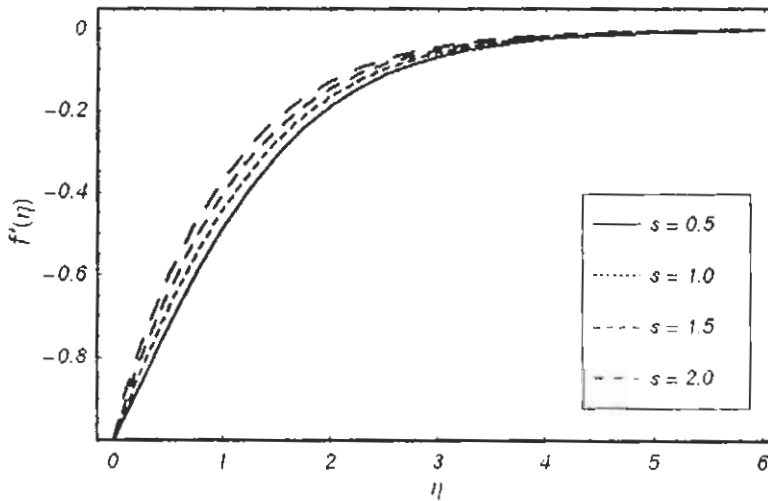


Fig. 5.3 (a). Variations of f' with s for case of suction.

Fig. 5.3 (b)

$\alpha_1 = 0.5, M = 0.1, \gamma = -0.5, \lambda = 0.3$

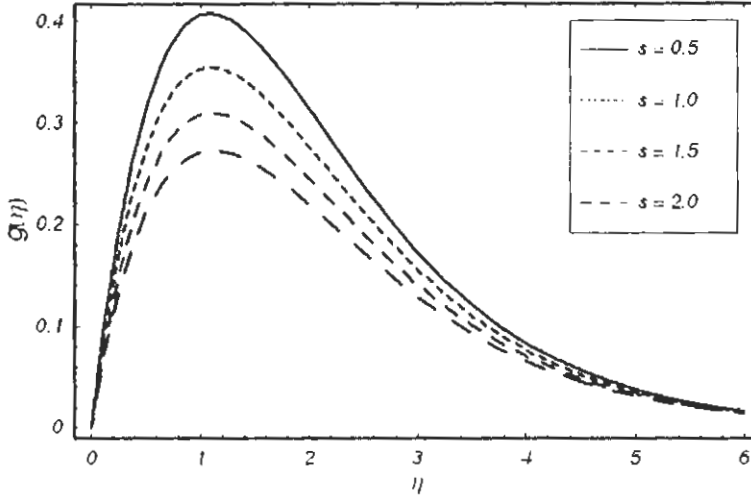


Fig. 5.3 (b). Variations of g with s for case of suction.

Fig. 5.4 (a)

$\alpha_1 = 0.5, M = 0.1, \gamma = -0.5, s = 0.5$

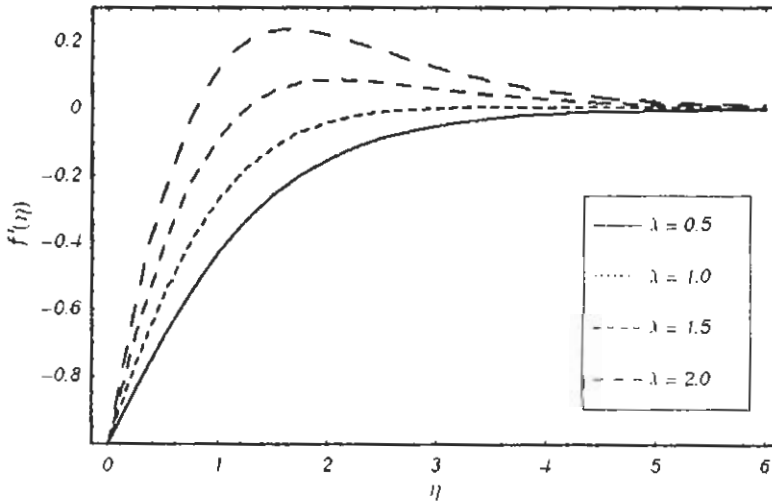


Fig. 5.4 (a). Variations of f' with an increase in λ .

Fig. 5.4(b)

$\alpha_1 = 0.5, M = 0.5, h = -0.5, s = 0.5$

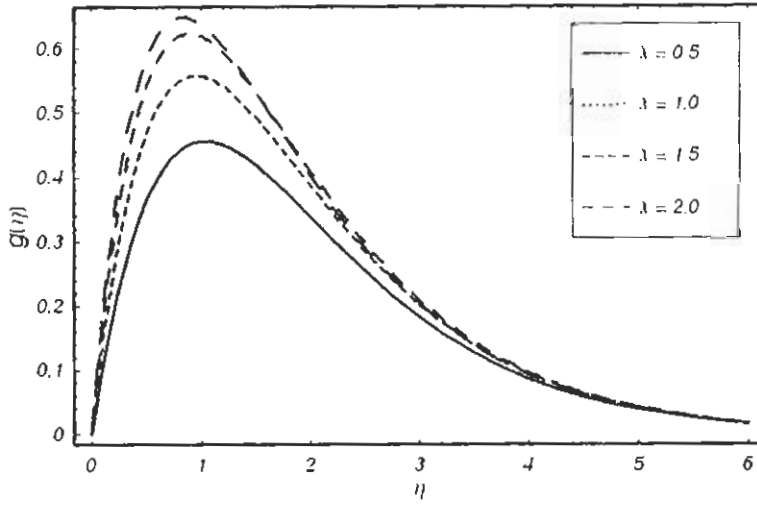


Fig. 5.4 (b). Variations of g with an increase in λ .

Fig. 5.5(a)

$\alpha_1 = 0.5, s = 0.5, h = -0.5, \lambda = 0.3$

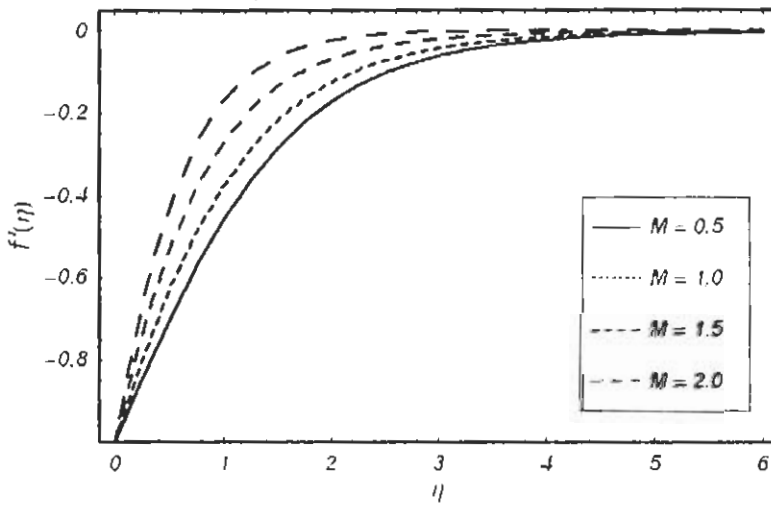


Fig. 5.5(a). Variations of f' with an increase in M .

Fig. 5.5 (b)

$\alpha_T = 0.1, s = 0.5, \beta = -0.5, \lambda = 0.3$

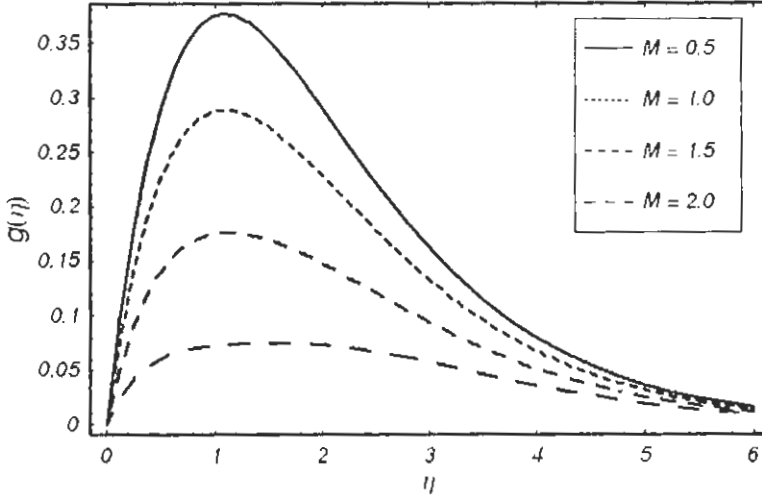


Fig. 5.5 (b). Variations of g with an increase in M .

Fig. 5.6 (a)

$\alpha_T = 0.5, M = 0.1, \beta = -0.5, \lambda = 0.3$

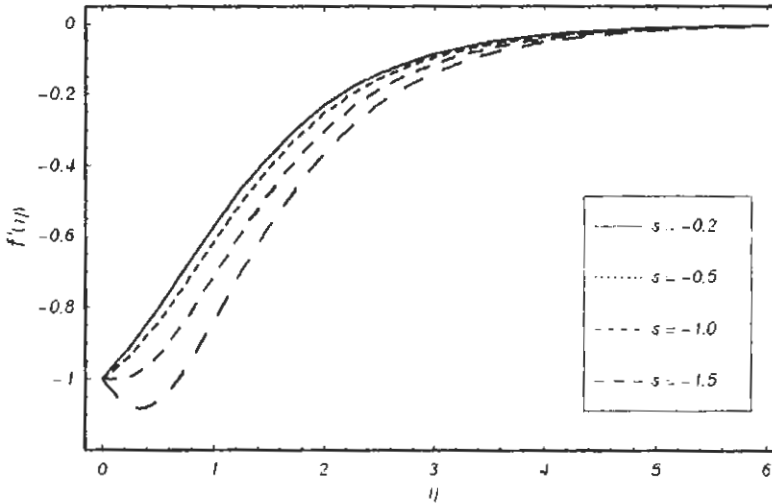


Fig. 5.6 (a). Variations of f' with s for the case of injection.

Fig. 5.6 (b)

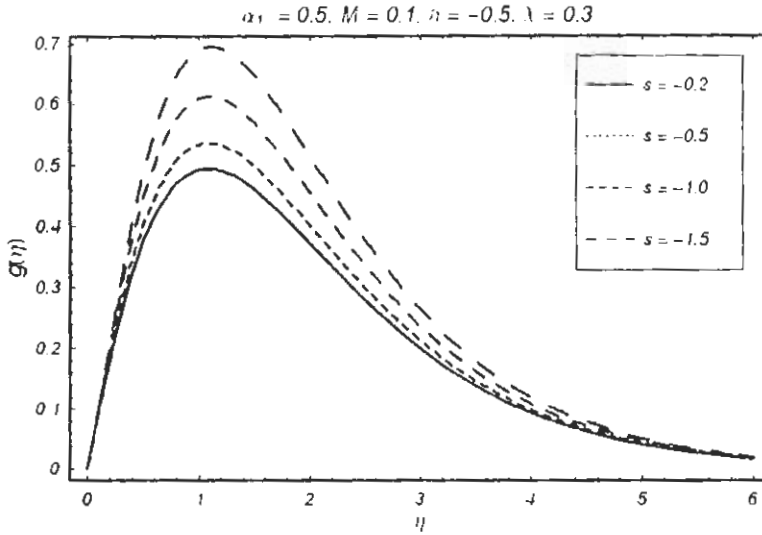


Fig. 5.6 (b). Variations of g with s for the case of injection.

It is found from Fig. 5.2(a) that the magnitude of f' decreases by increasing α_1 . Fig. 5.2(b) shows that the behavior of α_1 on g is quite opposite to that of f' . Fig. 5.3 (a) depicts that the velocity f' increases by increasing s . Furthermore, the boundary layer thickness decreases when s is increased. This is in agreement with the observation that suction causes reduction in the boundary layer thickness. The effect of s on g is similar to that of f' . However in this case boundary layer thickness increases as shown in Fig. 5.3(b). Fig. 5.4(a) and 5.4(b) elucidate the behavior of λ on f' and g . It can be seen that the effect of λ (which is the ratio of the rotation rate to the shrinking rate) is quite similar to that of α_1 on f' and g . Fig. 5.5(a) and 5.5(b) illustrates the effects of M on f' and g . The variation for M is similar to that of s . The boundary layer thickness decreases by increasing M . It is evident that the effect of rotation parameter on g is quite opposite when compared with the suction parameter s and Hartman number M . Fig. 5.6 (a) elucidates the variation in f' for the injection parameter s . It is noted that velocity decreases by increasing injection. These effects are quite opposite in the case of velocity field g as shown in Fig. 5.6 (b).

Chapter 6

The influence of Hall current on rotating flow of a third grade fluid in a porous medium

This chapter investigates the effect of Hall current on the steady and rotating flow of a third grade fluid in a porous medium. The hydromagnetic flow between the two stationary plates is induced by a constant applied pressure gradient. Modified Darcy's law has been used in the flow modelling. The series solution of the resulting non-linear problem is developed by means of the homotopy analysis method. The effects of various interesting parameters on the velocity components are seen through graphs and discussion.

6.1 Mathematical formulation

Let us consider the steady flow of an incompressible third grade fluid between two parallel plates at a distant d apart. Both plates and fluids are rotating with constant angular velocity Ω about an axis normal to the plates. We select the Cartesian coordinate system $OXYZ$. The x -axis and z -axis are perpendicular to the parallel plates respectively and y -axis normal to the xz -plane. The third grade fluid fills the porous space between the two stationary plates. Since the plates are infinite along x -and y -directions, all physical quantities except pressure depend upon z only. Denoting velocity components u and v along x -and y - directions, respectively,

the velocity \mathbf{V} is defined as

$$\mathbf{V} = [u, v, 0]. \quad (6.1)$$

For third order fluid, the Cauchy stress tensor $\boldsymbol{\tau}$ is defined in Eq. (1.11).

In a porous medium, the equations governing the incompressible rotating flow with Hall effect are

$$\operatorname{div} \mathbf{V} = 0, \quad (6.2)$$

$$\rho \left[\frac{d\mathbf{V}}{dt} + 2\boldsymbol{\Omega} \times \mathbf{V} + \boldsymbol{\Omega} \times \boldsymbol{\Omega} \times \mathbf{r} \right] = -\nabla p + \operatorname{div} \mathbf{S} + \mathbf{J} \times \mathbf{B} + \mathbf{R}, \quad (6.3)$$

where \mathbf{J} is the current density, \mathbf{B} is the total magnetic field, \mathbf{R} is the Darcy's resistance and the extra stress tensor \mathbf{S} in a third grade fluid is defined as

$$\mathbf{S} = (\mu + \beta_3 \operatorname{tr} \mathbf{A}_1^2) \mathbf{A}_1 + \alpha_1 \mathbf{A}_2 + \alpha_2 \mathbf{A}_1^2 + \beta_1 \mathbf{A}_3 + \beta_2 (\mathbf{A}_1 \mathbf{A}_2 + \mathbf{A}_2 \mathbf{A}_1) \quad (6.4)$$

where the apparent viscosity μ_{app} is defined by

$$\mu_{app} = \mu + \beta_3 \operatorname{tr} \mathbf{A}_1^2. \quad (6.5)$$

$$\mathbf{J} + \frac{\omega_c \tau_c}{B_0} (\mathbf{J} \times \mathbf{B}) = \sigma \left[\mathbf{E} + \mathbf{V} \times \mathbf{B} + \frac{1}{en_n} \nabla p_e \right], \quad (6.6)$$

where ω_c is the cyclotron frequency of electrons, τ_c is the electron collision time, σ is electrical conductivity, e is the electron charge and p_e is the electron pressure. The ion-slip and thermo-electric effects are not included in Eq. (6.6). Further it is assumed that $\omega_c \tau_c \sim o(1)$ and $\omega_i \tau_i < 1$ where ω_c and τ_i are cyclotron frequency and collision time for ions respectively.

For fluid flow in a porous media, it is a common practice to treat the porous medium as a continuous medium, but in this case we have two continuum medium: fluid in motion and the solid matrix that is rigid and stationary. For low speed fluid the Darcy's law holds in an unbounded porous medium. This law relates the pressure drop caused by the frictional drag and velocity and ignores the boundary effects on the flow. By this law the induced pressure drop is directly proportional to the velocity. For the porous medium with boundaries, Brinkman suggested an equation describing the locally averaged flow. Although an equation proposed by Brinkman holds only for steady viscous flows but there are several modified Darcy's law available

in the literature for viscous flows. Due attention has not been given to the mathematical macroscopic filtration models concerning viscoelastic flows in a porous medium. Due to this fact and keeping in view the constitutive equation of an Oldroyd-B fluid, the following expression has been proposed

$$\left(1 + \lambda \frac{\partial}{\partial t}\right) \nabla p = -\frac{\mu\phi}{k} \left(1 + \lambda_r \frac{\partial}{\partial t}\right) \mathbf{V}, \quad (6.7)$$

in which k is the permeability, λ and λ_r are respective relaxation and retardation times and ϕ is the porosity of the medium. It is pertinent to mention that for $\lambda = \lambda_r = 0$, Eq. (6.7) gives the well known Darcy's law for a viscous flow. For $\lambda_r = 0$, Eq. (6.7) reduces to a Maxwell fluid. When $\lambda = 0$ and $\mu\lambda_r = \alpha_1$ (second grade fluid parameter), Eq. (6.7) holds for second grade fluid. It should be pointed out that for $\lambda = \lambda_r = 0$, Eq. (6.7) is valid for a viscous fluid. Employing a similar procedure as in reference [10], the Darcy's resistance \mathbf{R} in a third grade fluid is

$$\mathbf{R} = -\frac{\phi}{k} \left[\mu + 2\beta_3 \left(\left(\frac{du}{dz}\right)^2 + \left(\frac{dv}{dz}\right)^2 \right) \right] \mathbf{V}. \quad (6.8)$$

In view of above equations, the incompressibility condition is automatically satisfied and Eq. (1.7) give the following scalar equations

$$-2\rho\Omega v = -\frac{\partial \hat{p}}{\partial x} + \frac{dT_{13}}{dz} + R_1 - \frac{\sigma\beta_0^2}{1-im}u, \quad (6.9)$$

$$2\rho\Omega u = -\frac{\partial \hat{p}}{\partial y} + \frac{dT_{23}}{dz} + R_2 - \frac{\sigma\beta_0^2}{1-im}v, \quad (6.10)$$

where

$$\hat{p} = -T_{33} - \frac{\rho}{2}\Omega^2(x^2 + y^2), \quad (6.11)$$

$$T_{13} = \mu \frac{du}{dz} + 2\beta_3 \frac{du}{dz} \left[\left(\frac{du}{dz}\right)^2 + \left(\frac{dv}{dz}\right)^2 \right], \quad (6.12)$$

$$T_{23} = \mu \frac{dv}{dz} + 2\beta_3 \frac{dv}{dz} \left[\left(\frac{du}{dz}\right)^2 + \left(\frac{dv}{dz}\right)^2 \right], \quad (6.13)$$

$$T_{33} = -p + (2\alpha_1 + \alpha_2) \left[\left(\frac{du}{dz}\right)^2 + \left(\frac{dv}{dz}\right)^2 \right] \quad (6.14)$$

$m(= \omega_e \tau_e)$ is the Hall parameter and the z -component of equation of motion indicates that

the modified pressure $\hat{p} \neq \hat{p}(z)$.

The equations which are to be solved are Eqs. (6.9) and (6.10), subject to the following boundary conditions:

$$u = v = 0 \text{ at } z = 0 \text{ and } z = d. \quad (6.15)$$

Writing

$$f = u + iv, \quad \bar{f} = u - iv \quad (6.16)$$

Eqs. (6.9) – (6.14) and boundary conditions (6.15) give

$$2i\Omega f = -\frac{1}{\rho} \left(\frac{\partial \hat{p}}{\partial x} + i \frac{\partial \hat{p}}{\partial y} \right) + \frac{1}{\rho} \left[\begin{array}{l} \mu \frac{d^2 f}{dz^2} - \left(\frac{\phi \mu}{k} + \frac{\sigma \beta_0^2}{1+m^2} \right) f \\ -i \frac{m\sigma \beta_0^2}{1+m^2} f - 2 \frac{\phi \beta_3}{k} \frac{df}{dz} \frac{d\bar{f}}{dz} f \\ + 2\beta_3 \left[2 \frac{df}{dz} \frac{d\bar{f}}{dz} \frac{d^2 f}{dz^2} + \frac{d^2 \bar{f}}{dz^2} \left(\frac{df}{dz} \right)^2 \right] \end{array} \right], \quad (6.17)$$

$$f(0) = 0, \quad f(d) = 0. \quad (6.18)$$

It is expedient to write the above equations in non-dimensional form. To do this, we introduce nondimensional variables and parameters as follows:

$$\begin{aligned} f^* &= \frac{f}{U_0}, & z^* &= \frac{z}{d}, & \Omega^* &= \frac{\Omega d^2}{\nu}, & \phi^* &= \frac{\phi d^2}{k} \\ \beta_3^* &= \frac{\beta_3 U_0^2}{\rho d^2 \nu}, & C &= -\frac{d^2}{\mu U_0} \left(\frac{\partial \hat{p}}{\partial x} + i \frac{\partial \hat{p}}{\partial y} \right), & M^* &= \frac{\sigma \beta_0^2 d^2}{\rho \nu}. \end{aligned} \quad (6.19)$$

We write Eqs. (6.17) and (6.18) in terms of these dimensionless parameters as

$$2i\Omega f = C + \left[\begin{array}{l} \frac{d^2 f}{dz^2} - i \frac{mM}{1+m^2} f - \left(\phi + \frac{M}{1+m^2} \right) f - 2\phi\beta_3 \frac{df}{dz} \frac{d\bar{f}}{dz} f \\ + 2\beta_3 \frac{df}{dz} \left[2 \frac{d\bar{f}}{dz} \frac{d^2 f}{dz^2} + \frac{d^2 \bar{f}}{dz^2} \frac{df}{dz} \right] \end{array} \right], \quad (6.20)$$

$$f(0) = 0, \quad f(1) = 0, \quad (6.21)$$

where C is dimensionless pressure gradient and asterisks have been suppressed for simplicity.

6.2 Analytic solution

For HAM solution we choose

$$f_0(z) = z^2 - z, \quad (6.22)$$

$$\mathcal{L}_4(f) = f'', \quad (6.23)$$

as initial approximation of f and auxiliary linear operator \mathcal{L}_4 satisfying

$$\mathcal{L}_4(C_6 z + C_7) = 0, \quad (6.24)$$

where C_6 and C_7 are arbitrary constants. If $q \in [0, 1]$ is the embedding parameter and \hbar is the auxiliary nonzero parameter then

$$(1 - q) \mathcal{L}_4[F(z, q) - f_0(z)] = q \hbar \mathcal{N}_9[F(z, q)], \quad (6.25)$$

$$F(0, q) = 0, \quad F(1, q) = 0, \quad (6.26)$$

in which

$$\begin{aligned} \mathcal{N}_9[F(z, q)] = & C + \frac{\partial^2 F(z, q)}{\partial z^2} - i \left(\frac{mM}{1+m^2} + 2\Omega \right) F(z, q) - \left(\phi + \frac{M}{1+m^2} \right) F(z, q) \\ & + 2\beta_3 \frac{\partial F(z, q)}{\partial z} \left[2 \frac{\partial \bar{F}(z, q)}{\partial z} \frac{\partial^2 F(z, q)}{\partial z^2} - \phi \frac{\partial \bar{F}(z, q)}{\partial z} F(z, q) + \frac{\partial^2 \bar{F}(z, q)}{\partial z^2} \frac{\partial F(z, q)}{\partial z} \right]. \end{aligned} \quad (6.27)$$

When $q = 0$ and $q = 1$, one can write

$$F(z, 0) = f_0(z), \quad F(z, 1) = f(z). \quad (6.28)$$

As q increases from 0 to 1, $F(z, q)$ varies from the initial guess $f_0(z)$ to the solution $f(z)$.

Using Taylor's theorem and Eq. (6.28) one obtains

$$F(z, q) = f_0(z) + \sum_{m=1}^{\infty} f_m(z) q^m, \quad (6.29)$$

$$f_m(z) = \frac{1}{m!} \frac{\partial^m F(z, q)}{\partial q^m} \Big|_{q=0}. \quad (6.30)$$

Clearly, the convergence of the series (6.29) depends upon \hbar_7 . We select \hbar_7 in such a way that the series (6.29) is convergent at $q = 1$, then due to Eq. (6.28) we can write

$$f(z) = f_0(z) + \sum_{m=1}^{\infty} f_m(z). \quad (6.31)$$

The resulting m th order deformation problem is

$$\mathcal{L}_4 [f_m(z) - \chi_m f_{m-1}(z)] = \hbar_7 \mathcal{R}7_m(z) \quad (6.32)$$

$$f_m(0) = f_m(1) = 0, \quad (6.33)$$

$$\begin{aligned} \mathcal{R}7_m(z) = & \hbar_7 \left[(1 - \chi_m) C - i \left(\frac{mM}{1+m^2} + 2\Omega \right) f_{m-1} \right. \\ & \left. + \frac{d^2 f_{m-1}}{dz^2} - \left(\phi + \frac{M}{1+m^2} \right) f_{m-1} \right] \\ & + \hbar_7 \sum_{k=0}^{m-1} \sum_{l=0}^k \left[2\beta_3 \frac{df_{m-1-k}}{dz} \left[2 \frac{d^2 f_{k-l}}{dz^2} \frac{d^2 f_l}{dz^2} + \frac{d^2 f_{k-l}}{dz^2} \frac{df_l}{dz} \right] \right. \\ & \left. - 2\phi\beta_3 \frac{df_{m-1-k}}{dz} \frac{d^2 f_{k-l}}{dz^2} f_l \right], \quad (6.34) \end{aligned}$$

To obtain the solution of above equation upto first few order of approximations, the symbolic computation software MATHEMATICA is used and the series solution is found to be

$$f_m(z) = \sum_{n=0}^{4m+2} a_{m,n} z^n, \quad m \geq 0. \quad (6.35)$$

Inserting Eq. (6.35) into Eq. (6.32) we get the following recurrence formulas for the coefficients $a_{m,n}$, of $f_m(z)$ as follows for $m \geq 1$, $0 \leq n \leq 4m+2$

$$a_{m,1} = \chi_m \lambda_{4m+1} a_{m-1,1} - \hbar_7 (1 - \chi_m) \frac{C}{2} - \sum_{n=0}^{4m+2} \frac{\Delta_{m,n}}{(n+1)(n+2)}, \quad (6.36)$$

$$a_{m,2} = \chi_m \lambda_{4m} a_{m-1,2} + \hbar_7 (1 - \chi_m) \frac{C}{2} + \frac{\Delta_{m,0}}{2}, \quad (6.37)$$

$$a_{m,n} = \chi_m \lambda_{4m-n+2} a_{m-1,n} + \frac{\Delta_{m,n-2}}{n(n-1)}, \quad 3 \leq n \leq 4m+2, \quad (6.38)$$

$$\begin{aligned} \Delta_{m,n} = & \hbar_7 \chi_{4m-n+2} \begin{bmatrix} c_{m,n} - i \left(\frac{mM}{1+m^2} + 2\Omega \right) a_{m,n} \\ - \left(\phi + \frac{M}{1+m^2} \right) a_{m,n} \end{bmatrix} \\ & + \hbar_7 \begin{bmatrix} 2\beta_3 (2\Sigma_{m,n} + \Pi_{m,n}) \\ -2\phi\beta_3 \Gamma_{m,n} \end{bmatrix}. \end{aligned} \quad (6.39)$$

Here the coefficients $\Gamma_{m,n}$, $\Pi_{m,n}$, $\Sigma_{m,n}$, where $m \geq 1$, $0 \leq n \leq 4m + 2$, are

$$\Gamma_{m,n} = \sum_{k=0}^{m-1} \sum_{l=0}^k \sum_{k_1=\max\{0, n-4(m-k)+2\}}^{\min\{n, 4k+2\}} \sum_{j=\max\{0, k_1-4(k-l)\}}^{\min\{k_1, 4l+2\}} b_{m-1-k, n-k_1} \bar{b}_{k-l, k_1-j} a_{l,j}, \quad (6.40)$$

$$\Pi_{m,n} = \sum_{k=0}^{m-1} \sum_{l=0}^k \sum_{k_1=\max\{0, n-4(m-k)+2\}}^{\min\{n, 4k+2\}} \sum_{j=\max\{0, k_1-4(k-l)\}}^{\min\{k_1, 4l+2\}} b_{m-1-k, n-k_1} \bar{c}_{k-l, k_1-j} b_{l,j}, \quad (6.41)$$

$$\Sigma_{m,n} = \sum_{k=0}^{m-1} \sum_{l=0}^k \sum_{k_1=\max\{0, n-4(m-k)+2\}}^{\min\{n, 4k+2\}} \sum_{j=\max\{0, k_1-4(k-l)\}}^{\min\{k_1, 4l+2\}} b_{m-1-k, n-k_1} b_{k-l, k_1-j} \bar{c}_{l,j}, \quad (6.42)$$

$$b_{m,n} = (n+1) a_{m, n+1}, \quad (6.43)$$

$$c_{m,n} = (n+1) b_{m, n+1}, \quad (6.44)$$

where $\bar{b}_{m,n}$, $\bar{c}_{m,n}$, are complex conjugate of $b_{m,n}$, $c_{m,n}$ respectively. One can calculate all coefficients using the first three

$$a_{0,0} = 0, \quad a_{0,1} = -1, \quad a_{0,2} = 1 \quad (6.45)$$

given by the initial guess approximation (6.22).

The corresponding M th-order approximation of Eqs. (6.20) and (6.21) is

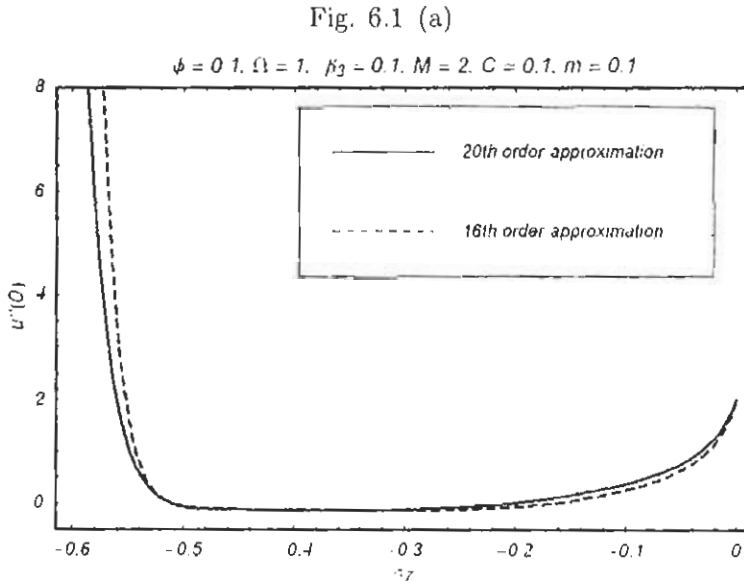
$$\sum_{m=0}^M f_m(z) = \sum_{n=1}^{4M+2} \left(\sum_{m=n-1}^{4M+1} a_{m,n} z^n \right) \quad (6.46)$$

and the explicit analytic solution is

$$f(z) = \sum_{m=0}^{\infty} f_m(z) = \lim_{M \rightarrow \infty} \left[\sum_{n=1}^{4M+2} \left(\sum_{m=n-1}^{4M+1} a_{m,n} z^n \right) \right]. \quad (6.47)$$

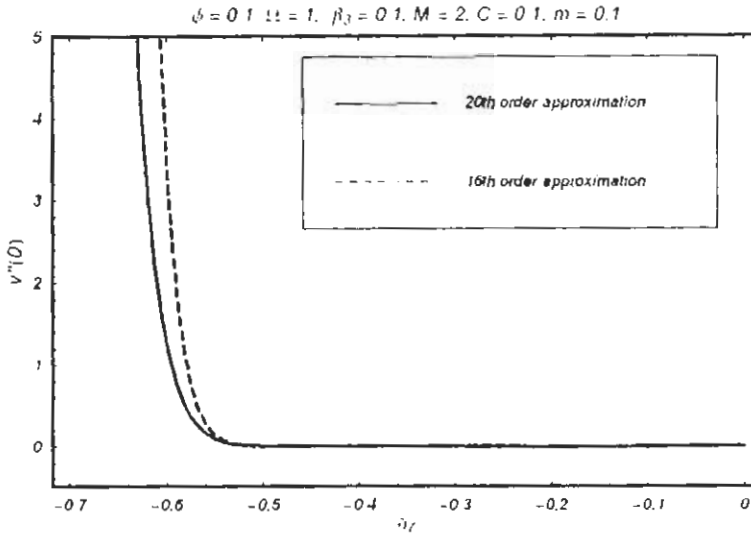
6.3 Convergence of the analytic solution

The explicit analytic solution given in Eq. (6.47) contains the auxiliary parameter \hbar_7 which gives the convergence region and rate of approximation for the HAM solution. In Fig. 6.1 (a,b), the \hbar -curves are plotted for two different order of approximations for the dimensionless velocity components u and v for $\phi = 0.1$, $\Omega = 1$, $\beta_3 = 0.1$, $M = 2$, $C = 0.1$ and $m = 0.1$. As we can see that the change in the order of approximation does not produce any change for the valid region of the auxiliary parameter \hbar_7 . Fig. 6.1 (a and b) clearly elucidates that the range for the admissible value of \hbar_7 is $-0.6 \leq \hbar_7 \leq 0$. Similar we can draw \hbar -curve for all other different values of the parameter involved. Our calculation indicates that the x and y -components of the velocity field f converges in the whole region of z when $\hbar_7 = -0.4$.



Figs. 6.1(a) \hbar -curves are plotted for 16th and 20th order of approximations for the velocity component u .

Fig. 6.1 (b)



Figs. 6.1(b) \bar{h} -curves are plotted for 16th and 20th order of approximations for the velocity component v .

6.4 Results and discussion

The graphs for the functions $u(z)$ and $v(z)$ for 15th order approximations are drawn against z for different values of the parameters β_3 , m , M , ϕ , Ω and the constant pressure gradient C for $C > 0$. Similarly, the graphs can be obtained for $C < 0$. To see the effects of emerging parameters on the velocity components u and v , Figs. 6.2(a)–6.7(b) are displayed. In each case, Figs (a) and (b) indicate the behavior for the velocity components u and v , respectively.

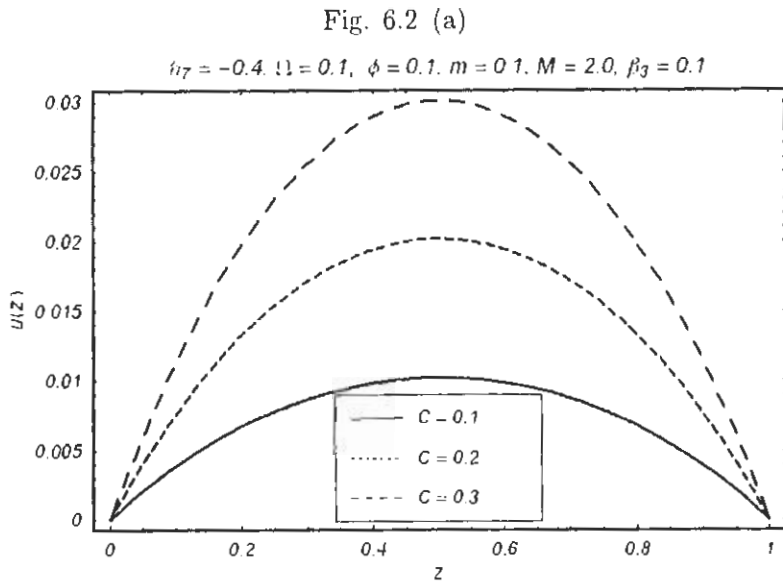


Fig. 6.2 (a). Variations of velocity components u with the increase in parameter C .

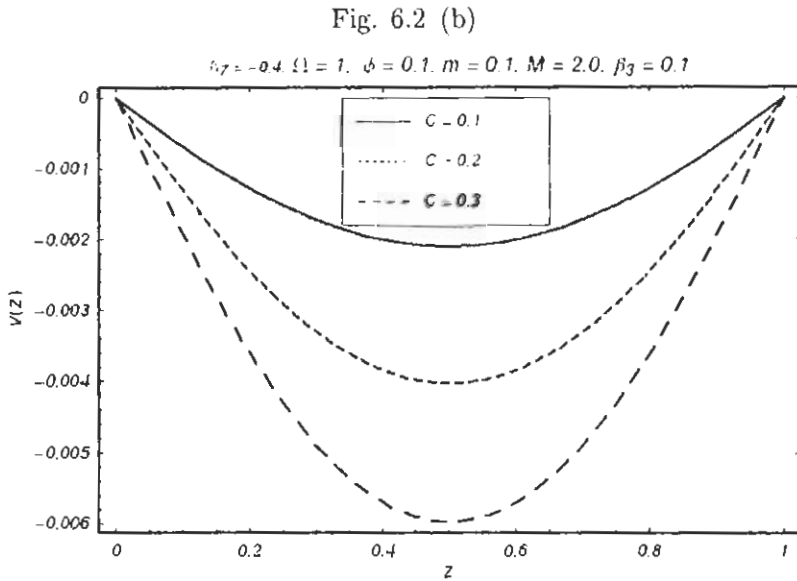


Fig. 6.2 (b). Variations of velocity components v with the increase in parameter C .

Fig. 6.3 (a)

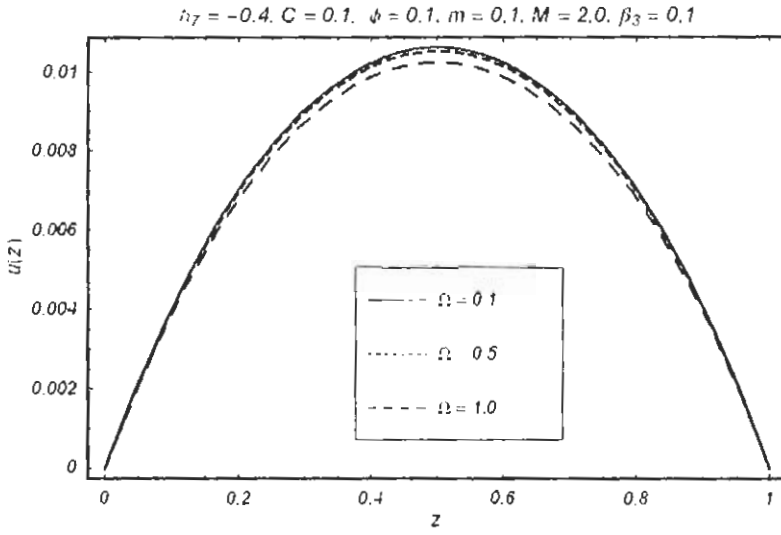


Fig. 6.3 (a). Variations of velocity component u with the increase in parameter Ω .

Fig. 6.3 (b)

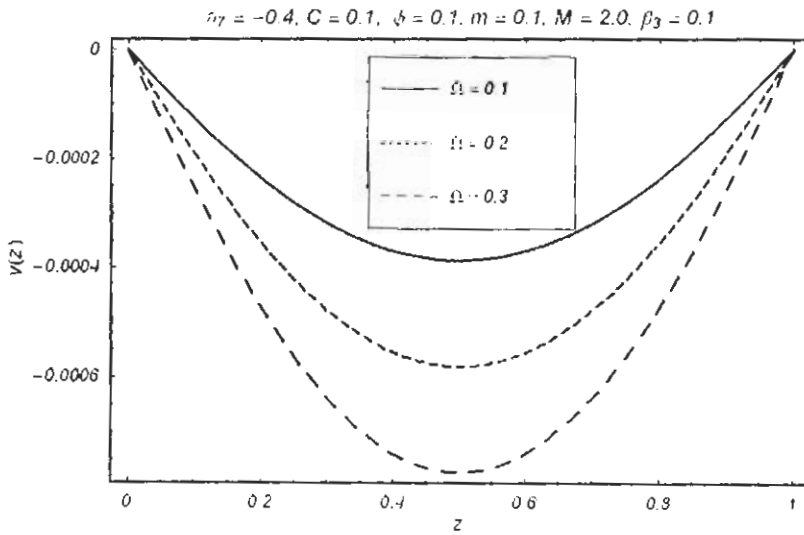


Fig. 6.3 (b). Variations of velocity component v with the increase in parameter Ω .

Fig. 6.4 (a)

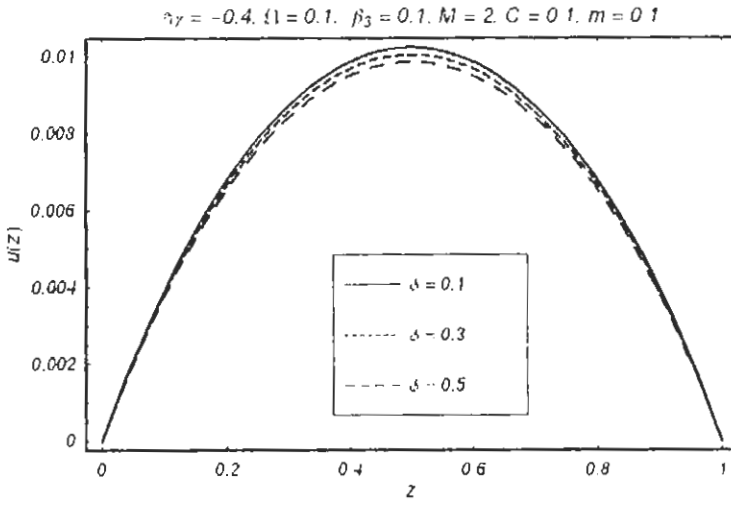


Fig. 6.4 (a). Variations of velocity component u with the increase in parameter ϕ .

Fig. 6.4 (b)

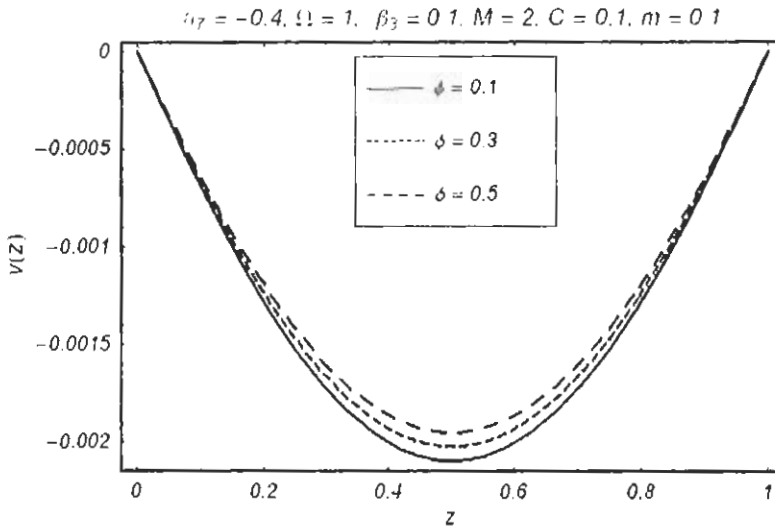


Fig. 6.4 (b). Variations of velocity component v with the increase in parameter ϕ .

Fig. 6.5 (a)

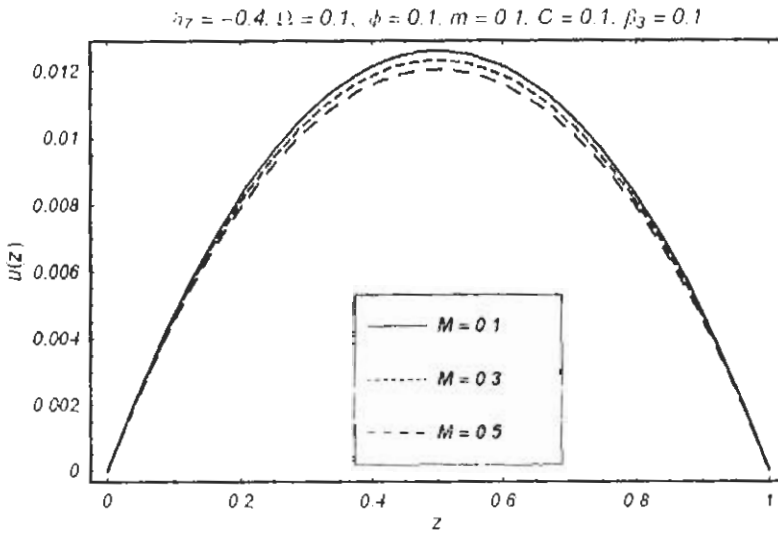


Fig. 6.5 (a). Variations of velocity component u with the increase in M .

Fig. 6.5 (b)

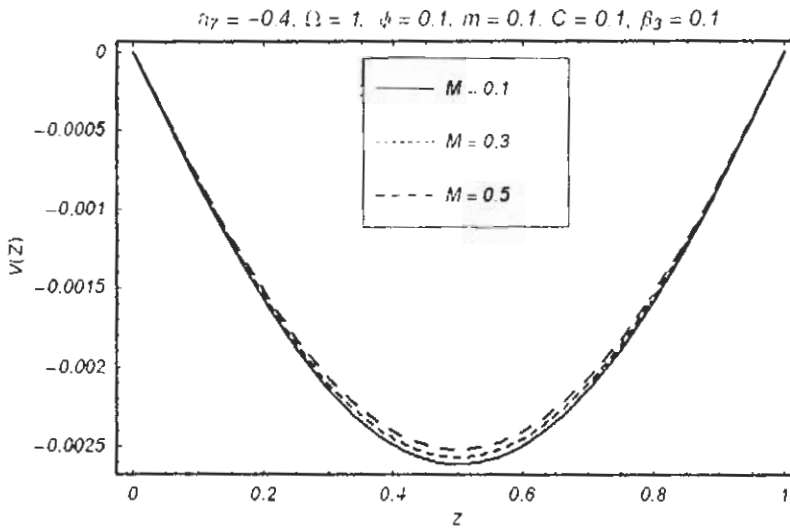


Fig. 6.5 (b). Variations of velocity component v with the increase in M .

Fig. 6.6 (a)

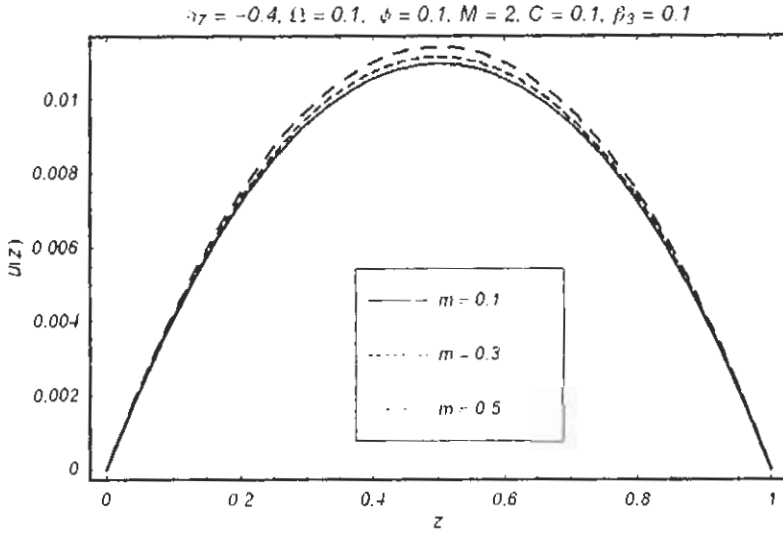


Fig. 6.6 (a). Variations of velocity component u with the increase in parameter m .

Fig. 6.6 (b)

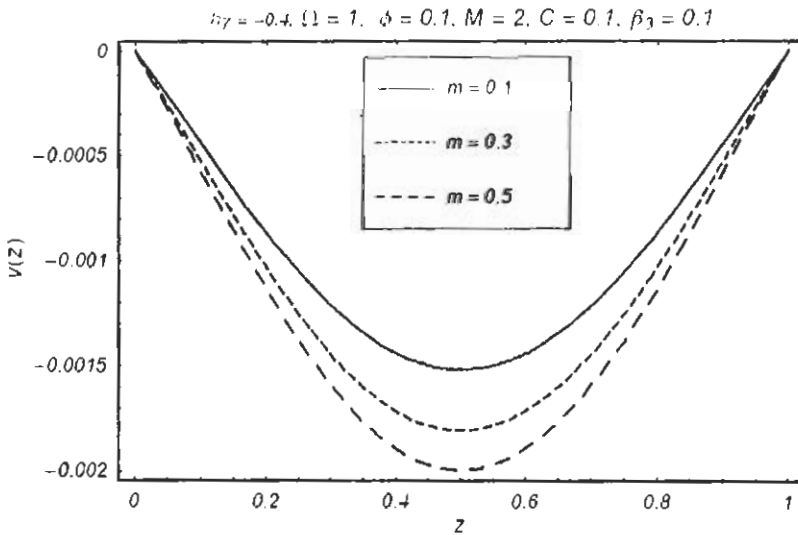


Fig. 6.6 (b). Variations of velocity component v with the increase in parameter m .

Fig. 6.7 (a)

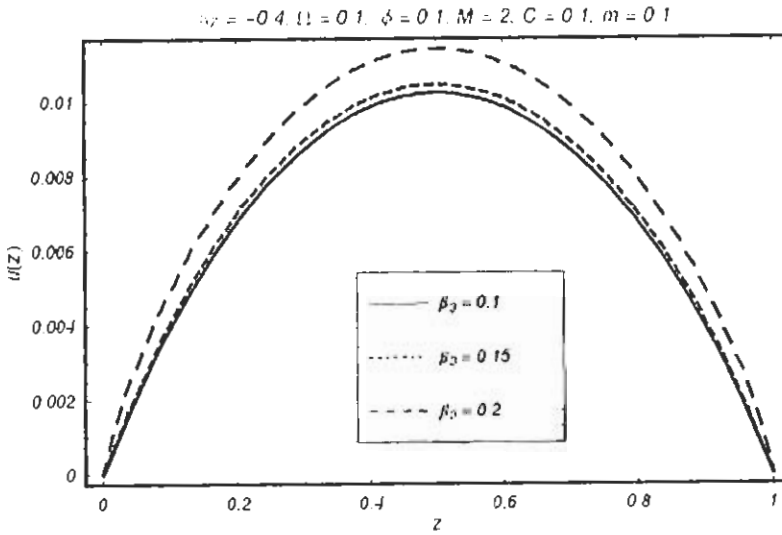


Fig. 6.7 (a). Variations of velocity component u with the increase in parameter β_3 .

Fig. 6.7 (b)

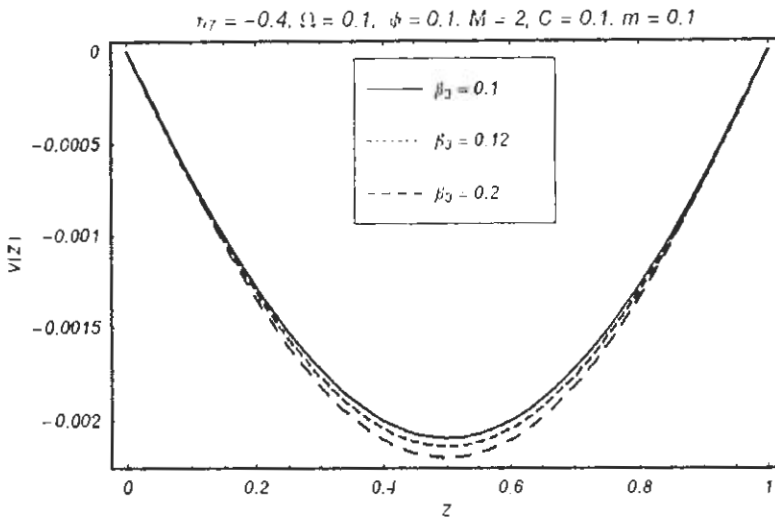


Fig. 6.7 (b). Variations of velocity component v with the increase in parameter β_3 .

Fig. 6.2(a) and 6.2(b) depicts the variation of C on the velocities u and v respectively. These Figs. show that by increasing constant pressure gradient C , the magnitude of u and v

increases. It is found from Fig. 6.3(a and b) that the magnitude of u decreases by increasing rotation parameter Ω , where this effect is opposite on velocity component v . Fig. 6.4 shows the effect of porosity parameter ϕ on u and v . It is observed that the effect of ϕ is quite opposite to that of C . Fig. 6.5(a and b) illustrates that the behavior of the parameter M on u and v is similar to that of ϕ . Figs. 6.6(a, b) and 6.7(a, b) show the variation of m and β_3 on u and v . These Figs. explore that magnitudes of u and v increase by increasing the value of m and β_3 .

Chapter 7

Heat transfer analysis on the rotating flow of a third grade fluid

The present work is concerned with the flow of a third grade fluid and heat transfer analysis between two stationary porous plates. The governing non-linear flow problem is solved analytically using homotopy analysis method (HAM). After finding the solution for velocity, the temperature profile is determined for the constant surface temperature case. Graphs for the velocity and temperature profiles are made and discussed for various values of pertinent parameters entering the problem.

7.1 Formulation of the problem

Let us consider the steady flow of a third grade fluid bounded by two porous parallel plates at $z = 0$ and $z = d$. The lower plate is subjected to a uniform suction W_0 and the upper plate is under the action of constant blowing W_0 . In the undisturbed state, both the fluid and plates are in a state of rigid body rotation with the uniform angular velocity Ω about the z -axis normal to the plates. The fluid is driven by a constant pressure gradient and heat transfer is due to constant temperature of the lower plate. By Cartesian coordinate system $Oxyz$, the motion in this rotating frame is governed by the momentum equation, the continuity equation and the

energy equation as follows

$$\rho \left[\frac{d\mathbf{V}}{dt} + 2\boldsymbol{\Omega} \times \mathbf{V} + \boldsymbol{\Omega} \times (\boldsymbol{\Omega} \times \mathbf{r}) \right] = \text{div}\boldsymbol{\sigma}, \quad (7.1)$$

$$\text{div}\mathbf{V} = 0, \quad (7.2)$$

$$\rho c \frac{d\mathbf{T}}{dt} = \boldsymbol{\sigma} \cdot \mathbf{L} - \text{div}\mathbf{q}, \quad (7.3)$$

where ρ is the fluid density, c is the specific heat, \mathbf{T} is the temperature, \mathbf{L} is the velocity gradient, t is the time, \mathbf{q} is the heat flux vector, $\boldsymbol{\sigma}$ is the Cauchy stress tensor which for a thermodynamic third grade fluid is

$$\boldsymbol{\sigma} = -p\mathbf{I} + (\mu + \beta \text{tr}\mathbf{A}_1^2) \mathbf{A}_1 + \alpha_1 \mathbf{A}_2 + \alpha_2 \mathbf{A}_1^2 \quad (7.4)$$

in which p is the pressure, \mathbf{I} is the identity tensor, μ , α_1 , α_2 , and β are material constants. The velocity field for the present flow is

$$\mathbf{V} = [u(z), v(z), w(z)], \quad (7.5)$$

which together with Eq. (7.2) gives $w = -W_0$ ($W_0 > 0$ corresponds to the suction velocity and $W_0 < 0$ indicates blowing).

The Eqs. (7.1 – 7.5) after using the following non-dimensional variables

$$\begin{aligned} F^* &= \frac{F}{U_0}, \quad z^* = \frac{z}{d}, \quad \beta^* = \frac{\beta U_0^2}{\nu \rho d^2}, \quad W_0^* = \frac{W_0 d}{\nu}, \quad \Omega^* = \frac{\Omega d^2}{\nu}, \\ \alpha_1^* &= \frac{\alpha_1}{\rho d^2}, \quad C = \frac{d^2}{\rho \nu U_0^2} \left(\frac{\partial p}{\partial x} + i \frac{\partial p}{\partial y} \right), \quad \theta(z^*) = \frac{T - T_d}{T_0 - T_d}. \end{aligned} \quad (7.6)$$

give

$$-W_0 \frac{dF}{dz} + 2i\Omega F = -C + \frac{d^2 F}{dz^2} - \alpha_1 W_0 \frac{d^3 F}{dz^3} + 2\beta \frac{d}{dz} \left[\left(\frac{dF}{dz} \right)^2 \frac{d\bar{F}}{dz} \right], \quad (7.7)$$

$$\frac{d^2 \theta}{dz^2} + \text{Pr} \left[W_0 \frac{d\theta}{dz} - E_c \left\{ \frac{\alpha_1 W_0}{2} \frac{d}{dz} \left(\frac{dF}{dz} \frac{d\bar{F}}{dz} \right) - 2\beta \left(\frac{dF}{dz} \frac{d\bar{F}}{dz} \right)^2 - \frac{dF}{dz} \frac{d\bar{F}}{dz} \right\} \right] = 0, \quad (7.8)$$

where $F = u + iv$, $\bar{F} = u - iv$, the Prandtl number $\text{Pr} = \mu c_p / k$, the Eckert number

$E_c = U_0^2/c_p(T_0 - T_d)$, ν the kinematic viscosity and asterisks have been suppressed for brevity.

The non-dimensional boundary conditions are

$$F(0) = 0, \quad F(1) = 0, \quad \theta(0) = 1, \quad \theta(1) = 0. \quad (7.9)$$

7.2 HAM solution for $F(z)$

Here the initial approximation $F_0(z)$ and the auxiliary linear operator \mathcal{L}_5 are

$$F_0(z) = \frac{C}{2}(z^2 - z), \quad (7.10)$$

$$\mathcal{L}_5(F) = F'' - C, \quad \mathcal{L}_5(Cz^2 + C_{12}z + C_{13}) = 0, \quad (7.11)$$

where C is a constant pressure gradient and C_{12} and C_{13} are arbitrary constants. By employing the similar procedure as in the previous chapters, the HAM solution of F is given by

$$F(z) = \lim_{M \rightarrow \infty} \left[\sum_{n=1}^{4M+2} \left(\sum_{m=n-1}^{4M+1} a_{m,n} z^n \right) \right], \quad (7.12)$$

where for $m \geq 1$, $0 \leq n \leq 4m + 2$ we have

$$a_{m,1} = \chi_m \lambda_{4m-1} a_{m-1,1} + \frac{C}{2} - \sum_{n=0}^{4m+2} \frac{\Gamma_{m,n}}{(n+1)(n+2)}, \quad (7.13)$$

$$a_{m,2} = \chi_m \lambda_{4m-2} a_{m-1,2} - \frac{C}{2} + \frac{\Gamma_{m,0}}{2}, \quad (7.14)$$

$$a_{m,n} = \chi_m \lambda_{4m-n} a_{m-1,n} + \frac{\Gamma_{m,n-2}}{n(n-1)}, \quad 3 \leq n \leq 4m+2, \quad (7.15)$$

$$\Gamma_{m,n} = \begin{cases} \hbar_8 \left[\begin{array}{l} C(1 - \chi_m) - W_0 b_{m-1,0} + 2i\Omega a_{m-1,0} \\ + (\alpha_1 W_0 - 1) c_{m-1,0} - 2\beta(2\delta_{m,0} + \Delta_{m,0}) \end{array} \right], & n = 0, \\ \hbar_8 \left[\begin{array}{l} \chi_{2m-n+1} \{-W_0 b_{m-1,n} + 2i\Omega a_{m-1,n} + (\alpha_1 W_0 - 1) c_{m-1,n}\} - \\ 2\beta(2\delta_{m,n} + \Delta_{m,n}) \end{array} \right], & n \geq 1, \end{cases} \quad (7.16)$$

$$\delta_{m,n}^q = \sum_{k=0}^{m-1} \sum_{l=0}^k \sum_{p=\max\{0, n-2m+2k+1\}}^{\min\{n, 2k+2\}} \sum_{s=\max\{0, p-2k+2l-1\}}^{\min\{p, 2l+1\}} \bar{b}_{l,s} b_{k-l, p-s} c_{m-1-k, n-p}, \quad (7.17)$$

$$\Delta_{m,n}^q = \sum_{k=0}^{m-1} \sum_{l=0}^k \sum_{p=\max\{0, n-2m+2k+1\}}^{\min\{n, 2k+2\}} \sum_{s=\max\{0, p-2k+2l-1\}}^{\min\{p, 2l+1\}} \bar{c}_{l,s} b_{k-l, p-s} b_{m-1-k, n-p}, \quad (7.18)$$

$$b_{m,n} = (n+1) a_{m, n+1}, \quad c_{m,n} = (n+1) b_{m, n+1}, \quad (7.19)$$

$$a_{0,0} = 0, \quad a_{0,1} = -\frac{C}{2}, \quad a_{0,2} = \frac{C}{2}. \quad (7.20)$$

7.3 HAM solution for $\theta(z)$

Here we select the following initial approximation (θ_0) and an auxiliary linear operator (\mathcal{L}) in the form

$$\theta_0(z) = 1 - z, \quad (7.21)$$

$$\mathcal{L}_A(\theta) = \theta'', \quad \mathcal{L}(C_{10}z + C_{11}) = 0, \quad (7.22)$$

in which C_{10} and C_{11} are arbitrary constants.

Following the same methodology of solution as for F one can get

$$\theta(z) = \lim_{M \rightarrow \infty} \left[\sum_{n=1}^{4M+4} \left(\sum_{m=n-1}^{4M+3} \alpha_{m,n} z^n \right) \right], \quad (7.23)$$

where for $m \geq 1$, $0 \leq n \leq 4m+4$ we have

$$\alpha_{m,0} = \chi_m \lambda_{4m+2} \alpha_{m-1,0}, \quad (7.24)$$

$$\alpha_{m,1} = \chi_m \lambda_{4m+1} \alpha_{m-1,1} - \sum_{n=0}^{4m+4} \frac{\Gamma 1_{m,n}}{(n+1)(n+2)}, \quad (7.25)$$

$$\alpha_{m,n} = \chi_m \lambda_{4m-n+2} \alpha_{m-1,n} + \frac{\Gamma 1_{m,n-2}}{n(n-1)}, \quad 2 \leq n \leq 4m+2, \quad (7.26)$$

$$\Gamma 1_{m,n} = \hbar_9 \left[\chi_{4m-n+2} \left\{ \begin{array}{c} e_{m-1,n} + \Pr W_0 d_{m-1,n} \\ - \Pr E_c \left(\frac{\alpha_1 W_0}{2} (\Delta_{m,n} + \beta_{m,n}) - \gamma_{m,n} \right) \end{array} \right\} - 2 \Pr E_c \beta \delta_{m,n} \right], \quad (7.27)$$

$$\Delta_{m,n} = \sum_{k=0}^{m-1} \sum_{s=\max\{0, n-4(m-k)+2\}}^{\min\{n, 4k+2\}} c_{m-1-k, n-s} \bar{b}_{k,s}, \quad (7.28)$$

$$\beta_{m,n} = \sum_{k=0}^{m-1} \sum_{s=\max\{0, n-4(m-k)+2\}}^{\min\{n, 4k+2\}} b_{m-1-k, n-s} \bar{c}_{k,s}, \quad (7.29)$$

$$\gamma_{m,n} = \sum_{k=0}^{m-1} \sum_{s=\max\{0, n-4(m-k)+2\}}^{\min\{n, 4k+2\}} b_{m-1-k, n-s} \bar{b}_{k,s}, \quad (7.30)$$

$$\begin{aligned} \delta_{m,n} = & \sum_{k=0}^{m-1} \sum_{l=0}^k \sum_{i=0}^l \sum_{q=\max\{0, n-4(m-k)+2\}}^{\min\{n, 4k+6\}} \sum_{p=\max\{0, q-4(k-l)-4\}}^{\min\{q, 4l+4\}} \\ & \sum_{r=\max\{0, p-4(l-i)-2\}}^{\min\{p, 4i+2\}} \bar{b}_{i,r} \bar{b}_{l-i, p-r} b_{k-l, q-p} b_{m-1-k, n-q}, \end{aligned} \quad (7.31)$$

$$b_{m,n} = (n+1) a_{m, n+1}, \quad c_{m,n} = (n+1) b_{m, n+1}, \quad (7.32)$$

$$d_{m,n} = (n+1) \alpha_{m, n+1}, \quad e_{m,n} = (n+1) d_{m, n+1}, \quad (7.33)$$

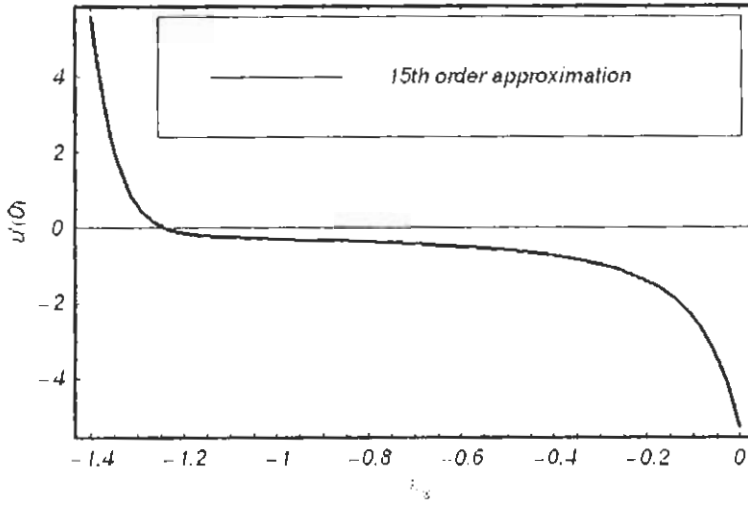
$$\alpha_{0,0} = 1, \quad \alpha_{0,1} = -1. \quad (7.34)$$

7.4 Convergence of the solution

The expressions given in Eqs. (7.12) and (7.23) contain two auxiliary parameters \hbar_8 and \hbar_9 . The \hbar -curves are plotted in Figs. 7.1 and 7.2 for 15th order of approximation for the non-dimensional velocity profiles u and v . Furthermore Fig. 7.3 is the \hbar_8 -curve for the non-dimensional temperature profile θ for 15th order of approximation. It is evident from Figs. 7.1 and 7.2 that the range for the admissible value \hbar_8 is $-1 \leq \hbar_8 < -0.3$ and for Fig. 7.3 the admissible value of \hbar_9 is $-1.8 \leq \hbar_9 < -0.3$. From the calculations it is noted that the real part of the series given by Eq. (7.12) converges in the whole region of z when $\hbar_8 = -0.6$ and the imaginary part for $\hbar_8 = -0.5$. The series (7.23) converges in the whole region of z when $\hbar_9 = -0.8$.

Fig. 7.1 (a)

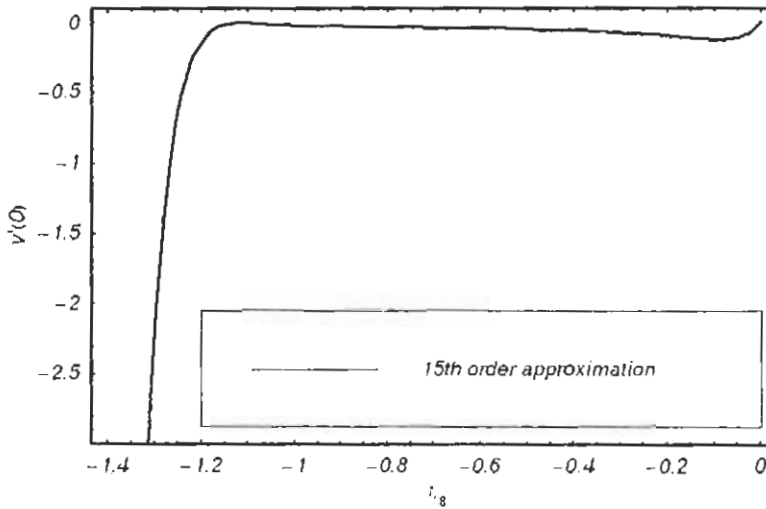
$$W_0 = 2, \alpha_1 = 1, \beta = 0.1, C = 0.1, \Omega = 1.$$



Figs. 7.1 (a). h -curve of velocity profile u for 15th order of approximation.

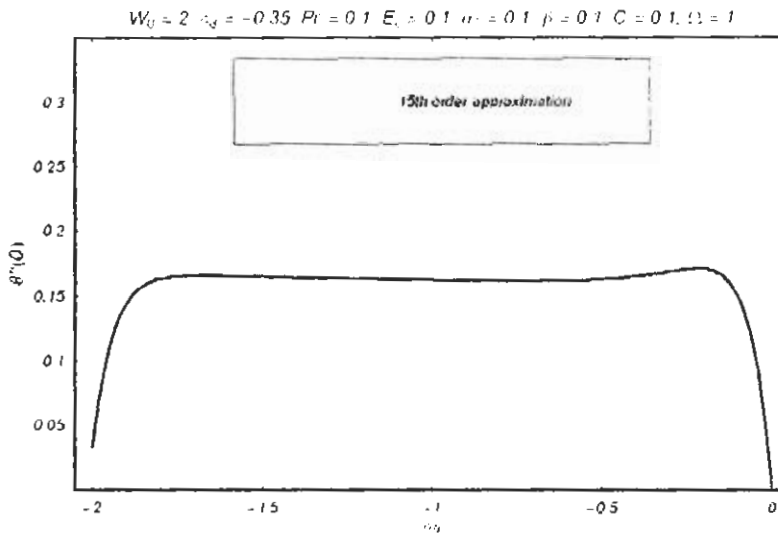
Fig. 7.1(b)

$$W_0 = 2, \alpha_1 = 1, \beta = 0.1, C = 0.1, \Omega = 1.$$



Figs. 7.1 (b). h -curve of velocity profile v for 15th order of approximation.

Fig.7.1(c)



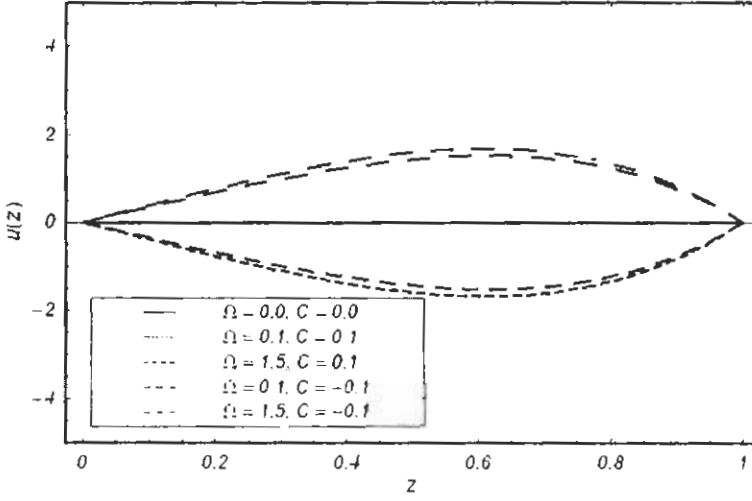
Figs. 7.1 (c). \bar{h} -curve of temperature profile θ for 15th order of approximation.

7.5 Results and discussion

This section is developed to observe the effects of different parameters W_0 , α_1 , β and Ω for the case when $C > 0$ and $C < 0$ on the velocity profiles u and v . For this purpose 7.2(a) – 7.5(b) have been plotted for variations in different parameters.

Fig. 7.2 (a)

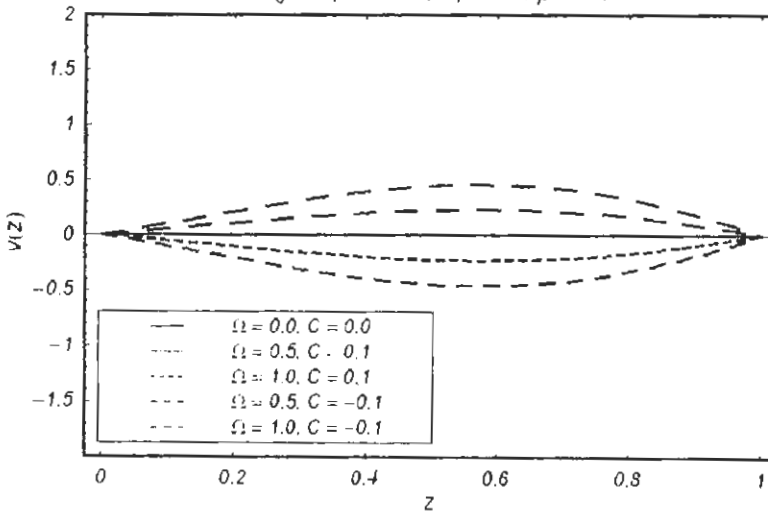
$$W_0 = 2, \nu = -0.5, \alpha_1 = 0.1, \beta = 0.1$$



Figs. 7.2 (a). Variations of velocity profile u with the change in parameter Ω .

Fig. 7.2 (b)

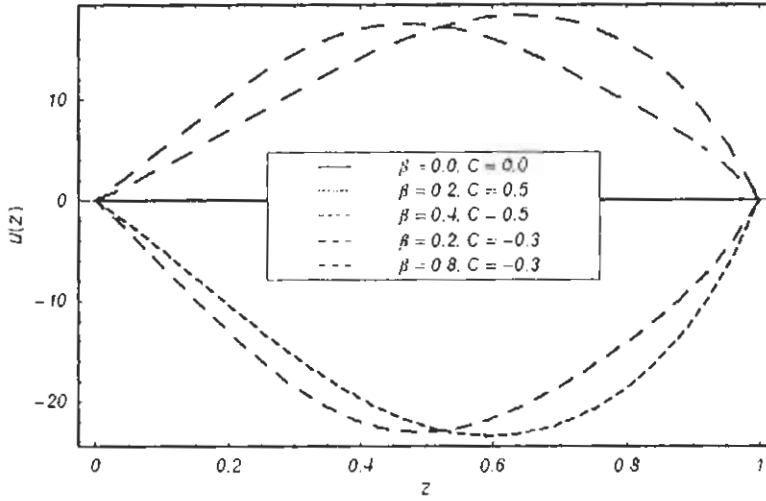
$$W_0 = 2, \nu = -0.5, \alpha_1 = 0.1, \beta = 0.1$$



Figs. 7.2 (b). Variations of velocity profile v with the change in parameter Ω .

Fig. 7.3 (a)

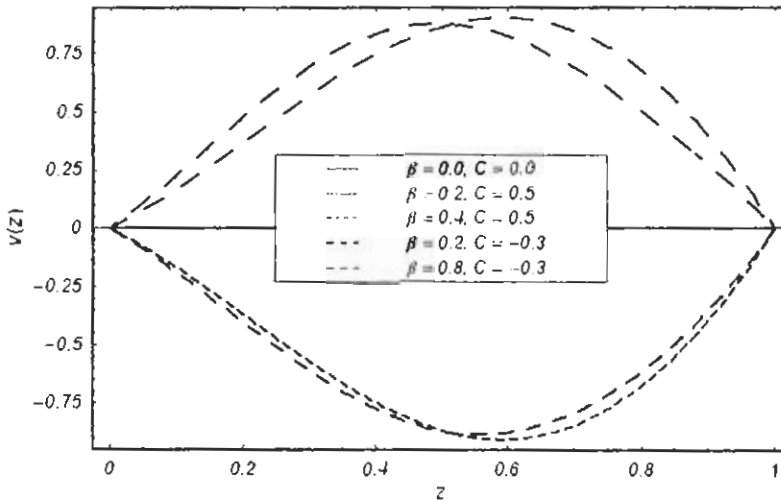
$W_0 = 2, \alpha = -0.5, \alpha_T = 0.1, \Omega = 0.1$



Figs. 7.3 (a). Variations of velocity profile u with the change in parameter β .

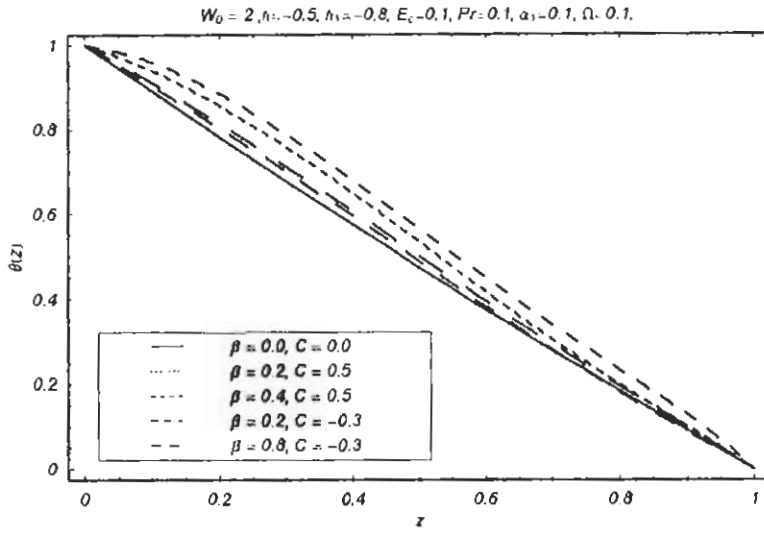
Fig. 7.3 (b)

$W_0 = 2, \alpha = -0.5, \alpha_T = 0.1, \Omega = 0.1$



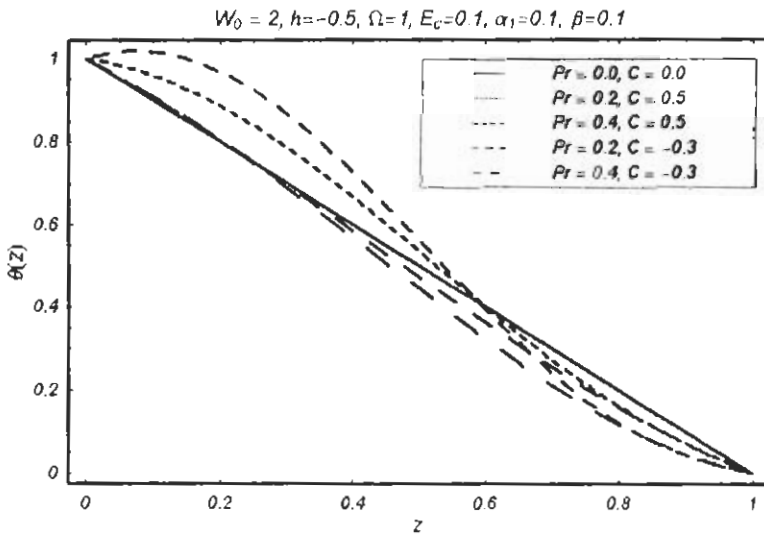
Figs. 7.3 (b). Variations of velocity profile v with the change in parameter β .

Fig. 7.4 (a)



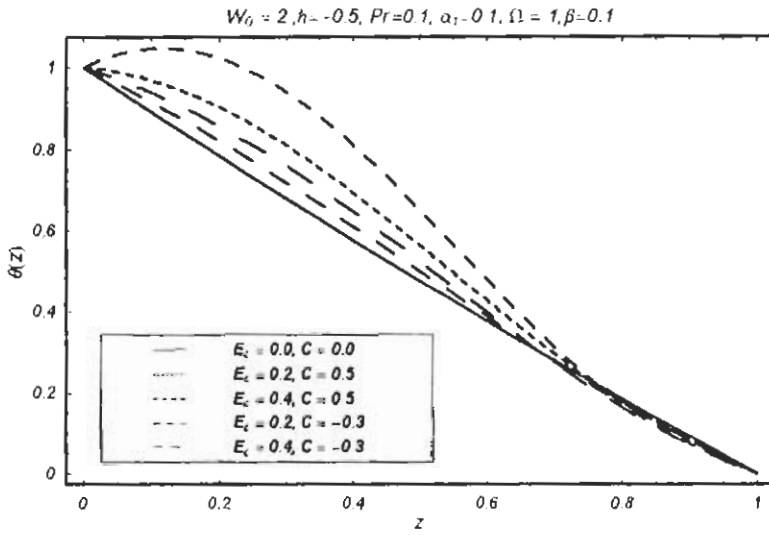
Figs. 7.4 (a). Variations of temperature profile θ with the change in parameter β .

Fig. 7.4 (b)



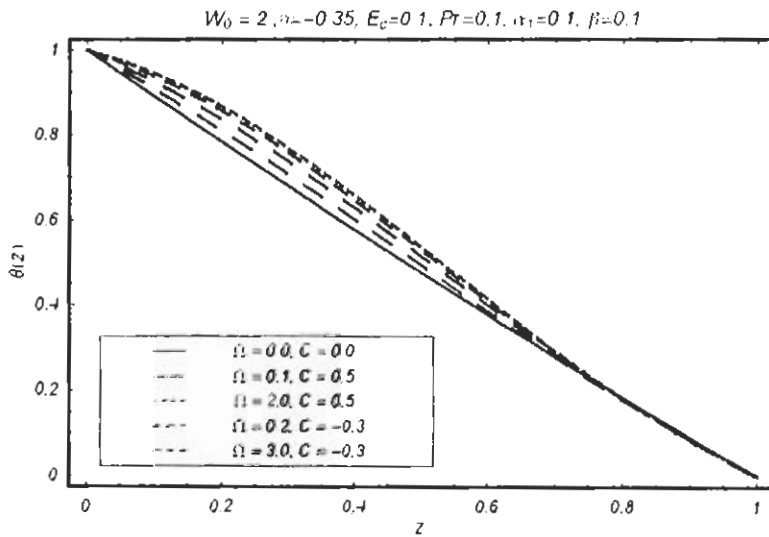
Figs. 7.4 (b). Variations of temperature profile θ with the change Prandtl number Pr .

Fig. 7.5 (a)



Figs. 7.5 (a). Variations of temperature profile θ with the change in number E_c .

Fig. 7.5 (b)



Figs. 7.5 (b). Variations of temperature profile θ with the change in rotation parameter Ω .

Figures. 7.2 – 7.5 are made just to analyze the variations of velocity profiles u and v for the rotation parameter Ω and third grade parameter β for different cases $C > 0$ and $C < 0$. It is obvious from the Figs. 7.2 (a) and 7.2 (b) that the magnitude of u decreases and v increases by increasing Ω when $C > 0$ and $C < 0$. The behavior of third grade parameter β is shown in Figs. 7.3 (a) and 7.3 (b). These figures show that the magnitude of velocity profiles u and v increases up to $z = 0.5$ and then decreases. Also third grade parameter causes the huge fluctuation in the magnitude of real component u of the velocity. To see the effect of the emerging parameters on the temperature distribution, Figs. 7.4 (a, b) – 7.5 (a, b) are prepared. The behavior of third grade parameter β on temperature is shown in Fig. 7.4 (a). It elucidates that an increase in β gives the decrease in the temperature profile. However positive pressure gradient causes the substantial change in temperature in comparison to the negative pressure gradient. It is shown in Fig. 7.4 (b) that the temperature increases with an increase in the Prandtl number but about $z = 0.6$ its behavior is quite opposite for the case of positive pressure gradient. On the other hand, for negative pressure gradient the temperature decreases with an increase in Prandtl number. The behavior of Eckert number (as shown in Fig. 7.5 (a)) initially is quite similar to the behavior of third grade parameter initially and at $z = 0.7$ its behavior changes abruptly. Fig. 7.5 (b). depicts the behavior of the rotation parameter Ω which is quite similar to the behavior of third grade parameter on the temperature distribution.

Chapter 8

Conclusions

This thesis is mainly concerned with the flows of second and third grade fluids in rotating frame. Linear and non-linear stretching/shrinking flows have been taken into an account. Fundamental concept of three dimensional stretching is considered. Chapter one of this thesis contains useful material for the subsequent chapters. Throughout the thesis the technique used is a homotopy analysis method (HAM). From the analysis presented in chapters two to seven, the following points have been noted.

- In semi-infinite domain, the researchers in the fluid mechanics dealt with the issue of extra boundary conditions through augmentation process. It is shown here that homotopy analysis method in such domain is able to give us meaningful solution without the augmentation process.
- Since Pade' approximation is used to accelerate the convergence of the series. It is noted that homotopy Pade' approximation is more useful than the usual Pade' approximation. It is further found that such approximation is independent upon an auxiliary parameter embedded in the equation to control and adjust the convergence for the series solution.
- Suction phenomenon causes reduction in the boundary layer thickness.
- The velocity components increases by increasing the injection velocity.
- The role of the Hartman number on the velocity components is similar to that of the suction velocity.

- Porosity if the medium decreases the magnitude of the velocity components.
- The magnitude of x-component of velocity in non-linear stretching case is much when compared with linear stretching.
- The magnitude of y-component of velocity in linear stretching is more than the non-linear stretching case.
- The normal stress coefficient in a second grade fluid increases the horizontal components of velocity. However it decreases the transverse component of velocity.
- The magnitude of velocity components increases by increasing an applied pressure gradient.
- Increase in the Hall parameter increases the magnitude of velocity components.
- The behavior of third grade parameter on the velocity is similar to that of hall parameter.
- Increase in the third grade parameter increases the temperature profile for both reverse and favorable pressure gradients.
- The variation of the Prandtl number for the positive pressure gradient is increases the temperature where as for negative pressure gradient, variation of temperature is reverse.
- Effects of Eckert and Prandtl number are same on the temperature for positive pressure gradient. However for negative pressure gradient their effects are opposite.

Bibliography

- [1] I. Hartman and HG-Dynamics, I: Theory of laminar flow of an electrically conductive liquid in a homogeneous magnetic field. Kg. 1. Danske Videnskabernes Selskab, Math. Fys. Medd. **15**, (1937).
- [2] V.J. Rossow: On flows of electrically conducting fluids over a flat plate in the presence of a transverse magnetic field, NASA report **1358**, 489 – 508 (1958).
- [3] Y. Wang and T. Hayat: Hydromagnetic rotating flows of a fourth order fluid past a porous plate, Math. Meth. Appl. Sci. **27**, 477 – 496 (2004).
- [4] T. Hayat, T. Haroon, S. Asghar and A.M. Siddiqui: MHD flow of a third grade fluid due to eccentric rotations of a porous disk and a fluid at infinity, Int. J. Non-Linear Mech. **38**, 501 – 511 (2003).
- [5] T. Hayat, K. Hutter, S. Asghar and A.M. Siddiqui: MHD flows of an Oldroyd-B fluid, Math. Comp. Model. **36**, 987 – 995 (2002).
- [6] J.C. Misra, G.C. Shit and H.J. Rath: Flow and heat transfer of a MHD viscoelastic fluid in a channel with stretching walls: Some applications to haemodynamics, Computers & Fluids **37**, 1 – 11 (2008).
- [7] M. Amkadni, A. Azzouzi and Z. Hammouch: On the exact solutions of laminar MHD flow over a stretching flat plate, Comm. Non-linear Sci. Numer. Simu. **13**, 359 – 368 (2008).
- [8] K. Sadeghy, N. Khabazi and S.M. Taghavi: Magnetohydrodynamic (MHD) flows of a viscoelastic fluids in converging/diverging channels, Int. J. Eng. Sci. **45**. 923 – 938 (2007).

- [9] M. Khan, C. Fetecau and T. Hayat: MHD transient flows in a channel of rectangular cross-section with porous medium, *Phys. Lett. A* **369**, 44 – 54 (2007).
- [10] M. Khan, S.H. Ali, T. Hayat and C. Fetecau: MHD flows of a second grade fluid between two side walls perpendicular to a plate through a porous medium, *Int. J. Non-Linear Mech.* (In press).
- [11] Z. Abbas and T. Hayat: Radiation effects on MHD flow in a porous space, *Int. J. Heat Mass Transfer* (In press).
- [12] T.V.S. Sekhar, R. Sivakumar, T.V.R. Kumar and K. Subbarayudu: High Reynolds number incompressible MHD flow under low R_m approximation, *Int. J. Non-linear Mech.* (In press).
- [13] F.S. Ibrahim, A.M. Elaiw and A.A. Bakr: Effect of the chemical reaction and radiation absorption on the unsteady MHD free convection flow past a semi infinite vertical permeable moving plate with heat source and suction, *Comm. Non-linear Sci. Numer. Simu.* **13**, 1056 – 1066 (2008).
- [14] R. Cortell: MHD flow and mass transfer of an electrically conducting fluid of second grade in a porous medium over a stretching sheet with chemically reactive species, *Chem. Eng. Proc.* **46**, 721 – 728 (2007).
- [15] A. Pantokratoras: Study of MHD boundary layer flow over a heated stretching sheet with variable viscosity, A numerical reinvestigation, *Int. J. Heat Mass Transfer* **51**, 104 – 110 (2008).
- [16] M.J. Pattison, K.N. Premnath, N.B. Morley and M.A. Abdou: Progress in lattice Boltzmann methods for magnetohydrodynamic flows relevant to fusion applications, *Fusion Engineering and Design* (In Press)
- [17] J. Liu, S. Tavener and H. Chen: ELLAM for resolving the kinematics of two-dimensional resistive magnetohydrodynamic flows, *J. Comput. Phys.* **227**, 1372 – 1386 (2007).

- [18] V. Aliakbar, A. Alizadeh-Pahlavan and K. Sadeghy: The Influence of thermal radiation on MHD Flow of Maxwellian fluids above stretching sheets, *Comm. Non-linear Sci. Numer. Simu.* (In Press).
- [19] H.F. Hakan, M. Oztop and Y. Varol: Numerical simulation of magnetohydrodynamic buoyancy-induced flow in a non-isothermally heated square enclosure, *Comm. Non-linear Sci. Numer. Simu.* (In press).
- [20] M.J. Ni, R. Munipalli, N. B. Morley, P. Huang and M.A. Abdou: A current density conservative scheme for incompressible MHD flows at a low magnetic Reynolds number. Part I: On a rectangular collocated grid system, *J. Comp. Phys.* **227**, 174 – 204 (2007).
- [21] M.J. Ni, R. Munipalli, P. Huang, N.B. Morley and M.A. Abdou: A current density conservative scheme for incompressible MHD flows at a low magnetic Reynolds number. Part II: On an arbitrary collocated mesh, *J. Comput. Phys.* **227**, 205 – 228 (2007).
- [22] E. Osalusi, J. Side and R. Harris: The effects of Ohmic heating and viscous dissipation on unsteady MHD and slip flow over a porous rotating disk with variable properties in the presence of Hall and ion-slip currents, *Int. Comm. Heat Mass Transfer* **34**, 1017 – 1029 (2007).
- [23] A. A. Pahlavan, V. Aliakbar, F. V. Farahani and K. Sadeghy: MHD flows of UCM fluids above porous stretching sheets using two-auxiliary-parameter homotopy analysis method, *Comm. Non-linear Sci. Numer. Simu.* (In press).
- [24] R. Samulyak, J. Du, J. Glimm and Z. Xu: A numerical algorithm for MHD of free surface flows at low magnetic Reynolds numbers, *J. Comput. Phys.* **226**, 1532 – 1549 (2007).
- [25] S.M.M. EL-Kabeir, M.A. EL-Hakiem and A.M. Rashad: Group method analysis of combined heat and mass transfer by MHD non-Darcy non-Newtonian natural convection adjacent to horizontal cylinder in a saturated porous medium, *App. Math. Model.* (In press)
- [26] A.M. Salem: Variable viscosity and thermal conductivity effects on MHD flow and heat transfer in viscoelastic fluid over a stretching sheet, *Phy. Lett. A* **369**, 315 – 322 (2007).

- [27] N.T.M. Eldabe, M.F. El-Sayed, A.Y. Ghaly and H.M. Sayed: Peristaltically induced transport of a MHD biviscosity fluid in a non-uniform tube, *Physica A* **383**, 253 – 266 (2007).
- [28] M.S. Abel and N. Mahesha: Heat transfer in MHD viscoelastic fluid flow over a stretching sheet with variable thermal conductivity, non-uniform heat source and radiation, *Appl. Math. Model.* (In press).
- [29] S. Chandrasekhar: The stability of viscous flow between rotating cylinders in the presence of a magnetic field, *Proy. Roy. Soc. A* **216**, 293 – 309 (1953).
- [30] S. Chandrasekhar: The instability of a layer of fluid heated below and subject to a Coriolis force, *Proc. Roy. Soc. A* **217**, 306 – 327 (1953).
- [31] S. Chandrasekhar: *Hydrodynamic and hydromagnetic stability*, Oxford University Press, 1961.
- [32] B. Lehnert: Magnetohydrodynamic waves under the action of the Coriolis force, *J. Astrophys* **119**, 647 – 753 (1954).
- [33] B. Lehnert: Magnetohydrodynamic waves under the action of the Coriolis force II, *J. Astrophys* **121**, 481 – 489 (1955).
- [34] V. Vidyanidhi: Secondary flow of a conducting fluid in a rotating channel, *J. Math. Phys. Sci.* **3**, 193 (1969).
- [35] R.S. Nanda and H.K. Mohanty: Hydromagnetic flow in a rotating channel, *Appl. Sci. Res.* **24**, 65 – 78 (1971).
- [36] A.S. Gupta: Ekman layer on a porous plate, *Phys. Fluids* **15**, 930 – 931 (1972).
- [37] I. Pop and V.M. Soundalgekar: Effects of Hall current on hydromagnetic flow near a porous plate, *Acta Mech.* **20**, 315 – 318 (1974).
- [38] D.E. Loper: Steady hydromagnetic boundary layer flow near a rotating electrically conducting plate, *Phys. Fluids* **13**, 2999 – 3002 (1970).

- [39] D.E. Loper: A linear theory of rotating, thermally stratified hydromagnetic flow, *J. Fluid Mech.* **72**, 1 – 16 (1975).
- [40] Y. Hsueh: Viscous fluid flow over a corrugated bottom in a strongly rotating system, *Phys. Fluids* **5**, 940 – 944 (1968).
- [41] M.C. Potter and M.D. Chawla: Stability of boundary layer subject to rotation, *Phys. Fluids* **11**, 2278 – 2281 (1971).
- [42] P.A. Gilman: Instabilities of the Ekman-Hartman boundary layer, *Phys. Fluids* **14**, 7 – 12 (1971).
- [43] K. Vajravelu and L. Debnath: A study of nonlinear convective flows in rotating wavy channels, *ZAMM* **64**, 303 – 308 (1984).
- [44] C. Thornley: On Stokes and Rayleigh layers in a rotating system, *Quart. J. Mech. Appl. Math.* **21**, 451 – 461 (1968).
- [45] L. Debnath: Inertial oscillations and hydromagnetic multiple boundary layers in a rotating fluid, *ZAMM* **55**, 141 – 147 (1975).
- [46] L. Debnath, S.C. Ray and A.K. Chatterjee: Effects of Hall current on unsteady hydro-magnetic flow past a porous plate in a rotating fluid system, *ZAMM* **59**, 469 – 471 (1979).
- [47] L. Debnath and S. Mukherjee: Unsteady multiple boundary layers on a porous plate in a rotating system, *Phys. Fluids* **16**, 1418 – 1421 (1973).
- [48] L. Debnath and S. Mukherjee: Inertial oscillations and multiple boundary layers in an unsteady rotating flow, *Phys. Fluids* **17**, 1372 – 1375 (1974).
- [49] G.S. Seth and R.N. Jana: Unsteady hydromagnetic flow in a rotating channel with oscillating pressure gradient, *Acta Mech.* **37**, 29 – 41 (1980).
- [50] B.S. Mazumder, A.S. Gupta and N. Data: Flow and heat transfer in the hydromagnetic Ekman layer on a porous plate with Hall effects, *Int. J. Heat Mass Transfer* **19**, 523 – 527 (1976).

- [51] B.S. Mazumder: An exact solution of oscillatory Couette flow in a rotating system, ASME J. Appl. Mech. **58**, 1104 – 1107 (1991).
- [52] R. Ganapthy: A note on oscillatory Couette flow in a rotating system, ASME J. Appl. Mech. **61**, 208 – 209 (1994).
- [53] K.D. Singh: An oscillatory hydromagnetic flow in a rotating system, ZAMM **80**, 429–432 (2000).
- [54] T. Hayat, C. Fetecau and M. Sajid: On MHD transient flow of a Maxwell fluid in a porous medium and rotating frame, Phys. Lett. A (In press).
- [55] T. Hayat, C. Fetecau and M. Sajid: Analytic solution for MHD transient rotating flow of a second grade fluid in a porous space, Nonlinear Anal. (In press).
- [56] T. Hayat, S. Mumtaz and R. Ellahi: MHD unsteady flows due to non-coaxial rotation of a disk and a fluid at infinity, Acta Mech. Sin. **19**, 235 – 240 (2003).
- [57] T. Hayat, S. Nadeem, A. M. Siddiqui and S. Asghar: An oscillating hydromagnetic non-Newtonian flow in a rotating system, Appl. Math. Lett. **17**, 609 – 614 (2004).
- [58] T. Hayat, S. Nadeem and S. Asghar: Hydromagnetic Couette flow of an Oldroyd-B fluid in a rotating system, I. J. Eng. Sci. **42**, 65 – 78 (2004).
- [59] A.M. Siddiqui, T. Haroon, T. Hayat and S. Asghar: Unsteady MHD flow of a non-Newtonian fluid due to eccentric rotations of a porous disk and a fluid at infinity, Acta Mech. **147**, 99 – 109 (2001).
- [60] A.M. Siddiqui, M. Khan, S. Asghar and T. Hayat: Exact solutions in MHD rotating flow, Mech. Research Comm. **28**, 485 – 491 (2001).
- [61] L. Howarth: On the solution of the laminar boundary layer equations, Proc. Roy. Soc. London A **164**, 547 – 579 (1938).
- [62] A.M.M. Abussita: A note on a certain boundary layer equation, Appl. Math. Comput. **64**, 73 – 77 (1994).

- [63] C.Y. Wang: A new algorithm for solving classical Blasius equation, *Appl. Math. Comput.* **157**, 1 – 9 (2004).
- [64] B.C. Sakiadis: Boundary layer behavior on continuous solid surface: I. Boundary-layer equations for two-dimensional and axisymmetric flow, *AIChE.* **7**, 26 – 28 (1961).
- [65] F.K. Tsou, E.M. Sparrow and R.J. Goldstein: Flow and heat transfer in the boundary layer on a continuous moving surface, *Int. J. Heat and Mass Transfer* **10**, 219 – 235 (1967).
- [66] B.C. Sakiadis: Boundary layer behavior on continuous solid surface: II. Boundary-layer equations on continuous solid surface, *AIChE.* **7**, 221 – 225 (1961).
- [67] L.E. Erickson, L.T. Van and V.G. Fox: Heat and mass transfer on a moving continuous flat plate with suction or injection, *Indust. Eng. Chem.* **5**, 19 – 25 (1966).
- [68] L.J. Crane: Flow past a stretching plate, *ZAMP* **21**, 645 – 647 (1970).
- [69] H.I. Andersson, J.B. Aerseth, B.S. Braud and B.S. Dandapat: Flow of a power-law fluid film on an unsteady stretching surface, *J. non-Newtonian Fluid Mech.* **62**, 1 – 8 (1996).
- [70] W.C. Troy and E.A. Overman, G.B. Ermentrout and J.P. Keener: Uniqueness of flow of a second-order fluid past a stretching surface, *Quart. Appl. Math.* **44**, 753 – 755 (1987).
- [71] P.D. Ariel: MHD flow of a viscoelastic fluid past a stretching sheet with suction, *Acta Mech.* **105**, 49 – 56 (1994).
- [72] P.S. Debnath and A.S. Gupta: Flow and heat transfer in a viscoelastic fluid over a stretching sheet, *Int. J. Non-Linear Mech.* **24**, 215 – 219 (1989).
- [73] W.T. Cheng and C.N. Huang: Unsteady flow and heat transfer on an accelerating surface with blowing or suction in the absence and presence of a heat source or sink, *Chem. Eng. Sci.* **59**, 771 – 780 (2004).
- [74] P.S. Gupta and A.S. Gupta: Heat and mass transfer on a stretching sheet with suction or blowing, *Can. J. Chem. Eng.* **55**, 744 – 746 (1977).
- [75] C.K. Chen and M. Char: Heat transfer of a continuous stretching surface with suction or blowing, *J. Math. Anal. Appl.* **135**, 568 – 580 (1988).

- [76] B.K. Dutta: Heat transfer from a stretching sheet with uniform suction and blowing, *Acta Mech.* **78**, 255 – 262 (1989).
- [77] K. Vajravelu: Hydromagnetic flow and heat transfer over a continuous moving porous flat surface, *Acta Mech.* **64**, 197 – 185 (1986).
- [78] T. Hayat and M. Sajid: Analytic solution for axisymmetric flow and heat transfer of a second grade fluid past a stretching sheet, *Int. J. Heat Mass Transfer* **50**, 75 – 84 (2007).
- [79] T. Hayat, Z. Abbas and T. Javed: Mixed convection flow of a micropolar fluid over a non-linearly stretching sheet, *Phys. Lett. A* (In press).
- [80] M. Sajid, T. Hayat and S. Asghar: Non-similar analytic solution for MHD flow and heat transfer in a third-order fluid over a stretching sheet, *Int. J. Heat Mass Transfer* **50**, 1723 – 1736 (2007).
- [81] M. Sajid, I. Ahmad, T. Hayat and M. Ayub: Series solution for unsteady axisymmetric flow and heat transfer over a radially stretching sheet, *Comm. Non-linear Sci. Numer. Simu.* (In press).
- [82] M. Sajid, I. Ahmad, T. Hayat and M. Ayub: Unsteady flow and heat transfer of a second grade fluid over a stretching sheet, *Comm. Non-linear Sci. Numer. Simu.* (In press).
- [83] K. Vajravelu and J.R. Cannon: Fluid flow over a nonlinearly stretching sheet, *Appl. Math. Comput.* **181**, 609 – 618 (2006).
- [84] T. Hayat, Masood Khan and M. Ayub: The effect of the slip condition on flows of an Oldroyd 6-constant fluid, *J. Comput. Appl. Math.* **202**, 402 – 413 (2007).
- [85] E. Magyari and B. Kellar: Heat and mass transfer in the boundary layers on an exponentially stretching continuous surface, *J. Phys. D: Appl. Phys.* **32**, 577 – 585 (1999).
- [86] M. Sajid and T. Hayat: Influence of thermal radiation on the boundary layer flow due to an exponentially stretching sheet, *Int. Comm. Heat and Mass Transfer* (In press).

- [87] K. Vajravelu and B. V. R. Kumar: Analytical and numerical solutions of a coupled non-linear system arising in a three-dimensional rotating flow, *Int. J. Non-Linear Mech.* **39**, 13 – 24 (2004).
- [88] C.Y. Wang: Liquid film on an unsteady stretching sheet. *Quart. Appl. Math.* **48**, 601 – 610 (1990).
- [89] M. Miklavcic and C.Y. Wang: Viscous flow due to a shrinking sheet, *Quart. Appl. Math.* **64**, 283 – 290 (2006).
- [90] R. Cortell: Viscous flow and heat transfer over a nonlinear stretching sheet, *Appl. Math. Comput.* **184** (2007) 864 – 873.
- [91] K. Vafai and C.L. Tien: Boundary and inertia effects on flow and heat transfer in porous media, *Int. J. Heat and Mass Transfer* **24**, 195 – 203 (1981).
- [92] J.E. Dunn and K.R. Rajagopal: Fluids of differential type, critical review and thermodynamic analysis, *Int. J. Eng. Sci.* **33**, (1958) 689 – 729.
- [93] R.L. Fosdick and K.R. Rajagopal: Thermodynamics and stability of fluids of third grade, *Proc. Roy. Soc. London* **339**, 351 – 377 (1980).
- [94] J.E. Dunn and R.L. Fosdick: Thermodynamics, stability and boundedness of fluids of complexity 2 and fluids of second grade, *Arch. Rat. Mech. Anal.* **56** 191 – 252 (1974).
- [95] S.J. Liao: *Beyond perturbation: Introduction to homotopy analysis method*, Boca Raton: Chapman & Hall/CRC Press; 2003.
- [96] S.J. Liao: Finding multiple solutions of nonlinear problems by means of the homotopy analysis method, *J. Hydrodynamics, Ser. B* **18**, 54 – 56 (2006).
- [97] S.J. Liao: An analytic solution of unsteady boundary-layer flows caused by an impulsively stretching plate, *Comm. Non-linear Sci. Numer. Simu.* **11**, 326 – 339 (2006).
- [98] C. Yang and S.J. Liao: On the explicit, purely analytic solution of Von Kármán swirling viscous flow, *Comm. Non-linear Sci. Numer. Simu.* **11**, 83 – 93 (2006).

- [99] S.J Liao: Comparison between the homotopy analysis method and homotopy perturbation method, *Appl. Math. Comput.* **169**, 1186 – 1194 (2005).
- [100] S.J. Liao: A new branch of solutions of boundary-layer flows over an impermeable stretched plate, *Int. J. Heat and Mass Transfer* **48**, 2529 – 2539 (2005).
- [101] S.J. Liao: On the homotopy analysis method for nonlinear problems, *Appl. Math. Comput.* **147**, 499 – 513 (2004).
- [102] C. Wang, S.J. Liao and J. Zhu: An explicit solution for the combined heat and mass transfer by natural convection from a vertical wall in a non-Darcy porous medium, *Int. J. Heat and Mass Transfer* **46**, 4813 – 4822 (2003).
- [103] S.J. Liao: On the viscous flow past a sphere: A simplified description, *Comm. Non-linear Sci. Numer. Simu.* **4**, 104 – 109 (1999).
- [104] S.J. Liao: General boundary element method: an application of homotopy analysis method, *Comm. Non-linear Sci. Numer. Simu.* **3**, 159 – 163 (1998).
- [105] S.J. Liao: Homotopy analysis method: A new analytical technique for nonlinear problems, *Comm. Non-linear Sci. Numer. Simu.* **2**, 95 – 100 (1997).
- [106] Y. Tan and S. Abbasbandy: Homotopy analysis method for quadratic Riccati differential equation, *Comm. Non-linear Sci. Numer. Simu.* **13**, 539 – 546 (2008).
- [107] S. Abbasbandy: Soliton solutions for the Fitzhugh–Nagumo equation with the homotopy analysis method, *Appl. Math. Model.* (In press).
- [108] S. Abbasbandy: Solitary wave solutions to the modified form of Camassa–Holm equation by means of the homotopy analysis method, *Chaos, Solitons & Fractals* (In press).
- [109] S. Abbasbandy: Approximate solution for the nonlinear model of diffusion and reaction in porous catalysts by means of the homotopy analysis method, *Chem. Eng. J.* (In press)
- [110] S. Abbasbandy: Homotopy analysis method for heat radiation equations, *Int. Comm. in Heat and Mass Transfer* **34**, 380 – 387 (2007).

- [111] S. Abbasbandy: The application of homotopy analysis method to solve a generalized Hirota-Satsuma coupled KdV equation, *Phys. Lett. A* **361**, 478 – 483 (2007).
- [112] S. Abbasbandy and F. Samadian Zakaria: Soliton solutions for the fifth-order Kdv equation with the homotopy analysis method, *Nonlinear Dyn.* **51**, 83 – 87 (2008).
- [113] S. Abbasbandy and E.J. Parkes: Solitary smooth hump solutions of the Camassa-Holm equation by means of the homotopy analysis method, *Chaos, Solitons & Fractals* **36**, 581 – 591 (2008).
- [114] R. Ellahi, T. Hayat, T. Javed and S. Asghar: On the analytic solution of non-linear flow problem involving Oldroyd 8-constant fluid, *Math. Comp. Model.* (In press).
- [115] T. Hayat, Z. Abbas and M. Sajid: Heat and mass transfer analysis on the flow of a second grade fluid in the presence of chemical reaction. *Phys. Lett. A* (In press).
- [116] T. Hayat, M. Sajid and M. Ayub: A note on series solution for generalized Couette flow, *Comm. Non-linear Sci. Numer.Simu.* **12**, 1481 – 1487 (2007).
- [117] T. Hayat, M.A. Farooq, T. Javed and M. Sajid: Partial slip effects on the flow and heat transfer characteristics in a third grade fluid, *Nonlinear Analysis: Real World Applications* (In press).
- [118] T. Hayat and T. Javed: On analytic solution for generalized three-dimensional MHD flow over a porous stretching sheet, *Phys. Lett. A*, **370**, 243 – 250 (2007).
- [119] M. Sajid and T. Hayat: Wire coating analysis by withdrawal from a bath of Sisko fluid, *Appl. Math. Comput.* (In Press).
- [120] M. Sajid and T. Hayat: Comparison of HAM and IIPM methods in nonlinear heat conduction and convection equations. *Nonlinear Analysis: Real World Applications* (In press).
- [121] M. Sajid and T. Hayat: Influence of thermal radiation on the boundary layer flow due to an exponentially stretching sheet, *Int. Comm. Heat and Mass Transfer* (In press).
- [122] T. Hayat, Z. Abbas, T. Javed and M. Sajid: Three-dimensional rotating flow induced by a shrinking sheet for suction, *Chaos, Solitons & Fractals* (In press).

- [123] M. Sajid and T. Hayat: The application of homotopy analysis method for MHD viscous flow due to a shrinking sheet, *Chaos, Solitons & Fractals* (In press).
- [124] M. Sajid, T. Hayat, S. Asghar and K. Vajravelu: Analytic solution for axisymmetric flow over a nonlinearly stretching sheet, *Arch. Appl. Mech.* **78**, 127 – 134 (2008).
- [125] S.J. Liao: On the homotopy analysis method for nonlinear problems, *Appl. Math. Comp.* **147**, 499 – 513 (2004).
- [126] P.M. Fitzpatrick: *Advanced Calculus*. PWS publishing company. Boston, MA (1996).
- [127] S.J. Liao and K.F. Cheung: Homotopy analysis of a nonlinear progressive waves in deep water, *J. Eng. Math.* **45**, 105 – 116 (2003).